University of Arkansas, Fayetteville

ScholarWorks@UARK

8-2016

Evaluating a Measure-Calculate Method for Determining Sediment Oxygen Demand in Lakes

Adrian Beirise
University of Arkansas, Fayetteville

Citation

Evaluating a Measure-Calculate Method for Determining Sediment Oxygen Demand in Lakes

A thesis submitted in partial fulfillment
of the requirements for the degree of
Master of Science in Biological Engineering

by

Adrian Beirise
University of Arkansas
Bachelor of Science in Mechanical Engineering, 2011

August 2016
University of Arkansas

This thesis is approved for recommendation to the Graduate Council.

_____
Dr. G. Scott Osborn
Thesis Director

_____
Dr. Benjamin Runkle
Committee Member

_____
Dr. J. Thad Scott
Committee Member

ABSTRACT

A steady-state mass diffusion model used with simple measurable and calculable inputs for determining sediment oxygen demand (SOD) is compared to an intact core incubation (ICI) SOD method using samples from three lakes. The mass diffusion model coupled with inputs is known as the measure-calculate method (M-C) and is a potential alternative to existing methods for measuring SOD which are more complex, time-consuming, and costly. The M-C method requires inputs for volumetric sediment oxygen uptake ($\dot{N}_{sed}$), sediment density and porosity, and water properties. $\dot{N}_{sed}$ was determined by suspending sediment in oxygen-saturated water with a DO probe and determining the steady state rate of oxygen decline for the volume of sediment suspended. The SOD values determined using the M-C method were not significantly different from SOD determined using the ICI method using water property inputs representative of lake conditions. Thus, the study confirms the method's efficacy under test conditions and encourages further research. A separate comparison using water property inputs representative of conditions within incubated cores showed that M-C SOD correlated negatively against ICI SOD despite having similar mean values. This appears to be a result of different boundary conditions for flow velocity and DO within the core, and may discourage the ICI method's use, as tested, for determining actual *in-situ* lake SOD.

ACKNOWLEDGEMENTS

TABLE OF CONTENTS

LIST OF FIGURES

LIST OF TABLES

1. INTRODUCTION

1.1 Problem

In its most recent report, the EPA lists Organic Enrichment/Oxygen Depletion as the fourth most frequent cause of waterbody impairment, affecting 6,712 monitored fresh waters and 300 marine environments nationally (US EPA, 2015; Committee on Environmental and Natural Resources, 2010). Oxygen depletion is often caused by eutrophication, which leads to increased primary productivity (photosynthetic life). Increased productivity can cause short term oxygen depletion because of dark respiration, but also long term oxygen depletion as the increasingly abundant organisms die and settle in the sediment, thereby increasing organic matter that decomposes and consumes oxygen from overlying water. Truax et al. (1995) define sediment oxygen demand (SOD) as the rate of dissolved oxygen consumption due to a waterbody's benthos. SOD is used as a metric to aid in determining the oxygen mass balance budget in aquatic systems.

Previous research has shown that sediments can account for as much as 85% of hypolimnetic respiration in lakes (Cornett and Rigler 1987). Others have found that sediments were responsible for up to approximately 50% of total respiration in Chesapeake Bay (Kemp and Sampou, 1992). Fennel et al. (2013) analyzed models for the prediction of hypoxia in the Gulf of Mexico, and concluded that one of the most sensitive inputs was the rate of sediment oxygen consumption.

Because of the magnitude to which SOD can affect its environment, it often becomes necessary to quantify it. Generally speaking, any attempt to understand the dissolved oxygen (DO) balance in a water body requires knowing SOD, with the notable exception of methods that do not distinguish between water and sediment oxygen consumption, such as Areal

Hypolimnetic Oxygen Deficit (AHOD) or Relative Areal Hypolimnetic Oxygen Deficit (RAHOD). In streams, TMDL regulations are sometimes established using SOD data (Duchscherer, 2010). SOD can also be monitored over time to track changes in environmental dynamics. Finally, SOD can be useful for designing remediation treatments and measuring resulting effects.

However, measuring SOD is often time consuming and difficult, as well as requiring specialized equipment. Present methods for measuring or approximating SOD include benthic chambers, intact core incubation, areal hypolimnetic oxygen deficit, eddy correlation, and the measure-calculate method. Each of these methods has advantages and disadvantages which are outlined in this chapter. More detailed reviews of each method are presented in Chapter 2, Literature Review. No single method appears to have gained universal acceptance as the standard.

Benthic chambers are normally cylindrical or rectangular flat-topped chambers, open on the bottom, which are placed above and into the sediment to seal it off from its surroundings and any source or sink of oxygen other than the sediment. Numerous papers used benthic chambers in studying another phenomenon (Kasprzak, 2001; Lee et al., 2000; Matlock et al., 2003; Murphy and Hicks, 1986; Rounds and Doyle, 1997). Other studies compare benthic chambers to other methods for determining SOD (Bowman and Delfino, 1980; Hall and Berkas, 1988; James, 1974; Truax et al., 1995). SOD is determined by measuring the rate of oxygen depletion from the water in the chamber. Benthic chambers have the advantage of being used *in-situ*, allowing the measurement to be conducted using *in-situ* water at the *in-situ* temperature. However, the chamber is not able to replicate the *in-situ* flow regime of water over sediment, although some chambers attempt to artificially replicate *in-situ* flow using a constant rotational flow (Waterman

2

et al. 2011). In addition, the DO of water in the chamber necessarily differs from water outside the chamber. Tests often require a full day to allow for significant change of DO inside the chamber. Chamber placement can require divers to ensure a satisfactory seal with the sediment and ensure that sediment is not resuspended in the chamber, both of which can introduce error. Benthic chambers often leak outside water to inside the chamber, creating error.

A laboratory method using intact core incubation (ICI) also isolates a known volume of water above an area of sediment (Gardner et al., 2006; Haggard et al., 2012; McCarthy et al., 2007; Scott et al., 2008). The continuous flow ICI method involves extracting a core and overlying water from the sediment using a cylindrical tube, sealing both ends, and transferring it to a lab where it is placed in an incubator with oxygenated control water pumped in above the sediment and out of the cylinder top at a known rate. SOD is determined by measuring the difference in DO between the inflow and outflow water at steady-state conditions, multiplying by flow rate, and then dividing by the sediment surface area. ICI has the advantage of being able to conduct batch testing without a large fleet of equipment. ICI also allows the user to standardize the SOD environment with controlled flow, temperature, and inflow water. However, as with the benthic chamber, this prevents the test from representing *in-situ* conditions, particularly water flow regime. In addition, rocky or excessively loose sediments do not allow for the extraction of intact cores, as they prevent corer penetration into sediment or easily break apart during retrieval.

Eddy correlation (EC) involves using high-resolution Doppler 3D water velocity and DO data measured above the sediment to determine the net vertical flux of oxygen over time (Berg et al. 2003, Brand et al., 2008, Lorrai et al., 2010). EC has the distinct advantage of measuring SOD *in-situ* without altering the DO or velocity flow regime above the sediment, making it more inherently accurate than other methods. It also requires much less time per test than other

methods. However, this method is considerably more expensive than chambers or the ICI method. Also, because it measures differences in turbulent vertical flux, these fluxes can be below the measurable limit of the instrumentation given low enough flow velocities (Lorrai et al., 2010). It is possible that some stratified lakes might yield fluxes too small to be resolved by this method.

Areal hypolimnetic oxygen depletion (AHOD) determines the overall SOD rate of a stratified water body by monitoring DO-depth profiles over time after stratification begins in spring. SOD is calculated by multiplying this average rate of DO depletion by the estimated volume of the hypolimnion, and dividing by the estimated surface area of the lake bottom beneath it (Kalff, 2002). AHOD has the advantages of requiring only DO probes and precise bathymetry data. However, it has the disadvantages of requiring intensive sampling and being limited in application to only seasonally stratified inland water bodies not subject to wind-induced turnover (not polymictic) that also have negligible through-flow rates and sufficient bathymetry data.

The Measure-Calculate (M-C) method, developed by Osborn et al. (2008) and Charbonnet et al. (2006), uses a mathematical model based on Fick's Law mass-transfer equations to determine SOD using measurable and calculable sediment and environmental inputs. It carries several potential advantages. First, the M-C method requires only equipment typically available to water quality laboratories (DO probes, BOD meters, drying oven, scales), making it more accessible to water professionals. Second, it can be repeated quickly and easily for multiple tests, allowing many data points to be collected, improving replication and easier determination of spatial and temporal variability. Third, it can provide a dynamic output prediction of SOD given changes in any input parameter, such as overlying water DO, flow

4

velocity, and temperature, meaning it can be used to both calculate SOD for existing conditions and predict SOD for past or future conditions. Its main disadvantage is that it has only been correlated to another established SOD method on one system, which was a stream. Experiments showed that it correlated well to benthic chamber measured SOD in the Arroyo Colorado River in south Texas (Charbonnet et al. 2006). To the author's knowledge, there has been no attempt to correlate the M-C method with empirical measurements in lakes.

1.2 Objective

The objective of this study is to evaluate the efficacy of the M-C method for determining SOD in lakes by comparing its results to the ICI method.

1.3 Approach

This study evaluates the M-C method side by side with the ICI method in sample pairs collected from three small, temperate lakes during summer. It seeks to validate the ability of the M-C method to predict ICI results, to determine the relative repeatability of the M-C method compared to that of ICI, and to investigate interactions between variables and outputs for the two methods to gain insight into the function of each.

2. BACKGROUND AND LITERATURE REVIEW

2.1 Current Methods For Determining SOD

Accurately determining SOD presents a number of problems for the science and engineering community, as has been noted in previous works (Berg et al. 2003; Truax et al., 1995). Background and literature review of current methods for determining SOD including benthic chambers, ICI, EC, AHOD, and M-C will be explored in further detail. It should be noted that the methods discussed are categorizations rather than specific method standards. There are many different specific methods within these categories throughout the body of SOD research.

2.1.1 Benthic Chambers

Benthic chambers function by sealing a chamber over a known area of sediment *in-situ*, isolating a known volume of water above the sediment and measuring the rate of oxygen depletion from the isolated water. Benthic chambers have been used for many years and described at length (Bowman and Delfino 1980; Hall and Berkas 1988; James 1974; Kasprzak 2001; Lee et al., 2000; Matlock et al., 2003; Murphy and Hicks 1986; Truax et al., 1995; Rounds and Doyle 1997).

Benthic chambers typically use probes to measure both DO and temperature on the inside and outside of the chamber. The outside probes allows for detection of leaks of outside water into the chamber (as the inside DO will track outside DO if there is a significant leak). Typical DO probes used are of the datasonde type that log DO and temperature every few minutes. These datasondes typically cost around $5000 US each. Time required to collect data is such that the DO of the water inside the chamber is reduced from ambient DO to around 2 mg/L and generally

requires 24 hours. Therefore, for typical benthic chambers, one SOD reading per location can be determined per day with an equipment cost of around $10,000 USD per chamber.

Great care must be taken to seal the chamber into the sediment layer, often requiring a diver. An improper seal can lead to an artificially low SOD reading as oxygenated water from outside enters the chamber. The presence of large detritus such as wood, rocks, epifauna, macroalgae, or mussels on or in the sediment can prevent a proper seal or may interfere with DO measurements. Additionally, if sediment is disturbed while placing the chamber on the bottom or from mixing too aggressively, it can lead to an artificially inflated SOD rate as reduced material and biological elements that would otherwise remain contained in the sediment (with little or no access to oxygen) are resuspended in the water, where they increase the oxygen consumption rate inside the chamber beyond what would occur with *in situ* settled sediment.

Water flow velocity over sediment can affect SOD and placement of a chamber over sediment can change water velocity. At low flow velocities, SOD is limited by, and increases with, the flow velocity of the water above the sediment-water interface (Mackenthun and Stefan 1998; Whittemore, 1986). This is explained by convective boundary layer behavior. For higher water velocity, the boundary layer between DO in the water column and the sediment is thinner, allowing faster transfer. Lower water velocity results in a thicker boundary layer and slower mass transfer (Nakamura and Stefan, 1994). Thus, whether a particular environment has a relatively low or high flow velocity, it is important to accurately reproduce the boundary layer found *in-situ* inside the chamber in order to avoid under- or over-estimating *in-situ* SOD flux. Often, chambers use stirring impellers to approximate *in-situ* flow. However, the induced rotational flow in the chamber may not duplicate *in-situ* boundary layer thickness, resulting in an unnatural representation of the currents and/or waves (seiches) naturally occurring over the

sediment (Waterman et al. 2011). Replicating *in-situ* boundary layer thickness is not just a matter of replicating water velocity. Water flow patterns created within a chamber are very different from those resulting from water flow over a surface in an unbounded open system, potentially resulting in different boundary layer thicknesses for the same velocity. Recent efforts have been made to improve chamber design to address this inadequacy (He and Liu 2011), but the fundamental method may never accurately represent external *in-situ* conditions.

2.1.2 Intact Core Incubation

The ICI method, or family of similar methods, uses intact sediment cores (typically cylindrical, 5-10cm in diameter) of sediment removed from the sampling site and transported to a lab where they are incubated at constant temperature. Cores can be evaluated by aerating overlying water, then sealing and monitoring in a similar fashion to benthic chambers (Sweerts et al., 1991; Rabouille et al., 2003), or can be fed a slow, constant influent stream of water near the sediment surface which forces water out of the top of the core, as depicted in Fig. 1 (e.g. Gardner et al., 2006; Haggard et al., 2012; McCarthy et al., 2007; Scott et al., 2008). The difference in DO between influent water and effluent water, measured after steady state has been reached, reveals the rate of oxygen consumption by the sediment. This rate is divided by the cross sectional area of the sediment in the core to determine SOD. This method is also used for determining nutrient fluxes in sediments (e.g. Gardner et al., 2006; Haggard et al., 2012)
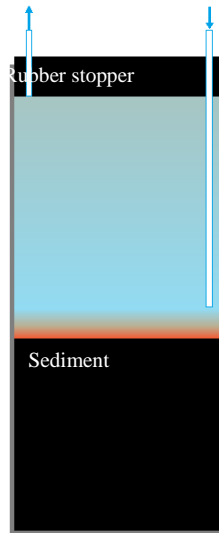
Figure 1: ICI schematic drawing, depicting possible oxygen gradients (blue representing high DO, red representing low DO) (not to scale)

While a few techniques attempt to mix the core water to varying degrees (Sweerts et al., 1989; Miller-Way and Twilley, 1996), few replicate the precise source *in-situ* environment and thus assume that pure diffusion is the primary vehicle for mass transport in/out of sediments (Lavery, et. al., 2001). ICI serves to effectively standardize environmental conditions between cores, and this provides an advantage when a relative comparison is desired. However, just as for the benthic chamber, DO and velocity may not accurately represent *in-situ* conditions, which limits how well the method represents *in-situ* SOD. The ICI method requires that sample cores be analyzed soon after collection. One study found that storing cores for 6 days or greater more than doubled the SOD rates of sediment cores (Edberg and Hofsten 1973). Intact core methods may also disturb or misrepresent bioturbation and bioirrigation caused by macrofauna in the sediment, causing an underestimation of SOD relative to the chamber method (Glud et al. 1998; 1999; 2003); however, not all sediments have significant macrofauna populations. Intact core incubation has been shown to be statistically equivalent with the chamber method in a freshwater river, except where sediments are extremely porous (Truax et al., 1995), and they have also been

shown to be similar in marine environments (Miller-Way et al., 1994). The difference with porous sediments was speculated to be due to disturbances during collection that collapse or compress the sediment and alter oxygen's ability to diffuse through it. Finally, ICI is limited to only those sediments which are both soft enough to penetrate with a corer and yet sufficiently cohesive to remain in the sampler when pulled from the sediment.

2.1.3 Eddy Correlation

A more recent development using EC technology (Berg et al. 2003, Brand et al., 2008, Lorrai et al., 2010) appears to solve some of the problems associated with chambers and intact cores. EC simultaneously measures, at high temporal resolution, the 3D velocity field (via acoustic Doppler velocimeter) and the DO concentration (via microelectrode or optical sensor) of a small, cylindrical water volume (approximately 1 cm^3) above the sediment surface for a period of 10-20 minutes. The flux of oxygen through the water and into the sediment is calculated from summing the vectors formed by multiplying instantaneous vertical flow components and their oxygen concentrations. According to its developer, EC can: measure SOD without disturbing natural light, sediment, or flow conditions, produce measurements rapidly, and can be used in environments where enclosure methods are difficult or impossible to apply. However it comes at the disadvantages of being costly and challenging to apply (Berg, n.d.). SonTek, who manufacturers the Doppler instrumentation used, estimated the cost of a complete SOD sensor at $20k USD. Another disadvantage is that EC measures advection (rather than diffusion) and requires turbulence, with sensor minimum velocities and minimum DO gradients that vary by model. In water bodies with fluctuations below these minimums, eddy correlation may be unreliable (Lorrai et al., 2010). EC has been applied in marine environments and in freshwater reservoirs. No studies could be found for the use of EC in streams.

2.1.4 Areal Hypolimnetic Oxygen Depletion

AHOD is the most sampling-intensive method for estimating SOD as it requires oxygen profiles to be collected throughout the water body with regularity until the hypolimnion becomes anoxic (Kalff, 2002; Matthews and Effler, 2006). It does not distinguish between oxygen consumed in the hypolimnetic water column and oxygen consumed in the sediment, but is measured in the same units of mass of oxygen per sediment area per time. Precise bathymetry data is required to compute the volume of the hypolimnion and the relevant sediment area. This bathymetric data, coupled with the overall rate of dissolved oxygen depletion in the hypolimnion (as calculated using the oxygen profiles) and accurate assumptions about vertical mixing, are then used to calculate an averaged SOD rate for the entire hypolimnion. This method can only be applied to seasonally stratified inland water bodies not subject to wind-induced turnover that also have negligible flow-through rates and sufficient data.

2.1.5 Measure-Calculate Method

The M-C method described by Osborn et al. (2008) and Charbonnet et al. (2006) uses mass balance equations based on a convective boundary layer of water over sediment and diffusion through sediment with oxygen consumption. The M-C method requires measurements of overlying DO, sediment density, and sediment volumetric oxygen uptake rate, along with estimation of oxygen diffusivity through sediment and the convective boundary layer determined by water flow velocity. These inputs are used in a mechanistic model based on mass diffusion equations to yield SOD. The M-C method is named as such to distinguish it from statistical or empirical models, as all model inputs are directly measured or determined based on physical/chemical properties of oxygen and water, then SOD is calculated from these

measurements from equations widely used for diffusion and convection from the literature. The M-C method was used to determine SOD in a Texas stream, the Arroyo Colorado, and was strongly correlated with empirical data from benthic chamber SOD tests (Charbonnet et al., 2006; Matlock et al., 2003). However, it has not yet been compared with empirical measurements in a lake system.

2.2 Previous SOD Models

In summarizing the field of SOD models, *Respiration in Aquatic Ecosystems* (Del Giorgio and Williams 2005) notes, "...the predictive ability of existing sediment respiration models has been rather poor and their generality tested more regionally." Empirical models have an inherently limited application when compared with mechanistic models because they are typically based on data from a specific location and are not broadly applicable. Mechanistic models are typically based on broadly applicable physical laws, properties and constants not limited to any specific location and are more likely to have the flexibility to account for changes in any input, although special care is needed to address assumptions regarding governing mechanisms and calculated inputs. Empirical models often do not have this flexibility and rely on statistical relationships. There does not appear to be any empirical model that has gained universal acceptance for predicting SOD. While one SOD model specific to lakes has proven accurate within study lakes in Ontario, Canada (Walker and Snodgrass 1986), this model must be fitted to each site using extensive testing. While other authors have used Fick's Law-based mass transfer to explore sediment-oxygen interaction (Hall et. al., 1989; Higashino and Gantzer, 2004; Lavery et. al, 2001; Rasmussen and Jorgensen, 1992), its use has been restricted to interpreting observations or to theoretical discussions, and has not until recently been proposed as the basis for a stand-alone method for determining SOD.

2.3 M-C Method In Depth– A Mass Diffusion Model

The M-C method was derived from Fick's Law of diffusion mass transfer within the oxic sediment only for one-dimensional transient mass transfer in Cartesian coordinates with consumption and is shown in Equation 1 (Osborn et al., 2008). Upper and lower boundary conditions are shown in Equations 2 and 3, respectively. Figure 2 is a diagram illustrating the model system and coordinate system. Fick's Law has previously been demonstrated to be capable of accurately representing mass transfer fluxes in intact sediment cores (Lavery, et. al., 2001). Equation 2 is the mass balance at the sediment-water interface and defines the boundary condition immediately above the interface to be convective. Equation 3 is the lower boundary condition of the oxic sediment stating that dissolved oxygen is reduced to zero where it transitions to anoxic sediment:
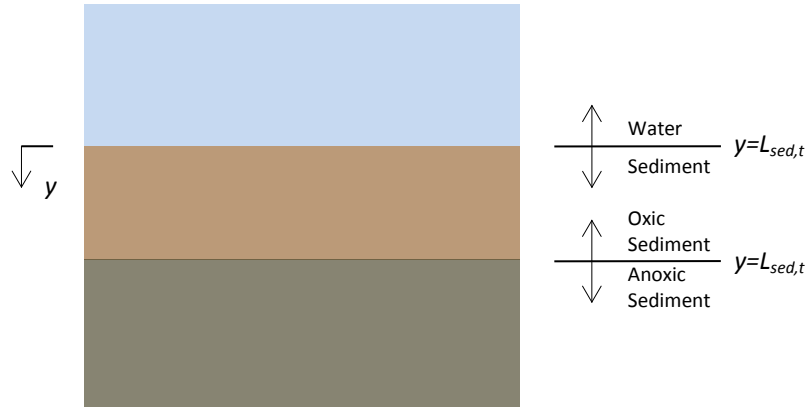
Figure 2: Diagram of sediment-water interface for equation orientation

$$\frac{\partial^2 C_{O2}}{\partial y^2} - \frac{\dot{N}_{sed}}{D_{O2,sed}} = \frac{1}{D_{O2,sed}}\left(\frac{\partial C_{O2}}{\partial t}\right) \tag{1}$$

$$-D_{O2,sed}\left.\frac{\partial C_{O2}}{\partial y}\right|_{y=0} = h_m\left(C_{O2-fs} - \frac{C_{O2-s}}{P_{sed}}\right) = SOD \tag{2}$$

$$C_{O2}|_{y=L_{sed,t}} = 0 \tag{3}$$

13

where

C_{O2} = concentration of oxygen (mg L^{-1})

y = depth below sediment/water interface (m)

$\dot{N}_{sed}$ = rate of sediment oxygen consumption per volume

   (g $m^{-3}s^{-1}$)

$D_{O2,sed}$ = Diffusivity of oxygen through sediment (m^2 s^{-1})

h_m = convective mass transfer convection coefficient (m s^{-1})

C_{O2-fs} = concentration of oxygen in water above the convective

   boundary layer (free stream)(mg L^{-1}_{water})

C_{O2-s} = sediment surface concentration of oxygen in sediment at

   $y = 0$ (mg $L^{-1}_{sediment}$)

P_{sed} = partition coefficient to relate oxygen solubility in sediment to

   that in water (m^3_{water} $m^{-3}_{sediment}$)

SOD = sediment oxygen demand (g $m^{-2}s^{-1}$)

$L_{sed,t}$ = oxic sediment depth below which DO = 0 (m)at any time, t

In order to calculate SOD, the equations must be solved simultaneously through either a steady state $\left(\frac{\partial c}{\partial t} = 0\right)$ or transient $\left(\frac{\partial c}{\partial t} \neq 0\right)$ condition. A numerical solution to the transient equations was developed by Osborn et al. (2008) and is available in a spreadsheet. The steady state solution was also developed by Osborn et al. (2008) (Eq. 4) and was solved assuming $\dot{N}_{sed}$ is constant throughout the oxic sediment depth at steady state and is therefore not reduced as

C_{O2-s} decreases with increasing sediment depth. The steady-state solution calculates SOD once equilibrium is established between oxygen diffusion (from water into sediment) and depth of sediment remaining oxic (in response to oxygen consumption from within the sediment). The transient solution calculates changing SOD over time and does reduce the value of $\dot{N}_{sed}$ as C_{O2-s} decreases. Charbonnet (2003) showed that the steady state solution gave similar results to the transient solution and is far simpler to use.

$$SOD = (\dot{N}_{sed}) \left\{ \left(\frac{D_{O2,sed}^2 * P^2_{sed}}{h_m^2} + \frac{2 * D_{O2,sed} * C_{O2-fs} * P_{sed}}{\dot{N}_{sed}} \right)^{\frac{1}{2}} - \left(\frac{D_{O2,sed} * P_{sed}}{h_m} \right) \right\} \qquad (4)$$

The primary driving force in the M-C model that creates the oxygen concentration gradient that forces diffusion is the volumetric sediment oxygen uptake rate, $\dot{N}_{sed}$. $\dot{N}_{sed}$ is the steady state rate at which a volume of oxic ($C_{O2-s} > 0$) sediment consumes oxygen at a standard temperature (20°C), expressed as g-O_2 s^{-1} m^{-3}-sediment. $\dot{N}_{sed}$ changes with temperature according to the kinetic equation developed by Chapra (2008), explained in more detail here in Ch. 3.7. When sediment becomes anoxic, $\dot{N}_{sed} = 0$. $\dot{N}_{sed}$ is a maximum potential rate occurring under oxic conditions.

The value of $\dot{N}_{sed}$ coupled with oxygen diffusivity through sediment and C_{O2-fs} determines L_{sed} and SOD. The relationship between these parameters is somewhat complex. An illustrative example is that if a sediment system is in steady-state with constant values for $\dot{N}_{sed}$, D_{O2-sed}, C_{O2-fs}, then L_{sed} is constant and the result of the oxygen balance between the rate consumed by the sediment and the rate entering the sediment based on diffusion from the free stream. If this baseline steady-state system is disturbed such that $\dot{N}_{sed}$ is increased and D_{O2-sed}, C_{O2-fs} are held constant, then the oxic sediment depth will decrease since the oxygen balance will shift as it is being consumed faster than it is diffusing into the sediment from the water. As oxic depth decreases, less sediment is actually consuming oxygen since oxic sediment near the bottom

layer in the baseline condition no longer has oxygen available to consume in the disturbed condition. Overall SOD may or may not change in the disturbed condition because the increase in $\dot{N}_{sed}$ will be somewhat offset by a decrease in the oxic depth and therefore amount of sediment consuming oxygen. The magnitude of this offset is also affected by $D_{O2\text{-}sed}$. If the baseline condition is disturbed such that $D_{O2\text{-}sed}$ is increased while $\dot{N}_{sed}$ and $C_{O2\text{-}fs}$ remain constant, L_{sed} will increase as oxygen can diffuse into the sediment more quickly than in the baseline condition. Since more sediment is oxic, SOD will increase. If the baseline condition is disturbed such that $C_{O2\text{-}fs}$ is increased while $\dot{N}_{sed}$ and $D_{O2\text{-}sed}$ remain constant, then the concentration gradient between water and sediment will increase resulting in faster transfer of oxygen into the sediment, so L_{sed} will increase resulting in more oxic sediment and an increase in SOD.

As a maximum potential, $\dot{N}_{sed}$ is not directly measurable *in-situ*, and may be difficult to measure consistently *ex-situ* because the oxic depth and therefore volume, may vary. To estimate values for $\dot{N}_{sed}$, Charbonnet et al. (2006) developed a method to place sediment of a known volume into oxygenated water. The sediment was homogenized and mixed with water such that the water-sediment mixture remained oxic throughout testing. The DO of the continuously-suspended mixture was measured to obtain a slope ($mg\text{-}L^{-1}\text{-}day^{-1}$) which was then multiplied by the volume of water then divided by the sediment volume to obtain ($g\text{-}m^{-3}\text{-}second^{-1}$).

The $\dot{N}_{sed}$ term does not appear widely in the research literature. Higashino and Gantzer's (2004) equivalent variable is called the "maximum oxidation rate", μ (units $mg\text{-}L^{-1}\text{-}d^{-1}$). They noted that the theoretical value for μ appeared to be highly unrepresentative of reality. The only available measured freshwater $\dot{N}_{sed}$ data was taken by two studies using the M-C method in a stream (Charbonnet et al., 2006; Matlock et al., 2003). A similar method used in Lake Wister (Oklahoma) measured the mass-based, rather than volumetric, sediment oxygen uptake rate

(Richardson, 2014). Unpublished data was used to convert Richardson's values into terms of $\dot{N}_{sed}$, which ranged from 0.029 – 0.097 g-m^{-3}-second^{-1}, which fell well within the range measured by the Arroyo Colorado studies (0.002 – 0.240 g-m^{-3}-second^{-1}).

Because accurate volume measurements on small amounts of sediment are difficult, $\dot{N}_{sed}$ is measured directly on a more accurate mass basis, and converted to a volume basis using separate settled sediment density measurements. The Osborn et al. (2008) $\dot{N}_{sed}$ measurement procedures attempt to determine this maximum rate using aggressive mixing and high DO concentrations with a small amount of sediment in order to remove any rate limitations imposed by oxygen diffusion. Because SOD is normally a relatively steady-state process in the environment (meaning that over time intervals of minutes or hours $\frac{\partial SOD}{dt} \approx 0, \frac{\partial \dot{N}sed}{dt} \approx 0$), only the steady-state portion of oxygen consumption rate is used for $\dot{N}_{sed}$ rather than the more rapid but short-term initial consumption rate.

Charbonnet (2003) performed a sensitivity analysis on the SOD determination model inputs. The analysis showed that the model is most sensitive to convection boundary layer h_m, temperature, and water free stream DO above the boundary layer. The model appears to be less sensitive to all other input parameters, including $\dot{N}_{sed}$. Therefore, values for h_m within the model will produce the largest effect on output SOD.

Despite the model's lower sensitivity to $\dot{N}_{sed}$, it is a variable that does not appear to have been sufficiently explored in previous studies. One impediment to quantifying $\dot{N}_{sed}$ is the degree to which it changes with depth below the sediment surface. It is generally known that sediments are composed of an aerobic region, defined by the availability of free oxygen and nearest to the overlying water, and an oxygen limited (anaerobic) region below. The aerobic region is often visually distinguishable, being a lighter color than underlying layers. This is likely due to

17

differences in metallic redox states (Huettel et al., 1998). Research shows that the majority of

SOD occurs within the topmost few millimeters of the sediment surface (Edberg and Hofsten

1973; Seiki et al., 1989), and this is responsible for the majority of SOD (Pamatmat and Banse

1969; Fillos and Molof 1972; Hatcher, 1986; Seiki et al. 1994). Both Jorgensen and Revsbech

(1985) and Rutherford et al. (1991) place the thickness of this layer between 2 and 5 mm. The

model to be used in this work has calculated an oxic depth of: 0.05-0.35mm (steady-state) or

0.65-1.03mm (transient) for a stream (Charbonnet et al., 2003). It is assumed that the anoxic

layer below this also has a large potential oxygen demand when exposed to available oxygen.

The experimentally determined $\dot{N}_{sed}$ does not distinguish between the contributions of biological

and chemical redox consumption . Often, it can be observed in sediment core samples that the

bulk of the core is a darker color, with a smaller "transition" zone between the uppermost

(presumably aerobic) and lower (presumably anaerobic) sediments. Values for $\dot{N}_{sed}$ by sediment

depth could not be found in the literature, but in order to capture $\dot{N}_{sed}$ that best represents *in-situ*

conditions, collecting the topmost aerobic layer of sediment and avoiding anaerobic sediment

would seem to be ideal for purposes of the M-C method.

2.3.1 M-C Method Potential Advantages

The M-C method appears to be worth investigating because it offers particular advantages

over all other current SOD methods. It is able to mathematically standardize the SOD

environment (i.e. water temperature, DO, velocity) in order to compare different sediment

samples. The effects of changing *in-situ* conditions can be modeled. It requires less costly

equipment than other methods, meaning it may be accessible to a greater number of water

professionals. The M-C method would likely allow a greater number of SOD determinations to

be made in the same amount of time as other test methods, allowing more data to be collected

and potentially reducing uncertainty when quantifying SOD in a water body. Easier and cheaper access to SOD data would likely fuel other studies and ultimately progress remediation and sustainability projects.

If studies can show that sediment property model inputs do not change significantly over time and the model remains accurate over a wide range of temperatures, then a single set of sediment samples could be coupled with future or historical water data for temperature, DO and bottom water velocity to create seasonal SOD profiles. Currently, this requires direct SOD measurements throughout the year, but with the proposed method and some testable assumptions, sampling could be reduced to only a few initial sediment samples, then environmental data for water conditions could be used at each time step for which SOD is desired. This would have applications in environmental software such as lake models and could also improve design of equipment to remediate lakes with high SOD and provide targets and validation of watershed scale remediation procedures. Lastly, improved SOD values would allow TMDLs to be set with more confidence, benefitting both the environment and permit-holding businesses.

2.3.2 Knowledge Gap

In summary, the M-C method has potential advantages over existing methods and could be a valuable tool. However, it lacks a substantial body of efficacy studies. Thus far, there has been a theoretical evaluation of a similar SOD model, a number of site-specific studies to develop empirical SOD models, and a direct comparison of this model to real data in a stream. There appears to be a gap in knowledge in comparing this type of SOD model side-by-side with observed data in lakes. The proposed research fills this gap.

3. METHODS & MATERIALS

3.1 Experimental Objective And Justification

Objective: In this experiment, the M-C method was tested against the ICI method using 20 paired sample cores from each of 3 lakes.

The ICI method was chosen as the benchmark in this study for several reasons: ICI data on lakes to be tested in this study is available, ICI is the best-suited available method for testing SOD in batches, sediment cores lend themselves well to collecting identical sediment sample pairs from a range of depths, and all necessary equipment was available.

3.2 Hypotheses

In order to evaluate the efficacy of the measure-calculate model as a stand-alone method for determining SOD in lakes, two hypotheses must be investigated:

1. H0: Mean M-C SOD is not significantly different from mean ICI SOD

2. H0: The coefficient of variation (CV) of M-C SOD is less than or equal to that of ICI SOD

3.3 Sampling Locations

The two methods for determining SOD were compared using samples collected from three lakes: Lake Wedington and Lake Fayetteville near Fayetteville, AR, and Lake Wister near Poteau, OK. Lake Wedington has been characterized as mesotrophic (medium primary productivity) (Scott and Grantz 2013). Lakes Fayetteville (Scott and Grantz 2013) and Wister (Buck 2014) have both been classified as eutrophic (high primary productivity). Lake Wister represents a unique set of conditions including frequent wind-driven turnover and high water

temperatures, whereas lakes Fayetteville and Wedington represent common conditions for small man-made lakes in temperate regions. SOD was measured in Lake Wister using ICI methods in previous studies. The number of sampling locations in each lake was 20, which were divided into at least two transects: one from inflow to outflow, and one approximately perpendicular to flow (Figures 3, 4, and 5). Sample locations were predetermined with GPS coordinates and found using a smartphone GPS application (GPS Essentials ®). Because of boat drift, GPS accuracy, and time constraints, locations reading within 3 meters of the preplanned sampling sites were considered sufficiently close to collect samples.

Figure 3: Lake Fayetteville sampling locations. Latitude/Longitude for each site can be found in Appendix A (image via Google Maps) N↑
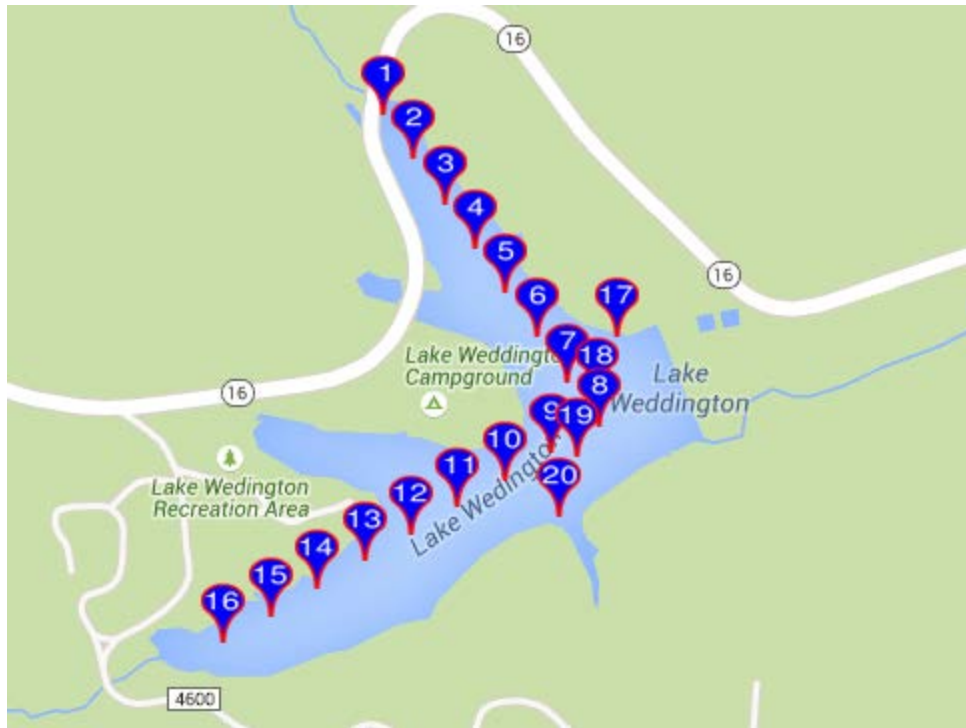
Figure 4: Lake Wedington sampling locations. Latitude/Longitude for each site can be found in Appendix A (image via Google Maps) N↑

Figure 5: Lake Wister sampling locations. Latitude/Longitude for each site can be found in Appendix A (image via Google Maps) N↑

3.4 Core Collection

1. Sediment core pairs (one for ICI, one for M-C) were collected at each site with a large size Uwitec hammer corer (Mondsee, Austria; www.uwitec.at/). The hammer corer was retrofitted with a custom rubber O-ring to use EnviroKing UVR Thinwall clear PVC core tubes, with dimensions 81.5mm ID x 610mm long. Cores ideally would have similar water column heights above the sediment, however absolute uniformity is difficult considering the manual operation of the corer, inability to see the corer during sample collection, and natural variation in sediment penetration ease. The goal was for the sediment to fill half of the 610mm core with the top half containing lake water.

2. At each sample location, sampling date, time and water depth were recorded.

3. During each collection trip, 10 locations were sampled plus one control core, which was filled with representative lake water.

4. For each batch of 10 samples, one randomly assigned location had an additional duplicate pair of core samples collected to examine repeatability.

5. Before removal from the water, cores were sealed on the bottom using slip-fit PVC endcaps with petroleum jelly applied inside to ensure that no water seeped out. Once removed from the water and from the corer, the top was sealed with a second slip-fit PVC endcap without petroleum jelly (so as not to potentially interfere with biochemical processes affecting SOD).

6. Cores were transported to the lab oriented vertically at ambient temperature.

3.5 Core Storage

1. All samples were stored as sealed intact cores to eliminate the possibility of further disturbing the sediments or prematurely satisfying any oxygen demand during repackaging or transfers.

2. Cores were placed immediately in either the incubator (for intact cores) or the testing laboratory (for M-C), both of which were temperature controlled to 20°C.

3. All cores were tested within 5 days of collection.

3.6 Intact Core SOD Testing Methods (Adapted from Grantz, et al., 2012)

1. 12 cores per batch (10 locations plus duplicate plus control core) were tested.

2. All cores and equipment were maintained at 20°C during testing using a precision incubator.

3. The upper PVC caps were removed from each core then replaced with a rubber stopper containing 1mm ID Teflon influent and effluent tubing. The inflow tube was positioned approximately 1 cm above the sediment, and the outflow tube was recessed into the rubber stopper so as to evacuate any remaining air bubbles from the core.

4. De-ionized water amended with vital minerals and trace metals (per Grantz et al., 2012) was used for influent water to the core and was constantly aerated to maintain oxygen saturation.

5. Influent water was pumped into all cores at a constant target rate of 0.7 mL/min as determined by per Grantz et al. (2012) for the entirety of the incubation using a peristaltic pump. The experimental setup is pictured in Fig. 6:

Figure 6: ICI experimental setup, with aerated amended water reservoir lower middle, pumps on either side of it, cores above supported with acrylic rack, and outflow receptacle on top, all within incubator.

6. Using the target influent rate and assuming plug flow in the core, the incubation was conducted for sufficient time to provide at minimum one water change, according to the time calculated using the largest core's overlying water volume divided by influent water target flow rate. Amended inflow water was periodically replaced as necessary and effluent discarded.

7. After the calculated time had elapsed to completely flush, effluent samples from each core were collected along with three influent samples. Water samples were placed into 12mL glass vials, preserved (to stop any further biological activity) by adding 0.15mL of 50% w:v $ZnCl_2$, sealed without bubbles, and wrapped in parafilm. Vials were stored inside the incubator submerged in tap water until analysis.

8. Preserved samples were analyzed for oxygen : argon ratio using a Membrane Inlet Mass Spectrometer (MIMS) set to 20°C. This data was then converted to DO (mg-L^{-1}) using the following equation:

$$DO = \left([O_2]:[Ar]_{sample} \times [Ar]_{exp}\right)\left(\frac{[O_2]:[Ar]_{exp}}{[O_2]:[Ar]_{standard}}\right) \tag{5}$$

where $[Ar]_{exp}$ is the theoretical saturated argon concentration calculated at the test temperature using solubility tables, $[O_2]:[Ar]_{exp}$ is the theoretical saturated dissolved gas ratio from solubility tables, and $[O_2]:[Ar]_{standard}$ is the ratio measured by the MIMS machine in well mixed, aerated, de-ionized water at the same temperature and atmospheric pressure as the samples.

9. SOD (g-m^{-2}-day^{-1}) was calculated using the sediment surface area (based on core inside diameter), the difference between equilibrium influent and effluent dissolved oxygen readings, and the oxygen uptake rate from a control core obtained using this procedure according to the following equation:

$$SOD = \frac{([O_2]_{out}-[O_2]_{in})\times Q_{core}-([O_2]_{control,out}-[O_2]_{in})\times Q_{control}}{A} \tag{6}$$

where Q denotes the peristaltic pumping rates through the cores and control (m^3-day^{-1}), and A is the core tube inside cross sectional area (m^2).

3.7 Measure-Calculate SOD Methods

The M-C method as tested uses the steady state solution to the differential equation rather than the transient solution. The steady state solution was chosen because it is more manageable in a spreadsheet with multiple input rows, has been shown to be nearly equal to the transient

solution, and was also more accurate than the transient solution when compared to the chamber data (Charbonnet, 2003).

3.7.1 Measured Sediment Inputs

The following M-C inputs were measured directly: $\dot{N}_{sed}$, sediment density, and sediment moisture content.

1. The following procedure for measuring $\dot{N}_{sed}$ was performed twice per core, and was adapted from Charbonnet (2003). The testing station is shown in Figure 7:

Figure 7: $\dot{N}_{sed}$ testing station, showing laptop computer (center), YSI 5100 DO probes, 300mL BOD bottles, and stir plates.

    a. The room thermostat was set to 20°C, and all equipment and water was stored overnight at this temperature before testing.

    b. The YSI 5100 DO probe (Yellow Springs, Ohio) was autocalibrated and its atmospheric oxygen concentration reading recorded.

    c. The core was opened by removing the top cap, slipping a piece of PVC larger than the core's outer diameter around the core, replacing the top cap to provide a vacuum on the core contents, and hammering the bottom cap off with the outer PVC piece, then placing it immediately onto a special-made core plunger that

consisted of an approximately 3 inch diameter by 1-inch thick machined Delrin ®
cylinder with a recessed 8mm OD rubber O-ring to seal inside of the core,
mounted on a 24 inch steel rod above a wooden base. Once the plunger piston was
sealed inside the bottom of the sediment core, the overlying water was carefully
siphoned off with a small piece of vinyl tubing.

d. The sediment was pushed to the top of the core where an Uwitec core cutter was
used to remove the uppermost 1.5 cm of sediment. The 1.5cm depth was chosen to
provide a balance between attempting to capture all aerobic sediment, attempting
to minimize inclusion of anoxic sediment, and collecting a sufficient volume of
sediment to perform all sediment tests on each core.

e. The removed upper sediment was mixed thoroughly and tested immediately.

f. $\dot{N}_{sed}$ was measured using a 300mL glass BOD bottle that was filled with aerated
DI water. A 2" magnetic stir bar was added to the bottle, which was placed on a
magnetic stir plate. The DO probe was inserted while the water was mixed to
measure initial DO in the test bottle prior to adding sediment.

g. Previously mixed sediment was portioned out into a dish and weighed for
placement into the test bottle. The amount of sediment used ranged from 4.06 g to
13.68 g and was adjusted as necessary to match a target consumption rate. Too
much sediment will consume DO from the water too quickly to measure
accurately, and too little sediment may consume DO at a slow enough rate that it
becomes difficult to distinguish from instrument measurement error. Oxygen
depletion from near saturation to 0.50 mg/L in 45 minutes (the maximum time the
YSI 5100 probe allows for it's OUR function) was the target in this study.

h. The YSI 5100 DO analyzer was set to OUR mode, then the probe moved
    temporarily to another bottle of clean test water while the sediment was added to
    the water in the test bottle.

i. The DO probe was then reinserted, the stir bar was activated, and the OUR
    program was started and set to output data. The stir bar was rotated at a sufficient
    velocity to suspend all sediment.

j. Data was recorded automatically every 15 seconds until either DO became less
    than 0.50 mg/L (approximately anoxic) or 45 minutes elapsed. This data was
    captured using an RS232-USB connection to a laptop computer and stored. It
    should be noted that the author demonstrated previously that the probe, although
    technically consumptive, does not consume a measurable amount of oxygen in the
    time and water volume considered, thus no corrections are taken to account for
    probe consumption in the test bottle.

k. Water temperatures were recorded to temperature-correct DO curves to 20°C.
    Recorded test temperature averages were between 19.3°C and 22.2°C, with a
    mean of 20.7°C.

l. The oxygen consumption rate per unit mass of wet sediment was determined using
    equation (7):

$$\dot{N}_{sed} = \frac{-b * \rho * volume_{test\ bottle}}{mass_{sediment\ added}} \qquad (7)$$

Where *b* is found using the following regression of the DO versus time curve
recorded by the DO probe. JMP 12 was used to fit the regression (equation 8) to
each run simultaneously and save the parameter estimates:

$$DO = a + b * t + c * \exp(d * t) + e * \exp(f * t) \qquad (8)$$

At steady state, $t \approx \infty$ and $\frac{dDO}{dt} = b$.

m. $\dot{N}_{sed}$ was temperature corrected according to the following:

$$\dot{N}_{sed,corected} = \dot{N}_{sed} * 1.08^{(T-20)} \tag{9}$$

where T = average test water temperature (°C) (developed for SOD by

Chapra, 2008).

2) Sediment density (ρsed, g-cm-3) was measured using a 25 mL subsample of the removed

and mixed sediment that was placed into a graduated cylinder of known dry weight.

Excess was wiped off, and the cylinder was re-weighed to calculate sediment density.

3) Sediment moisture content (MC) was measured accordingly:

a) The remainder of the removed upper 1.5cm of sediment was placed on an inert and

heat resistant dish of known dry weight, and weighed wet.

b) The sediment sample was then placed in a drying oven at 103°C for a minimum of

two days and re-weighed after completely desiccated.

c) The difference between the wet and dry sediment weights was lost water (MC, g$_{water}$-

g$_{wet\ sediment}^{-1}$), calculated as a decimal of the initial wet sediment weight.

3.7.2 Calculated M-C Method Inputs

1) The sediment partition coefficient (P_{sed}), diffusivity of oxygen through water ($D_{O2,w}$, m^2-

s^{-1}) and diffusivity of oxygen through the sediment ($D_{O2,s}$, m^2-s^{-1}) were calculated

accordingly (with T = temperature, °C):

$$P_{sed} = \frac{\rho_{sed}*MC}{\rho_{water}} \tag{10}$$

$$D_{O2,w} = 4.665378 * 10^{-13} * (T + 273.16)^{3/2} \tag{*11}$$

30

(*This equation is a regression of diffusivity vs. T

data; $D_{O2,w}$ may also be found using a water property

table at varying temperatures)

$$D_{O2,s} = D_{O2,w} * P_{sed} \tag{12}$$

At 20°C, $D_{O2,w}$ = 2.34E-09 m^2-s^{-1}, the value used in these calculations.

2) The mass transfer convection coefficient was calculated as follows, based on Osborn, et

al. (2008). To represent lake conditions, a representative value for water velocity over

sediment was necessary to estimate h$_m$. Three studies were referenced to estimate

representative minimum, mid-range, and maximum water velocities near lake bottoms

(Brand et al., 2008, 0.11m above sediment; Horn et. al., 1986, 6-10m below water

surface; Gloor et. al., 1994, 0.7-1.55m above sediment), determined as 0, 2, and 5 cm/s,

respectively. h_m was then calculated assuming water flow over a flat plate. It should be

noted that where Osborn et al. used the equation for Nusselt number (within equation 14)

for turbulent flow at a point ($Re>3*10^6$) to represent streams with typically greater

velocity that lakes, it is here replaced with the equation for average Nusselt number for

lower Reynolds Numbers ($Re<2*10^5$) (Datta, 2002) to better represent *in-situ* lake

conditions. Reynolds number was calculated as an average for a representative cross-

section 1m high by 10m wide above the lake bottom to approximate the large scale water

movements found in lakes.

$$h_m = \frac{h}{\rho_w * C_p * \left(\frac{\alpha}{D_{O2,w}}\right)^{2/3}} \tag{13}$$

$$h = \frac{Nu * k_w}{D_h} \tag{14}$$

$$Nu \ (Nusselt \ Number) = 0.664 Re^{1/2} Pr^{1/3} \tag{15}$$

$$\text{Pr } (Prandtl\ Number) = \frac{\mu * C_p}{k_w} \qquad *(16)$$

(*This input may also be found using a

water property table)

$$Re\ (Reynold's\ Number) = \frac{\rho_w * v * D_h}{\mu} \qquad (17)$$

where:

h_m = convection mass transfer coefficient (m-s^{-1})

h = convection heat transfer coefficient (W-m^{-2})

ρ_w = water density (kg-m^{-3})

c_p = heat capacity of water (kJ-kg^{-1}-K^{-1})

α = thermal diffusivity of water (m^2-s^{-1})

$D_{O2,w}$ = diffusivity of oxygen through water (m^2-s^{-1})

v = flow velocity (m-s^{-1})

D_h = hydraulic diameter = $\frac{4A}{P_w}$, estimated for horizontal cross section of water

10m*1m,=1.818m

k_w = thermal conductivity of water (W-m^{-1}-K^{-1})

μ = dynamic viscosity of water (Pa-s)

At 20°C, ρ_w = 998.3 kg-m^{-3}, c_p = 4182 kJ-kg^{-1}-K^{-1}, α = 1.49E-07 m^2-s^{-1}, $D_{O2,w}$ = 2.34E-09

m^2-s^{-1}, k_w = 0.5984 W-m^{-1}-K^{-1}, μ = 1.00E-03 Pa-s. These values were used to calculate

model inputs.

3) DO of water above the boundary layer input into the model was chosen to represent lake

conditions of minimum, median, and maximum typical DO. The minimum condition was

chosen as the delineation for hypoxia (2 mg-L^{-1}). The maximum condition was chosen as

saturation for the study temperature, 9.09 mg-L^{-1} (at 20°C, sea level). The median

condition was chosen as the mid-way point between these two, 5.5 mg-L^{-1}.

4) Finally, SOD is calculated using equation (4)

3.8 Analytical Methods

In order to calculate, organize, and analyze outcomes, Microsoft Excel 2010 and JMP 12

software were used. Raw data was collected and organized in Excel. DO versus time regressions

for $\dot{N}_{sed}$ were obtained using JMP 12 software. Final calculations for SOD were conducted using

Excel. Statistical analyses, outcome comparisons, and graphs used JMP 12. Spatial

representations of data were obtained using ArcMap software. All statistical analyses were

performed using $\alpha = 0.05$. Specific analyses performed include:

1. Paired t-test to evaluate differences between ICI and M-C SOD- as a whole dataset, and
   by lake.

2. Coefficients of variation (CV) for each dataset using the following equation:

$$CV = \frac{s}{\bar{X}} \qquad (18)$$

       where s is the sample standard deviation and $\bar{X}$ is the mean.

3. Box plots to compare literature values for SOD and $\dot{N}$sed with study values.

4. Graphs of sediment inputs and SOD outputs versus location to observe any resulting
   patterns.

5. Graphs of observed versus predicted SOD using ICI inputs.

6. Graphs of observed and predicted SOD using lake inputs, by lake.

7. Relative sensitivity (Haan, 2002) of model inputs under the three simulated lake
   conditions according to:

$$S_r = \left(\frac{O_2 - O_1}{P_2 - P_1}\right)\frac{P}{O} \tag{19}$$

where

$P =$ source parameter

$P_2 =$ increased source parameter (+1%)

$P_1 =$ decreased source parameter (-1%)

$O =$ model output

$O_2 =$ increased model output

$O_1 =$ decreased model output

8. Graphs of interactions between all SOD inputs and outputs for both methods to determine significant correlations.

4. RESULTS AND ANALYSIS

Not all proposed sample locations yielded usable data. In total, 37 of 60 proposed locations were evaluated to completion: 9 from Lake Fayetteville, 20 from Lake Wister, and 8 from Lake Wedington. At 12 of 20 locations in Lake Wedington, the sediment was either too rocky to penetrate with the corer (frequently the shallower sites) or else not cohesive enough to extract intact cores (frequently deeper sites). This issue is addressed later in Section 5.1.

4.1 Intact Core Incubation SOD Results

Cores from 9 sample locations were successfully extracted and tested in Lake Fayetteville instead of the proposed 20. Odd-numbered samples F1-F19 (10 samples) did not yield core incubation data because inflow DO samples were missing due to operator error, and the F6 outflow sample was damaged during analysis. All locations were tested successfully in Lake Wister. All 12 locations in Lake Wedington that produced core samples were tested successfully for ICI SOD. Successful ICI SOD determination results are mapped in Fig. 8:
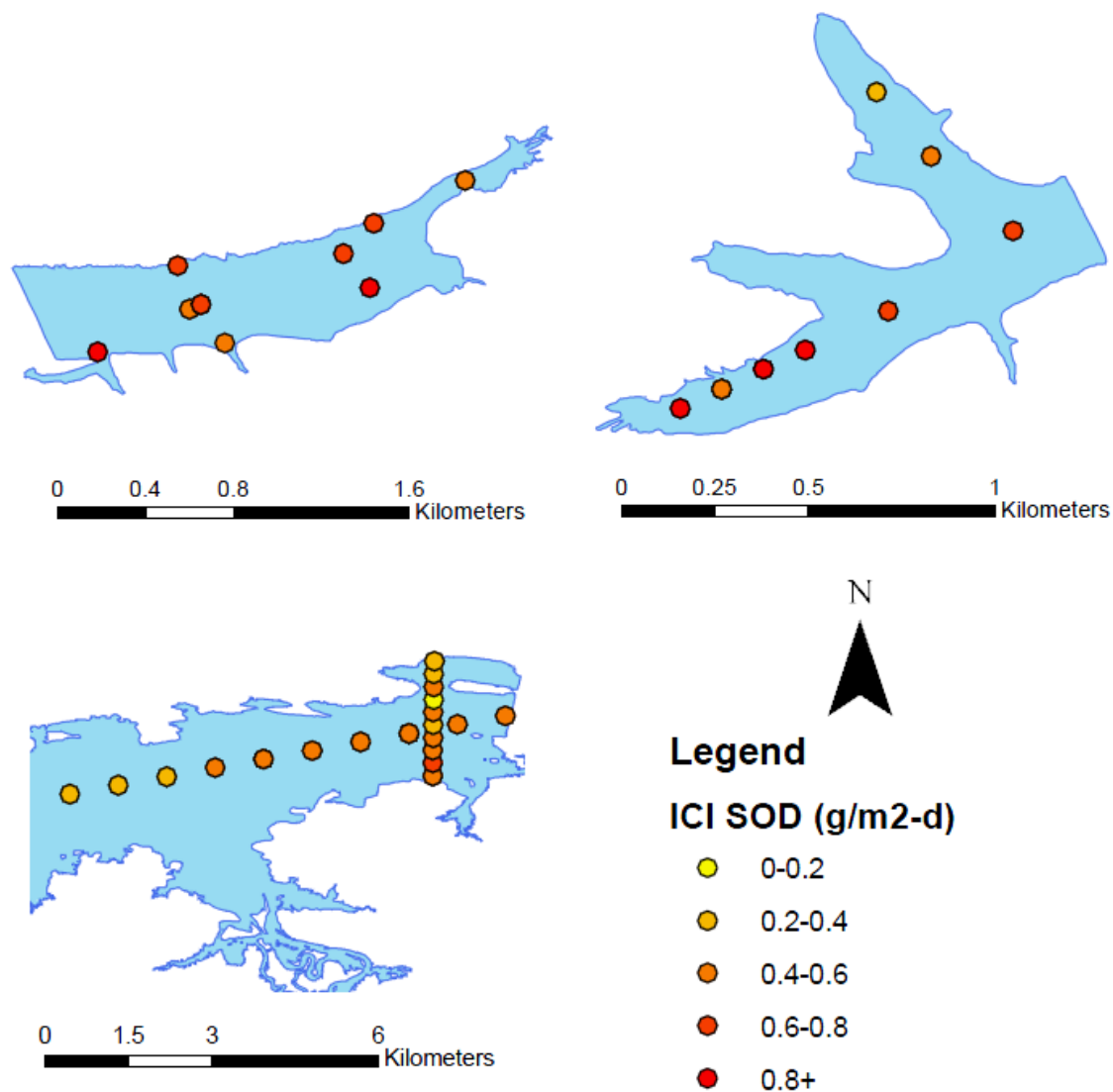
Figure 8: Sample site ICI SOD (g/m^2-d) by location and lake (clockwise from bottom left: Wister, Fayetteville, and Wedington)

Sample location R10 is used in Table 1 to illustrate how ICI SOD was calculated:

Table 1: Sample ICI SOD calculation for location R10

ID	Flow Rate Q (L/h)	O2 $_{Out}$ (mg/L)	O2 $_{In}$ (mg/L)	O2 $_{(out-in)}$ (mg/L)	[O2$_{(out-in)}$*Q]-[O2$_{ctrl}$*Q$_{ctrl}$] (mg/h)	Surface Area (m^2)	Delta O2*Q/SA (mg/m^2-h)	SOD (g/m^2-d)
R10B	0.03988	2.885	6.797	-3.912	-0.1227	0.005221	-23.50	0.5641
Control	0.039	5.943	6.797	-0.854		0.005221		

Overall, ICI SOD ranged from 0.13 to 1.03 $g\text{-}m^{-2}\text{-}d^{-1}$, with an overall mean of 0.55 $g\text{-}m^{-2}\text{-}$ d^{-1}. The overall coefficient of variation (CV) was 36.3 (Table 2). The literature does not appear to contain any previous SOD studies for Lake Fayetteville or Lake Wedington. Previous studies in Lake Wister show a range of measured SOD of 0.23 – 0.66 $g\text{-}m^{-2}\text{-}d^{-1}$, with a mean of 0.47 $g\text{-}$ $m^{-2}\text{-}d^{-1}$ (Haggard et al., 2012; Richardson, 2014). The SOD measured in this study appears to agree with these studies. ANOVA shows previous measurements and those from this study are not statistically different for Lake Wister (α=0.05; p=0.62) (Fig. 9).

Table 2: ICI SOD results from entire study

ICI SOD (g/m2-d)						
Lake	Min	Mean	Max	Lower 95%	Upper 95%	CV %
Fayetteville	0.4421	0.6691	1.035	0.5942	0.7440	25.194
Wedington	0.3837	0.6768	0.9768	0.6038	0.7498	33.047
Wister	0.1297	0.4390	0.6357	0.3903	0.4877	29.137
All	0.1297	0.5477	1.035	0.5042	0.5911	36.56
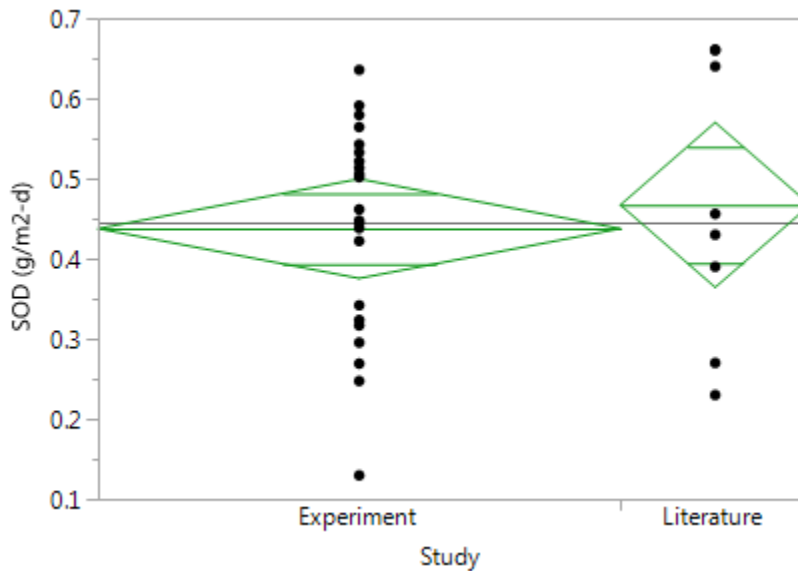
Figure 9: Distribution of experimental (ICI, n=22) and literature values (n=8) for SOD in Lake Wister, with diamond height representing 95% confidence interval around overall mean (center line) and diamond width representing sample size (Haggard et al., 2012; Richardson, 2014). ANOVA p=0.62

Other literature shows freshwater SOD rates from various waterbodies spanning 3 orders of magnitude (fig. 10) and contains all measured values in this study (Charbonnet et. al., 2006; Haggard et. al., 2012; Matlock et. al., 2006; Richardson, 2014; Truax et al., 1995). Thomann and Mueller (1987) state that SOD rates at 20°C should fall between 0.05 - 0.1 $g\text{-}m^{-2}\text{-}d^{-1}$ for mineral soils, 0.2 - 1.0 $g\text{-}m^{-2}\text{-}d^{-1}$ for sandy bottoms, and $1 - 2$ $g\text{-}m^{-2}\text{-}d^{-1}$ for estuarine mud. These data are in range of the data collected in this study. Sediments collected in this study could be described as varying mixtures of organic mud and fine clay or silt. Literature data appears to confirm the validity of the measured ICI values.
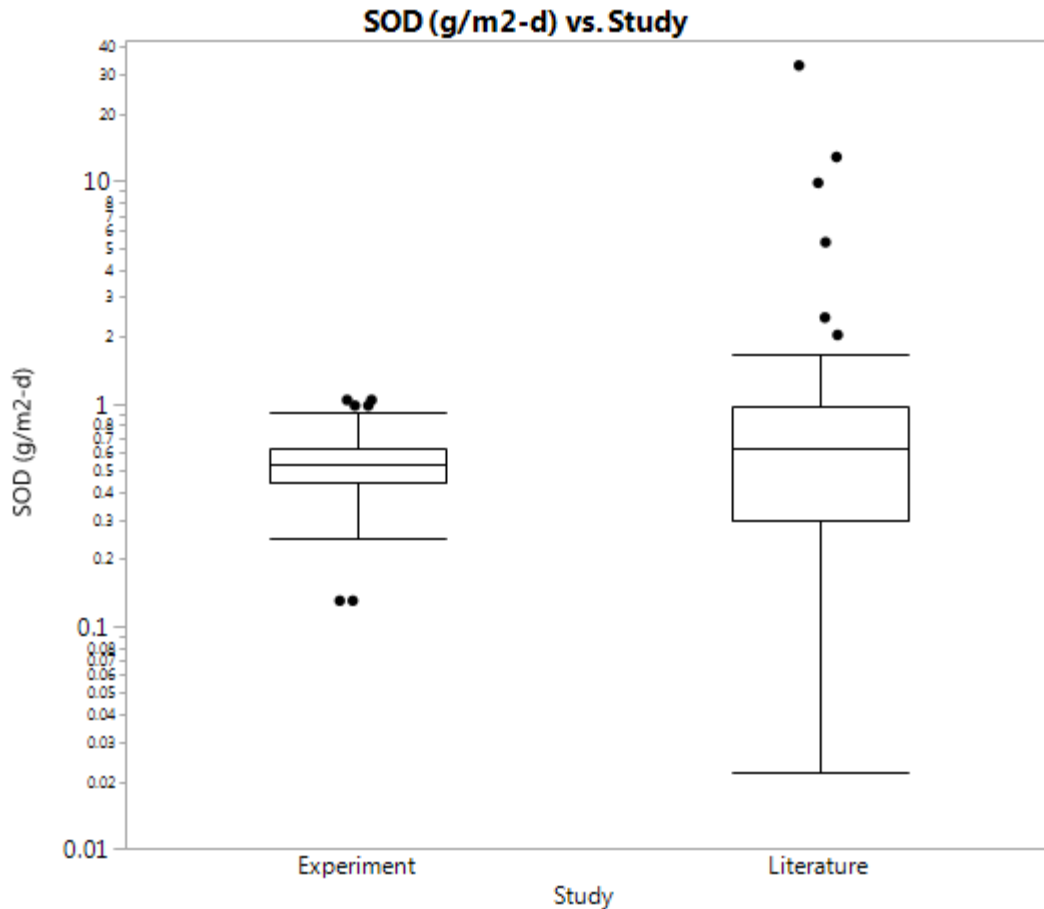
Figure 10: Box plot comparison of study SOD to literature freshwater SOD (g/m2-d) using log-10 scale. Central line in each box plot represents median, outer edges of box represent 25th and 75th quantiles, whiskers represent 1.5 times interquartile range, outside of which data are considered outliers. See Appendix C for detailed literature data (Charbonnet et. al., 2006; Haggard et. al., 2012; Matlock et. al., 2006; Richardson, 2014).

ICI SOD was significantly different between all lakes ($\alpha=0.05$; $p<0.0001$) (Fig. 11), but was not significantly different between lakes Fayetteville and Wedington ($p=0.90$). Lake Wister SOD measured significantly lower than the other lakes. The range of ICI SOD measured in any lake exceeded the difference in mean ICI SOD between any two lakes.
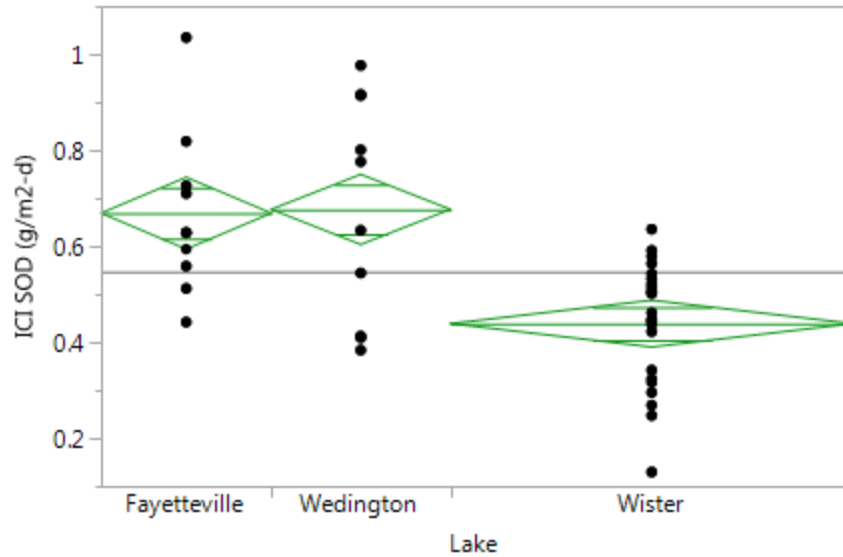
Figure 11: ICI SOD results by lake, with diamond height representing 95% confidence interval around overall mean (center line) and diamond width representing sample size. ANOVA p<0.0001.

Data reveal no significant correlations between lake water depth (shown in Fig. 12) and ICI SOD, evaluated both as a single dataset (α=0.05; p=0.18) and by lake (Fayetteville, p=0.38; Wedington, p=0.87; Wister, p=0.47).
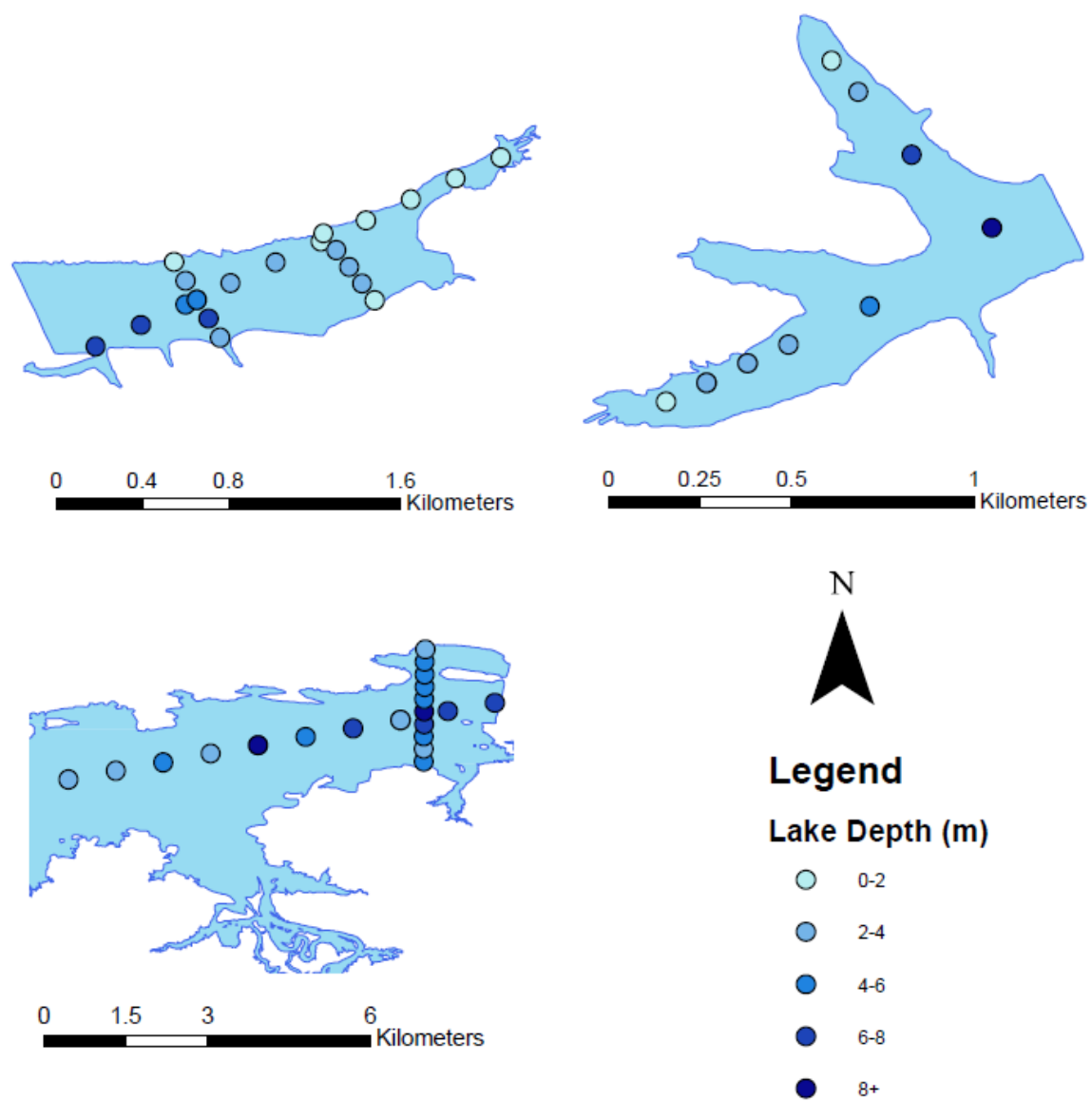
Figure 12: Sample site depth (m) by location and lake (Clockwise from bottom left: Wister, Fayetteville, and Wedington)

4.2 Measure-Calculate Lake SOD

4.2.1 $\dot{N}_{sed}$

Previous studies (Richardson, 2014; Charbonnet, 2003) used linear regressions of DO versus time curves to arrive at $\dot{N}_{sed}$. The curves obtained in this study did not lend themselves to linear regressions over the full time range measured. Further investigation revealed that the previous studies' published data, and that used in their linear regressions, were only for selected portions of the measured time curves. The complete curves (examples given in Fig. 13) resembled those collected in this study.
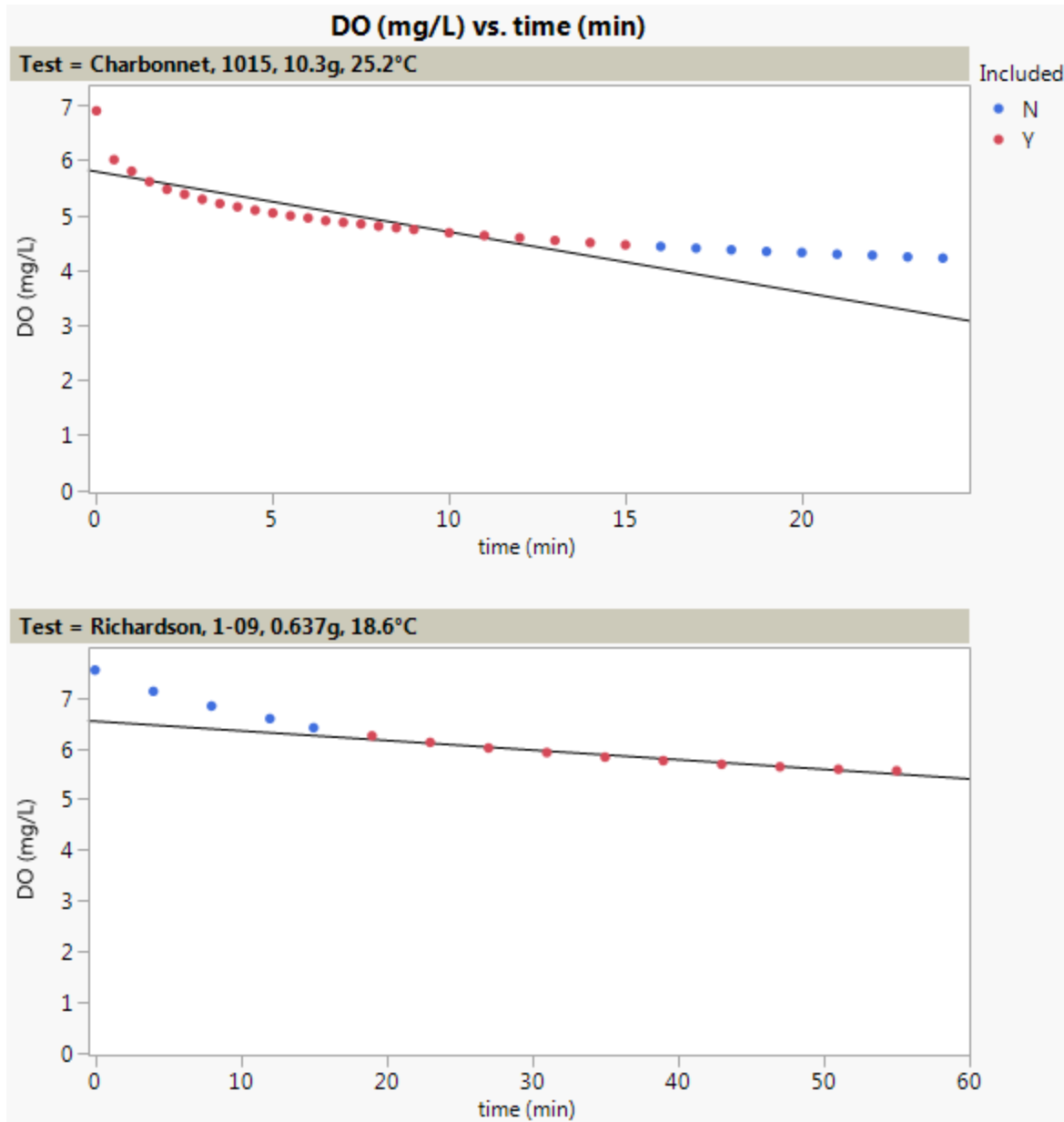
Figure 13: DO vs. time curves from Charbonnet (2003 and unpublished, top) and Richardson (2014 and unpublished, bottom), with their linear regressions shown (black) through published data (red) and unpublished data (blue). R^2=0.74 and 0.97 respectively, based on only the included published data.

Because the data curves are non-linear, linear regressions may misrepresent part of the

data. Non-linear regressions contain a multitude of slopes, and thus a multitude of potential $\dot{N}_{sed}$

values. These problems were remedied as follows. Because the M-C method is built on a steady

state solution to Fick's Law ($\frac{\partial SOD}{dt} \approx 0$), it is reasonable that the method would perform best

using the steady state $\dot{N}_{sed}$ ($\frac{\partial \ddot{N}sed}{dt} \approx 0$) rather than the initial, much greater $\dot{N}_{sed}$. Fast, initial

oxygen uptake was likely due to chemical consumption (such as oxidation of reduced metals in

anaerobic sediment suddenly exposed to oxygen), as it could be accounted for using multiple

first order terms. Many different regression formulae were tested to approximate the DO-time

curves, but equation (8) was chosen due to its ability to achieve R^{2s} of 0.999+ for the entire

dataset, and its inclusion of both first order terms (presumed to represent concentration-

dependent chemical demand) and linear terms (presumed to represent metabolically-regulated

biological demand). According to Equation 8, $\dot{N}_{sed}$ estimated at DO concentrations of 7, 4, and

2mg/L ($\dot{N}_{sed}7$, $\dot{N}_{sed}4$, $\dot{N}_{sed}2$) decreased expectedly. However, this raised the question: did the $\dot{N}_{sed}$

test run for a sufficient length of time to allow a steady state assumption to be made? A follow

up experiment was conducted to address this question.

After the $\dot{N}_{sed}$ stirring test would normally be finished (0.50 mg/L or 45 min), the

suspended sediment was re-aerated using a clean aquarium air stone for 5-10 minutes to near

saturation, then the experiment repeated for a total of three runs. In each of four replications

shown in Figures 14 and 15, it was shown that $\dot{N}_{sed}$ decreased over time then appeared to flatten

out to a very nearly linear rate of consumption, such that Equation 8, fitted using only data from

the initial run before re-aeration (to represent previously collected study data for DO versus

time), was able to predict experimental steady state $\dot{N}_{sed}$ within a factor of 2. Therefore, Equation

8 was used to determine the steady state slope of the DO versus time data (and thus $\dot{N}_{sed}$) for the

study data even if the test did not reach a constant slope and the extrapolated portion of the DO

versus time curve was used. This result has implications for future testing procedures for

determining accurate steady state values for $\dot{N}_{sed}$ including the length of time for testing and the

relative amount of sediment used in each test.
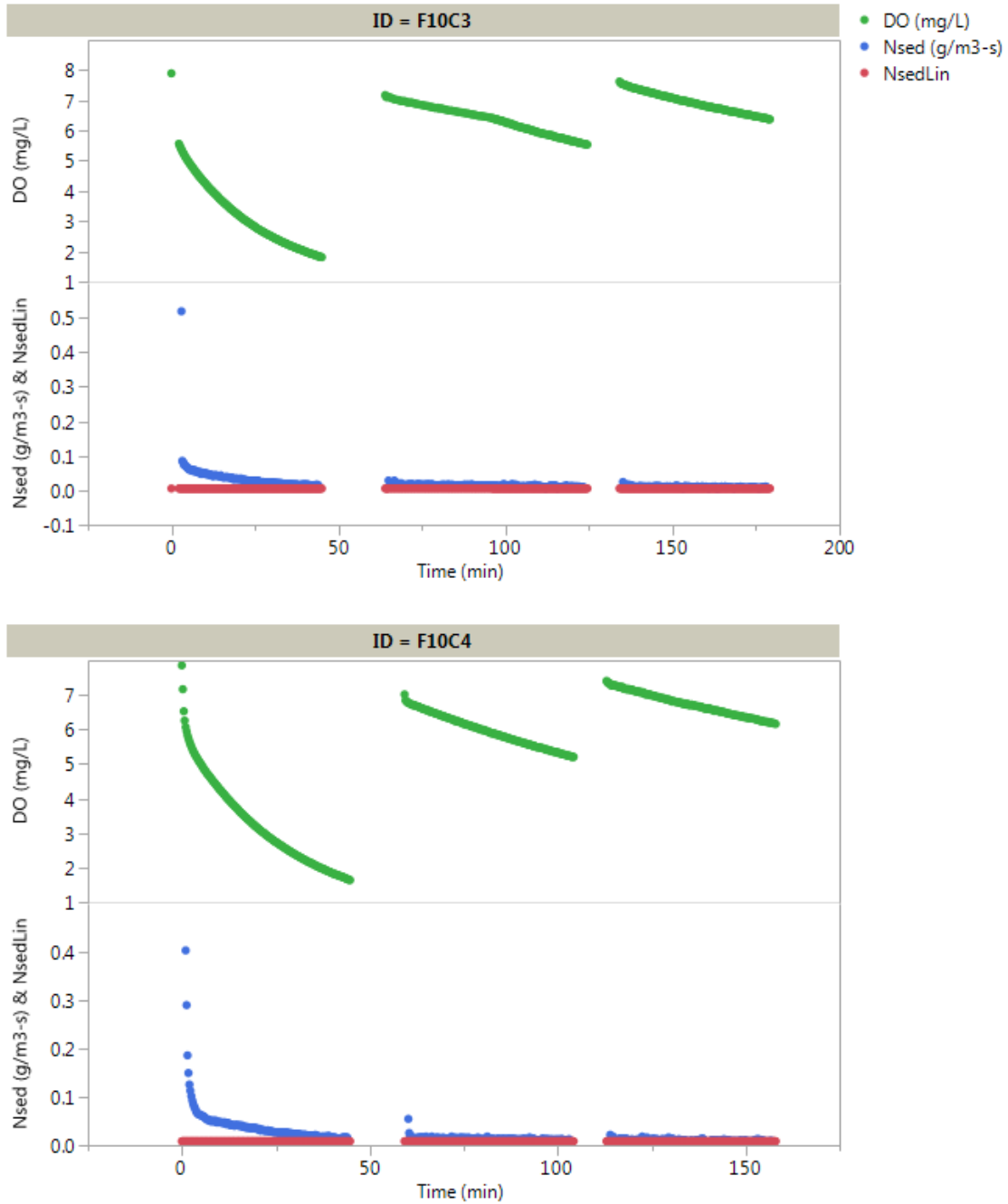
Figure 14: Extended experimental graph of DO (mg/L, green), instantaneous $\dot{N}_{sed}$ (g-m^{-3}-s^{-1}, blue), and linear $\dot{N}_{sed}$ from equation (8), (g-m^{-3}-s^{-1}red) vs. time (s) for runs F10C3 and F10C4.
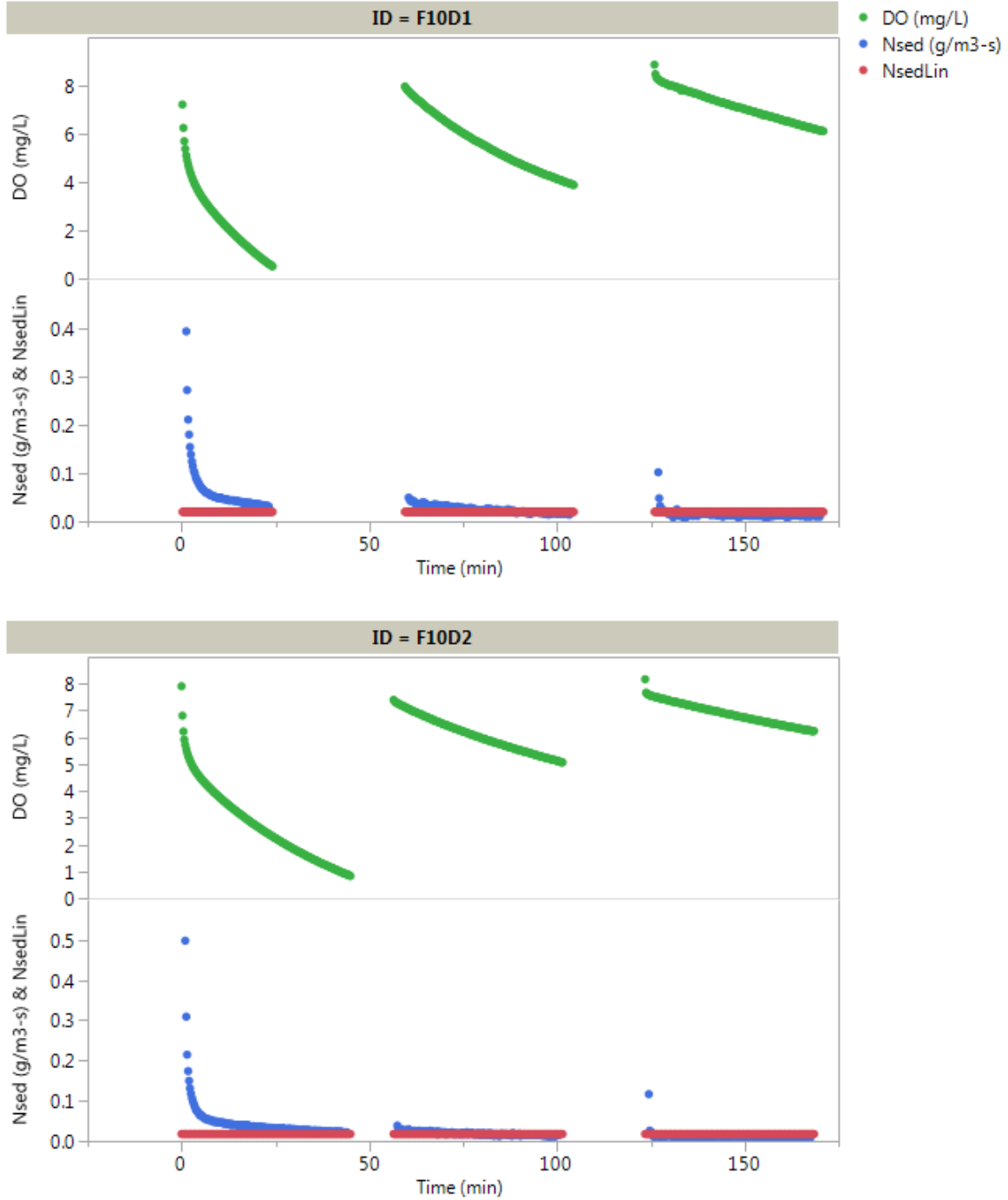
Figure 15: Extended experimental graph of time (s) vs. DO (mg/L, green), instantaneous $\dot{N}_{sed}$ (g-m^{-3}-s^{-1}, blue), and linear $\dot{N}_{sed}$ from equation (8), (g-m^{-3}-s^{-1} red) for runs F10D1 and F10D2.

Figures 16 and Table 3 show sample calculations for $\dot{N}_{sed}$. It should be noted that the regression can only be fitted properly if given reasonably close parameter estimate guesses (in this work: 2.5, -0.001, 2.5, -0.001, 2.5, -0.01 were used for a, b, c, d, e, and f respectively). It should also be noted that the first datapoint (t=0s) in the DO versus time dataset was sometimes excluded, as the DO analyzer may either have been still un-equilibrated in the test water or the DO had already dropped below the measured initial reading by the time the analyzer started logging. It is more important that the regression fit the end of the data rather than the beginning. The parameter estimates for b were then used in equation (7) to arrive at uncorrected $\dot{N}_{sed}$, which was then temperature corrected using equation (10) to arrive at $\dot{N}_{sed}$.
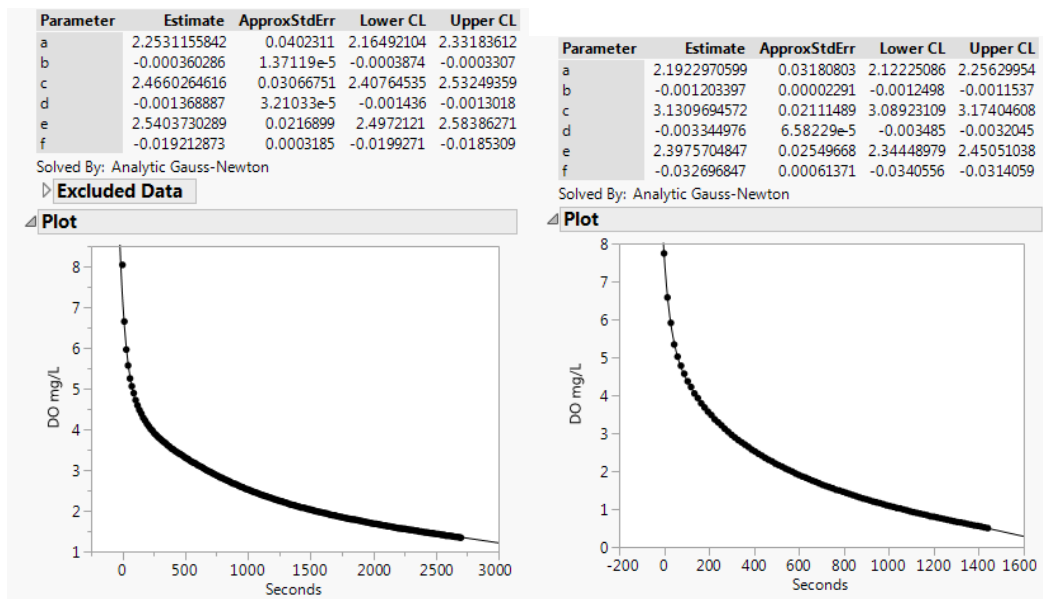
Figure 16: Graphs of DO (mg/L) vs. time (seconds) for runs F14AB (left) and R11BB (right), with 6-parameter regressions (black lines) fitted to data points. The t=0s datapoint was excluded from run F14AB to improve overall fit.

Table 3: Sample inputs and calculations required for $\dot{N}_{sed}$ for runs F14AB and R11BB.

Run	b (mg/L-s)	density (g/cm3)	wet sed (g)	Test Vol (L)	Uncorr. Nsed (g/m3-s)	Avg Test Temp (°C)	Corrected Nsed (g/m3-s)
F14AB	-0.0003603	1.254	7.48	0.3	0.01812	20.67	0.01907
R11BB	-0.0012034	1.207	6.71	0.3	0.06495	20.91	0.06964

$\dot{N}_{sed}$ data was determined twice from one core of every sample pair collected, with the exception of one duplicate run of sample F20, which did not produce results for $\dot{N}_{sed}$ as the sediment mass was not recorded. $\dot{N}_{sed}$ (data is shown in Table 4 and Fig. 17) ranged from 0.0069 to 0.1911 g/m^3-s, with an overall mean of 0.0534 g-m^{-3}-s^{-1}. The CV was 58.5, which was more than 50% greater than that of ICI SOD. $\dot{N}_{sed}$ was significantly different between lakes (α=0.05; p<0.0001) (Fig. 18). In contrast to ICI SOD, Lake Wister had the highest $\dot{N}_{sed}$, with Lake Wedington following and Lake Fayetteville with the lowest.

Table 4: $\dot{N}_{sed}$ (g-m^{-3}-s^{-1}) results from each lake and the entire dataset

Nsed (g-m^{-3}-s^{-1})				
Lake	Min	Mean	Max	CV (%)
Fayetteville	0.0149	0.0303	0.0716	48.58
Wedington	0.0194	0.0485	0.1223	59.02
Wister	0.0069	0.0721	0.1911	45.14
All	0.0069	0.0570	0.1911	58.17
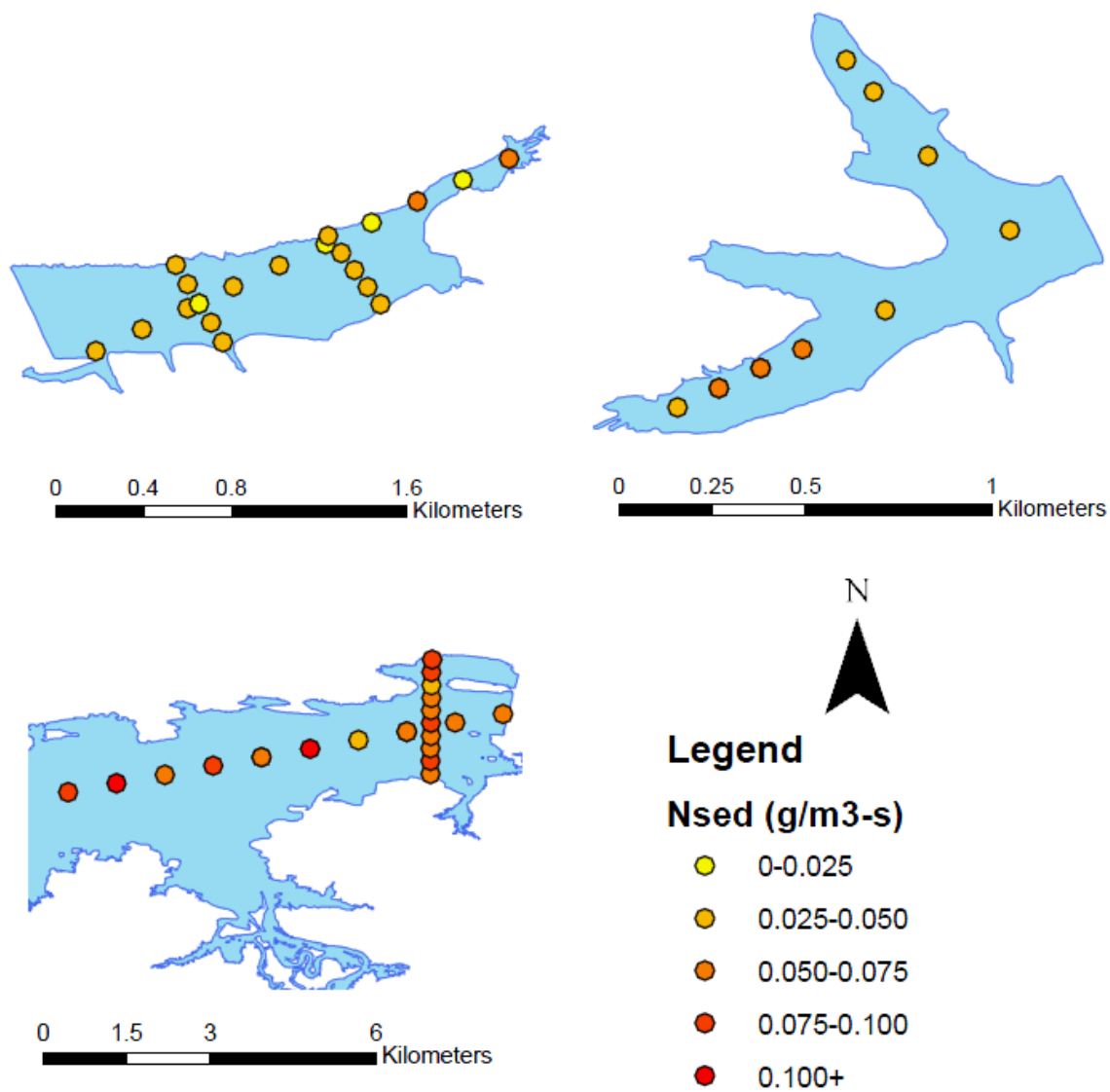
Figure 17: $\dot{N}_{sed}$ (g-m^{-3}-s^{-1}.) by location and lake (clockwise from bottom left: Wister, Fayetteville, and Wedington)
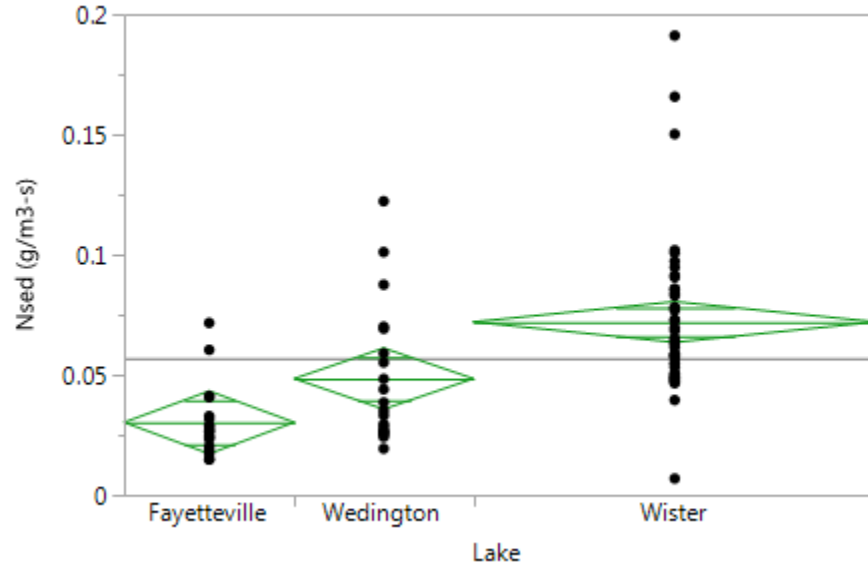
Figure 18: $\dot{N}_{sed}$ compared between lakes, with diamond height representing 95% confidence interval around overall mean (center line) and diamond width representing sample size. ANOVA p<0.0001.

A small number of previous studies show a range of measured and proposed $\dot{N}_{sed}$ values

that spans 3 orders of magnitude and contains all measured values in this study (Fig. 19)

(Charbonnet et. al., 2006; Higashino and Gantzer, 2004; Matlock et. al., 2003; Richardson,

2014). ANOVA shows values from this study are not significantly different than literature values

($\alpha=0.05$; p=0.70). When compared to $\dot{N}_{sed}$ values from a previous study on Lake Wister

(Richardson, unpublished), values from this study are significantly lower than the values

reported by Richardson (p<0.0001), but the ranges do overlap (see Fig. 20). This is likely due to

previously discussed differences in calculation methods to determine the DO versus time slope.

Overall mean $\dot{N}_{sed}$ in this study (0.053 g-m^{-3}-s^{-1}) falls between the average measured

consumption of two studies of the Arroyo Colorado stream: 0.166 g-m^{-3}-s^{-1} (Charbonnet et. al.,

2006) and 0.008 g-m^{-3}-s^{-1} (Matlock et. al., 2003).

50
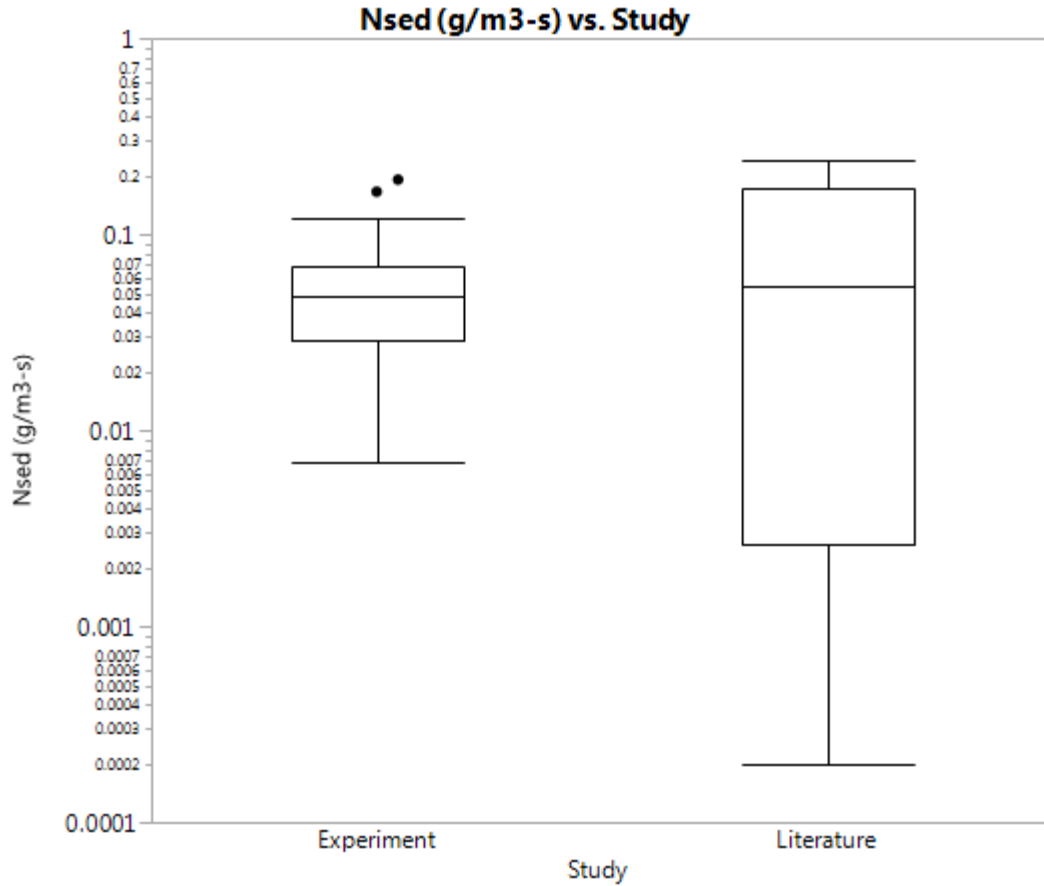
Figure 19: Box plot comparison of study $\dot{N}_{sed}$ to literature $\dot{N}_{sed}$ (g/m^3-s). Central line in each box plot represents median, outer edges of box represent 25th and 75th quantiles, whiskers represent 1.5 times interquartile range, outside of which are considered outliers. (Charbonnet et. al., 2006; Higashino and Gantzer, 2004; Matlock et. al., 2003; Richardson, unpublished)

51
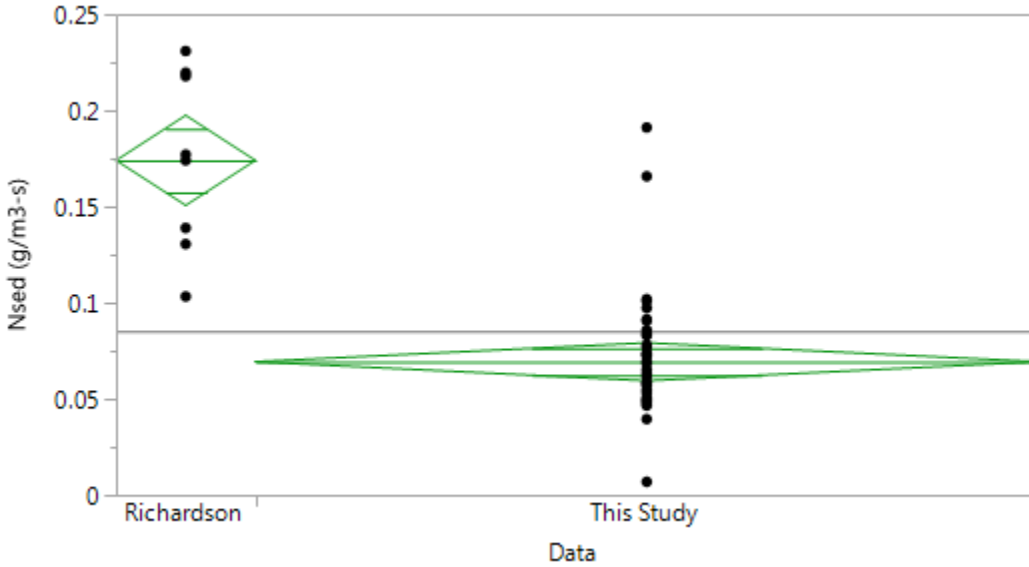
Figure 20: Lake Wister $\dot{N}_{sed}$ results compared with literature values, also from Lake Wister (Richardson, unpublished), with diamonds representing 95% confidence interval around overall mean (center line). ANOVA p<0.0001.

Data reveal no significant correlations between $\dot{N}_{sed}$ and lake depth at sample site (α=0.05; p=0.72), and there appear to be no visible geographic patterns related to $\dot{N}_{sed}$ variation (fig. 17). A multiple linear regression model of $\dot{N}sed$ using water depth, Latitude, Longitude, and Latitude*Longitude was performed for each lake. The only significant parameter estimate was Latitude*Longitude at Lake Wedington. $\dot{N}_{sed}$ was geographically distributed with higher values in the Southwest reach of the lake, but an explanation is not immediately obvious. It is possible that $\dot{N}_{sed}$ variation is inherent or is random error attributable to the testing method.

4.2.2 Density, Moisture Content, and P_{sed}

Physical sediment properties are summarized in Table 5. Sediment density for all data was between 1.02 and 1.37 g-cm^{-3}. Density was significantly different between lakes, with overlapping ranges (α=0.05; p=0.001; fig 21). Sediment density is mapped in Fig. 22. Richardson (unpublished data) reported sediment densities of 1.20 and 1.06 g-cm^{-3} in Lake Wister. Density correlated negatively with depth (p<0.0001 for the entire dataset, Lake Fayetteville, and Lake Wedington; p=0.004 for Lake Wister), with deeper water generally producing less dense sediments (Fig. 23).

Table 5: Summary of physical sediment properties

Lake	Density (g-cm^{-3})			Moisture Content (%)			P_{sed} (cm^3-cm^{-3})			
	Min	Mean	Max	Min	Mean	Max	Min	Mean	Max	CV%
Fayetteville	1.095	1.209	1.323	57.4%	71.1%	83.5%	0.759	0.851	0.932	7.11
Wedington	1.02	1.123	1.21	66.5%	79.5%	93.2%	0.802	0.886	0.954	5.42
Wister	1.088	1.187	1.37	48.0%	71.2%	81.8%	0.538	0.843	0.895	8.66
All	1.02	1.177	1.37	48.0%	73.2%	93.2%	0.538	0.855	0.954	7.81
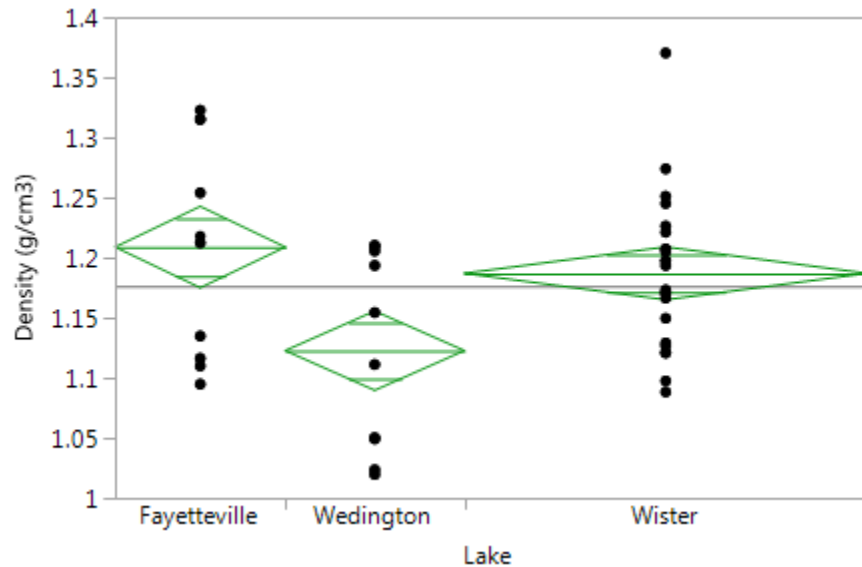
Figure 21: Sediment density results compared between lakes, with diamonds representing 95% confidence interval around overall mean (center line). ANOVA p=0.001.
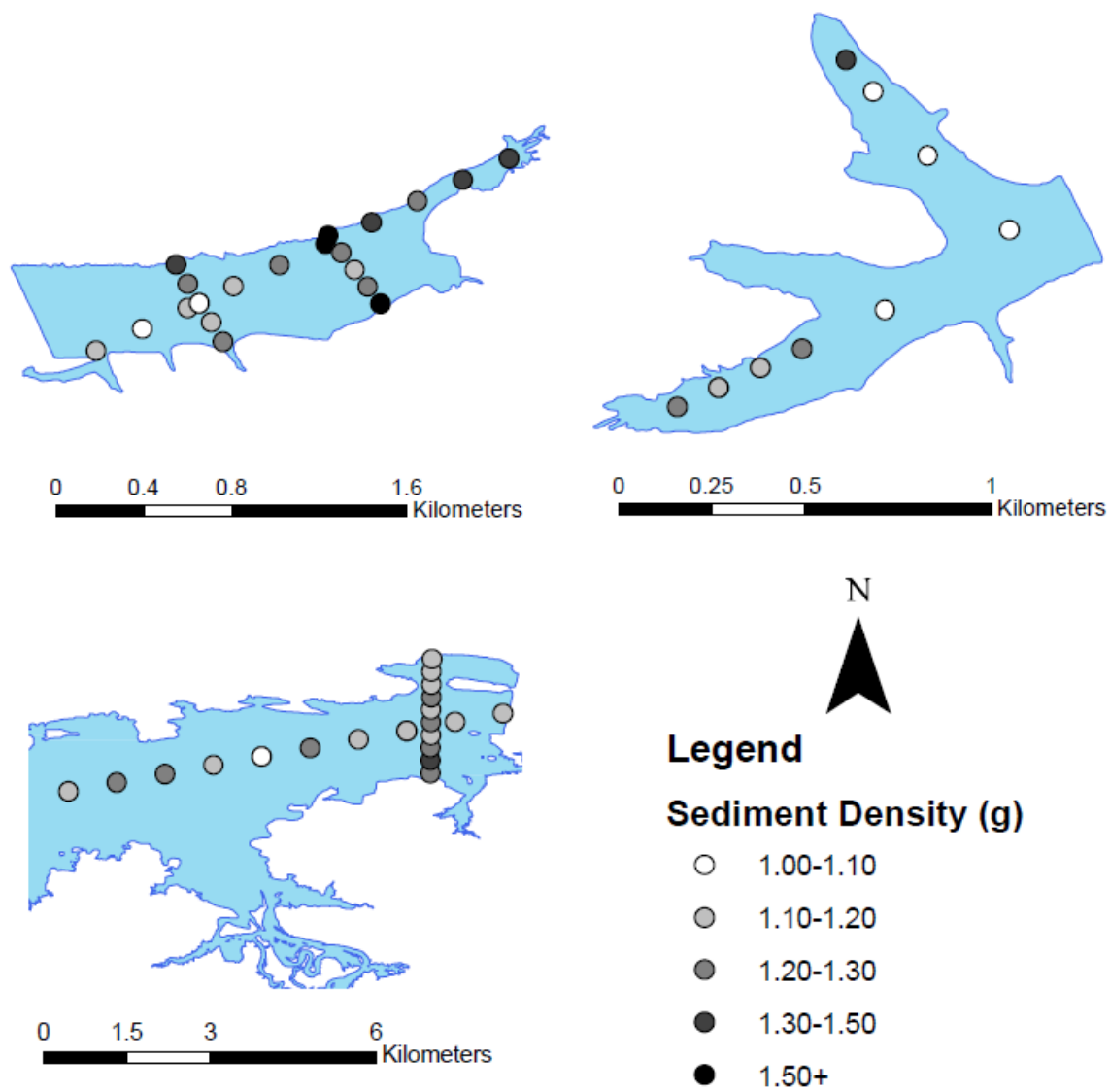
Figure 22: Sample site density (g-cm^{-3}) by location and lake (clockwise from bottom left: Wister, Fayetteville, and Wedington)
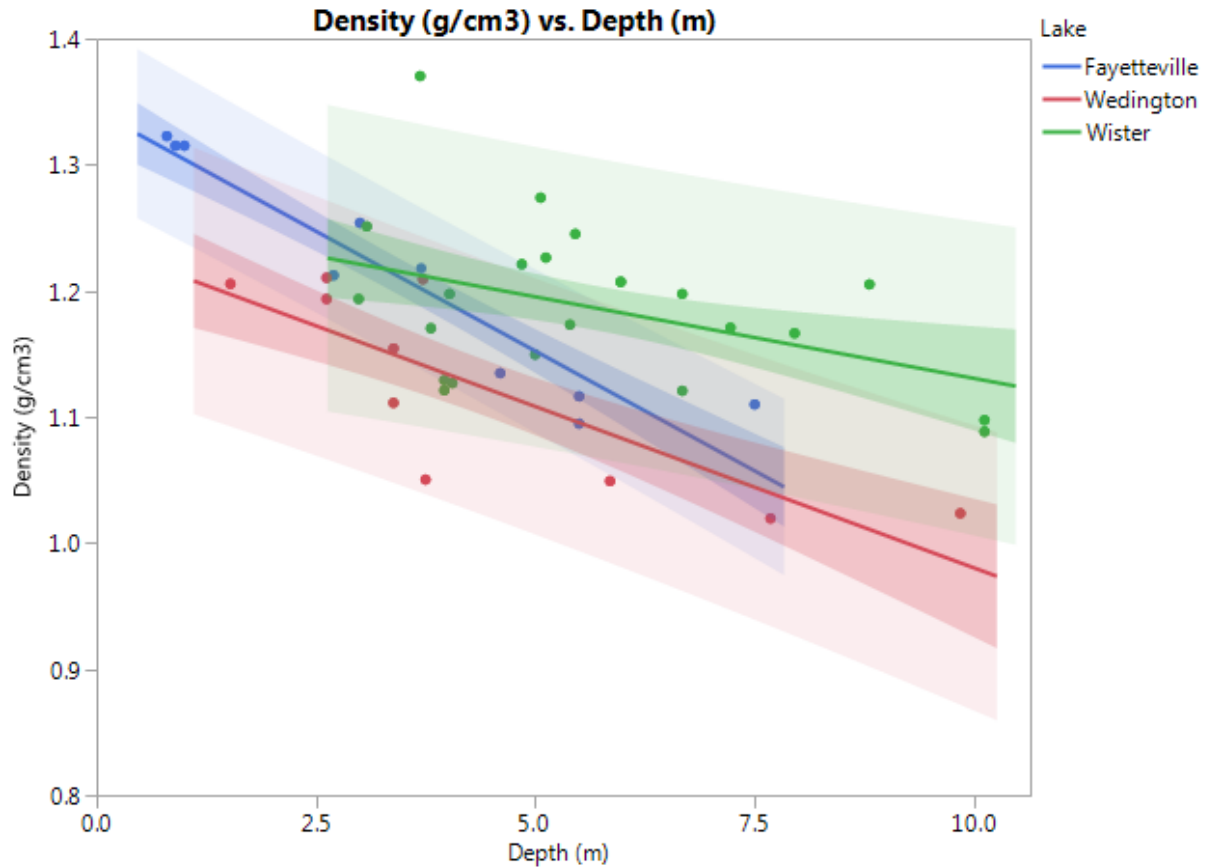
Figure 23: Graph of sediment density (g-cm^{-3}) vs. depth (m) by lake, with CIs of means and predictions. ANOVA p<0.0001 for whole dataset, Lake Fayetteville, and Lake Wedington; p=0.004 for Lake Wister.

Sediment moisture content fell between 48 and 93% water by weight. Richardson (unpublished data) reported moisture contents between 22.5 and 95.9% water by weight in Lake Wister. Moisture content correlated significantly and negatively with density, as expected (α=0.05; p<0.0001; fig. 24). Because of the high correlation (RMSE=0.05), density may be an estimator of moisture content or vice versa.
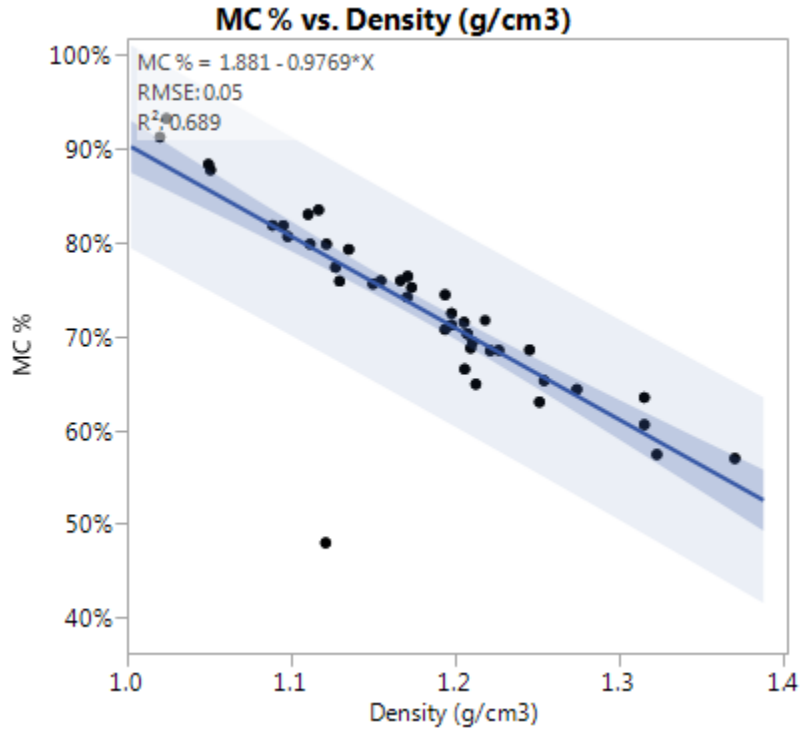
Figure 24: Graph of MC% vs. density (g-cm^{-3}) with CIs of means and predictions. ANOVA p<0.0001.

P_{sed} is the product of sediment density and moisture content (divided by water density), and is used as an input in the M-C method. Study values ranged from 0.538 to 0.945 g-cm^{-3}, and were significantly different between lakes by a small margin ($\alpha=0.05$; p=0.047) (Fig. 25). Variability (CV) was lower than either $\dot{N}_{sed}$ or ICI SOD.
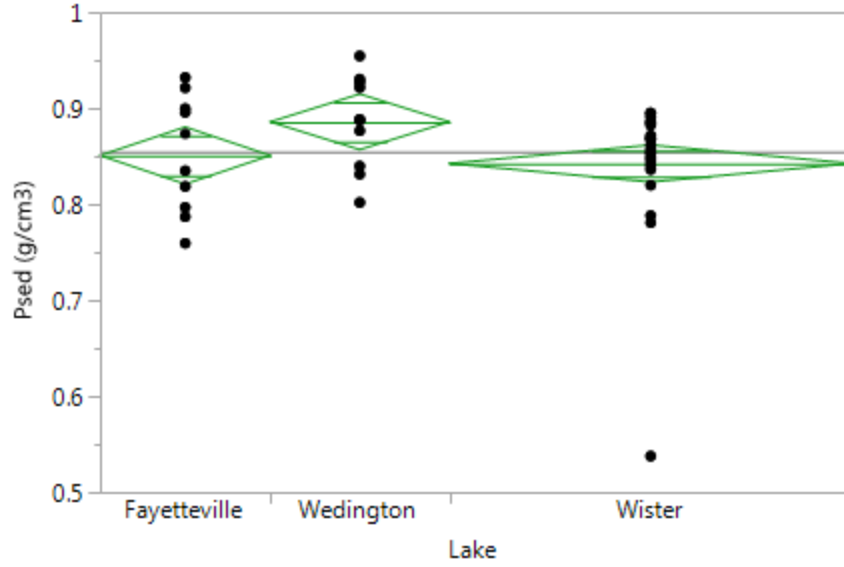
Figure 25: P$_{sed}$ results compared between lakes, with diamonds representing 95% confidence interval around overall mean (center line). ANOVA p=0.047.

A comparable parameter to P$_{sed}$ using the same inputs can be used to compare data to literature values. A study compiling dry bulk density values (g$_{dry\ sed}$-cm^{-3}$_{wet\ sed}$) from freshwater lakes worldwide showed a spread from 0.1 to 1.8 g-cm^{-3} (Avnimelech et al., 2001). Dry bulk density (DBD) can be calculated from study data as follows:

$$DBD = (1 - MC) * \rho_{sed} \tag{20}$$

Values from this study converted to DBD fell between 0.069 and 0.590 g$_{dry\ sed}$- cm^{-3}$_{wet\ sed}$, which were on the lower end of the worldwide study. Low DBD equates to high porosity, meaning the sediments from this study had a relatively high amount of pore water through which oxygen could be transferred.

4.2.3 Calculated Parameters Required for M-C Model

Necessary model inputs were calculated as discussed in section 3.7 at 20°C. Mass transfer convection coefficient results are shown in Appendix A, Tables 11 and 12.

57

4.2.4 M-C SOD

M-C SOD was calculated according to Section 3.7, as illustrated in the following sample

calculations for finding the h_m used in the middle range simulated lake conditions:

Table 6: Sample calculation for h_m under mid-range lake conditions

Pr	kw (W-m^{-1}-K^{-1})	μ (Pa-s)	ρ (kg-m^{-3})	Hd (m)	cp (kJ-kg^{-1}-K^{-1})	α (m^2-s^{-1})	v (m-s^{-1})	Re	hm LAKE mid (m-s^{-1})
7.01	0.5984	0.001	998.3	1.818	4182	1.49E-07	0.02	36302	1.199E-06

Table 7: Sample M-C SOD calculation inputs and output for sample location R10, run R10AA

ID	DO2s (m^2-s^{-1})	Psed (m^3-m^{-3})	Nsed (g-m^{-3}-s^{-1})	DO (mg/L)	hm Lake MID (m/s)	M-C SOD Lake MID (g/m^{2}s)	M-C SOD Lake MID (g/m^{2}d)
R10AA	1.26E-09	0.5377	0.07253	5.5	1.199E-06	6.137E-06	0.5302

Modeled SOD ranged from 0.0005 to 1.55 g-m^{-2}-d^{-1} using reasonable literature values to

model conditions of minimum [v=0.00001 m-s^{-1}, DO=2.0 mg-L^{-1}] and maximum consumption

[v=0.05 m-s^{-1}, DO= 9.09 mg-L^{-1}], respectively (Table 8). Minimum, median and maximum

water flow rate and DO conditions were assumed to likely occur at some point in time because of

seasonal changes within the three study lakes. The minimum values represent the condition when

SOD is likely to be low: bottom velocity is very nearly zero and the overlying water is borderline

hypoxic (likely in summer with no wind driven currents), while the maximum conditions

represent when SOD is likely to be high: oxygen saturated water and a moderately high lake

bottom velocity (likely in cooler weather during wind events or during thermally driven

turnover), based on two studies (Horn, et. al., 1986; Gloor, et. al., 1994). Gloor et. al. reported an

overall average bottom velocity to be 2 cm-s^{-1} in a Swiss lake, which was used to model mid-

level consumption. It was found that using this velocity and a mid-level DO of 5.5 mg-L^{-1}, the

M-C method achieved a mean model SOD statistically similar to the observed mean SOD

determined by ICI (p=0.77), with a CV of 3 %, compared to 36% CV for ICI SOD. All temperatures in model simulations were held at 20°C so valid comparisons could be made between M-C assumed temperatures and the temperature at which the ICI method was conducted.

Table 8: M-C SOD results using simulated lake inputs for flow velocity and DO.

Lake	M-C SOD Lake (g-m^{-2}-d^{-1})								
	MIN (2 mg-L^{-1}, 0.00001 m-s^{-1})			MID (5.5 mg-L^{-1}, 0.02 m-s^{-1})			MAX (9.09 mg-L^{-1}, 0.05 m-s^{-1})		
	Min	Mean	Max	Min	Mean	Max	Min	Mean	Max
Fay.	0.0046	0.0046	0.0046	0.4993	0.5266	0.5518	1.0204	1.1627	1.3208
Wed.	0.0046	0.0046	0.0046	0.5221	0.5415	0.5607	1.1314	1.2533	1.3946
Wis.	0.0046	0.0046	0.0046	0.4588	0.5488	0.5633	0.864	1.3063	1.4181
All	0.0046	0.0046	0.0046	0.4588	0.5421	0.5633	0.864	1.2612	1.4181

The M-C method bracketed observed SOD data from the ICI method (Fig. 26). Because model inputs for velocity, temperature, and DO are mathematically held constant, all variation in M-C SOD within each condition group is attributable to differences in measured P_{sed} and $\dot{N}_{sed}$. Results reveal that at minimum conditions, the CV is very low for predicted SOD, indicating that the variability in measured parameters P_{sed} and $\dot{N}_{sed}$ does not translate to variability of SOD, meaning P_{sed} and $\dot{N}_{sed}$ have a minimal effect on predicted SOD at minimum conditions. The CV increases for middle range values and increases further for maximum conditions, indicating that as water velocity and DO increase, the measured inputs have a greater effect on SOD variation.
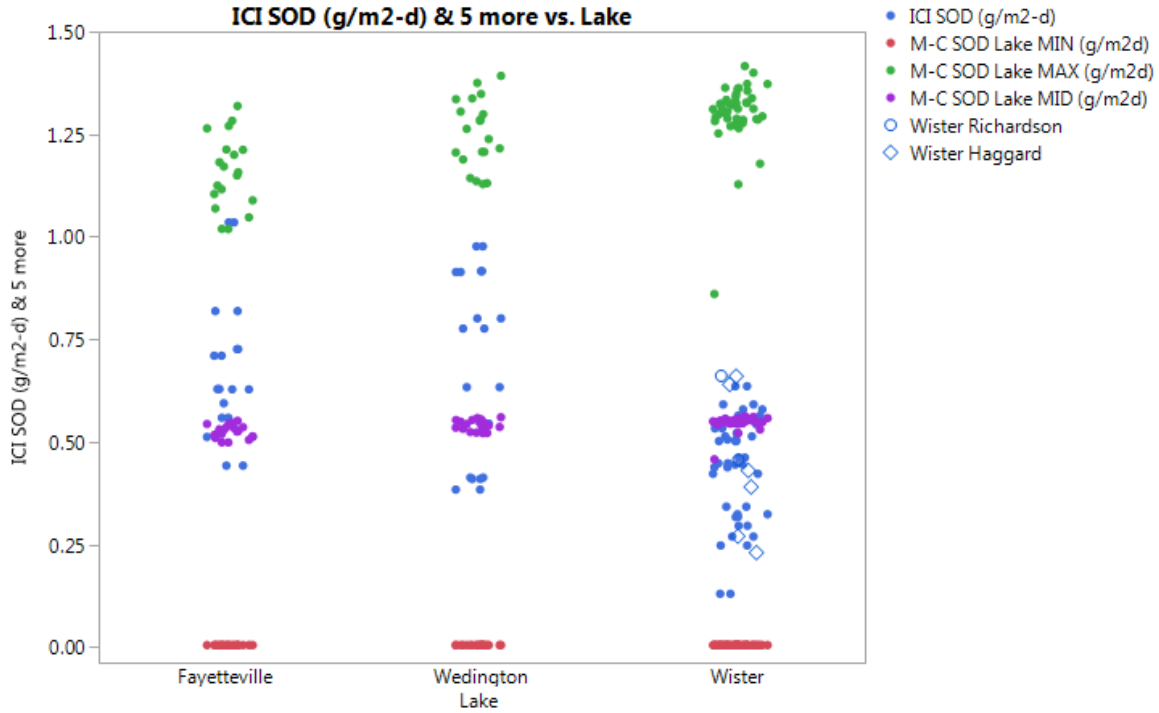
Figure 26: Graph of ICI (blue) vs. M-C SOD by longitude and lake under simulated minimum (red), median (purple), and maximum (green) mass transfer conditions. Previous research data for Lake Wister is included using open markers.

M-C SOD varied significantly between lakes (α=0.05; p<0.0001) under all three conditions, despite the seemingly negligible variation (CV=0.0008%) under minimum conditions. Lake Wister showed the highest M-C SOD (Fig. 26), in direct relation with having the highest $\dot{N}_{sed}$ despite having the lowest observed ICI SOD.
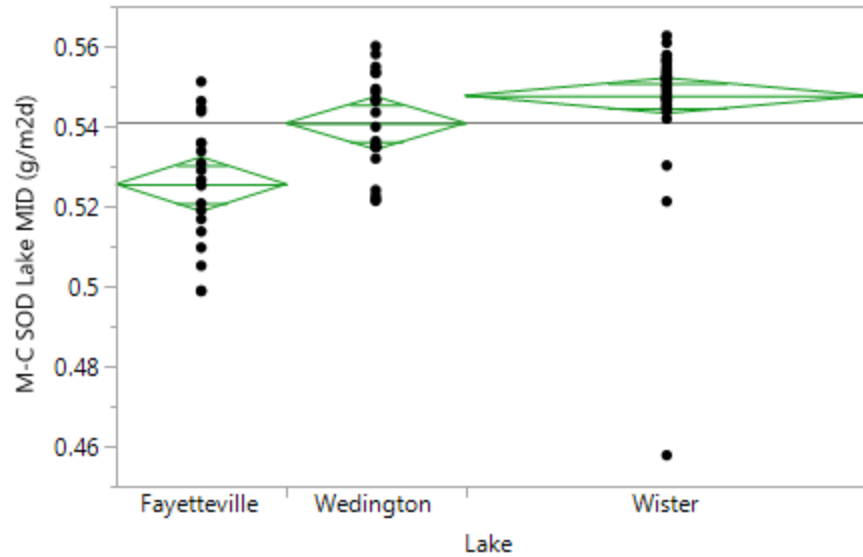
Figure 27: M-C SOD results under mid-range lake conditions compared between lakes, with diamonds representing 95% confidence interval around mean (center line). ANOVA p<0.0001

4.2.5 Relative Sensitivity Analysis

A sensitivity analysis was performed according to the procedure of Haan (2002) (Section 3.8) at each simulated lake condition for water velocity, free stream DO, P_{sed}, and $\dot{N}_{sed}$. Relative sensitivity (S_r) calculates the ratio of percent change in output to percent change in input, and is useful in comparing the sensitivity of inputs whose units differ. Analysis was performed using the minimum, median, and maximum conditions for water velocity and free stream DO, and values for P_{sed} and $\dot{N}_{sed}$ averaged from the entire dataset. All values were held constant except the input that was varied to show the response in relative sensitivity. The results showed relatively low sensitivity to P_{sed} (Fig. 28) and $\dot{N}_{sed}$ (Fig. 29), and high sensitivity to DO (Fig. 30) and velocity (Fig. 31), especially when these inputs are low (and therefore limiting).

61
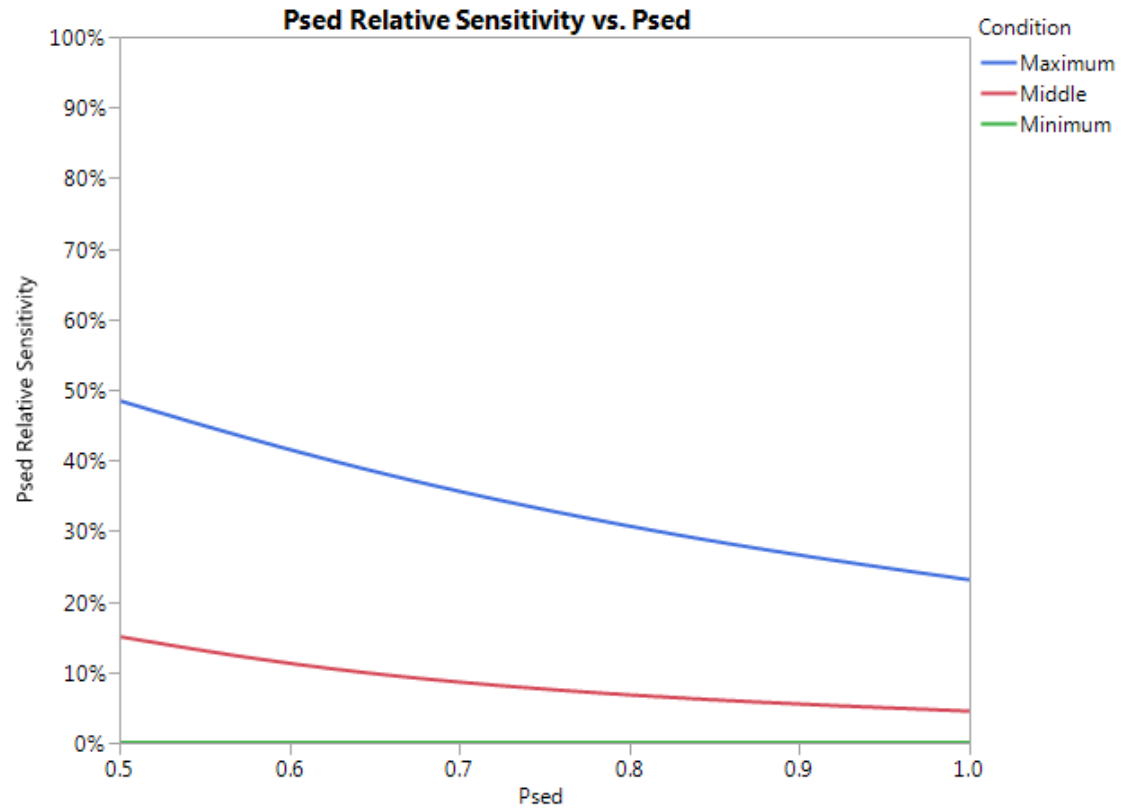
Figure 28: Graph of the M-C method's relative sensitivity to P_{sed} under simulated minimum (green), median (red), and maximum (blue) mass transfer conditions.
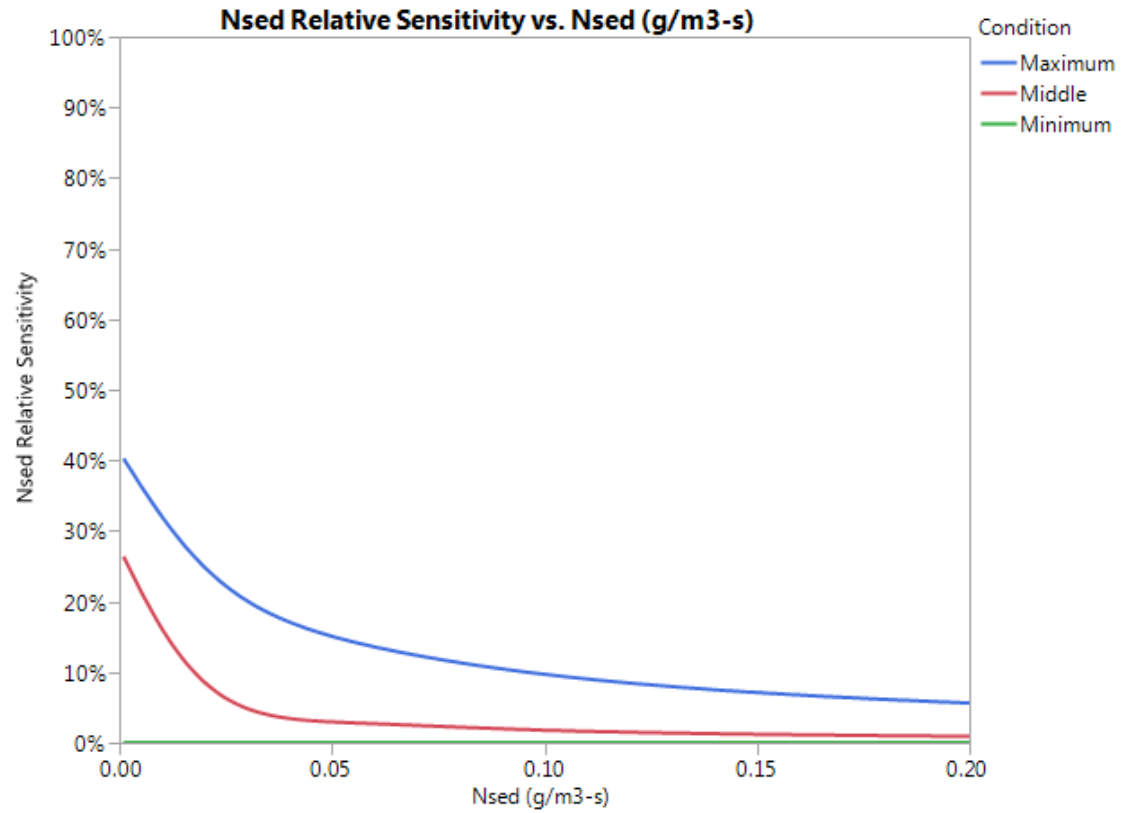
Figure 29: Graph of the M-C method's relative sensitivity to $\dot{N}_{sed}$ under simulated minimum (green), median (red), and maximum (blue) mass transfer conditions.
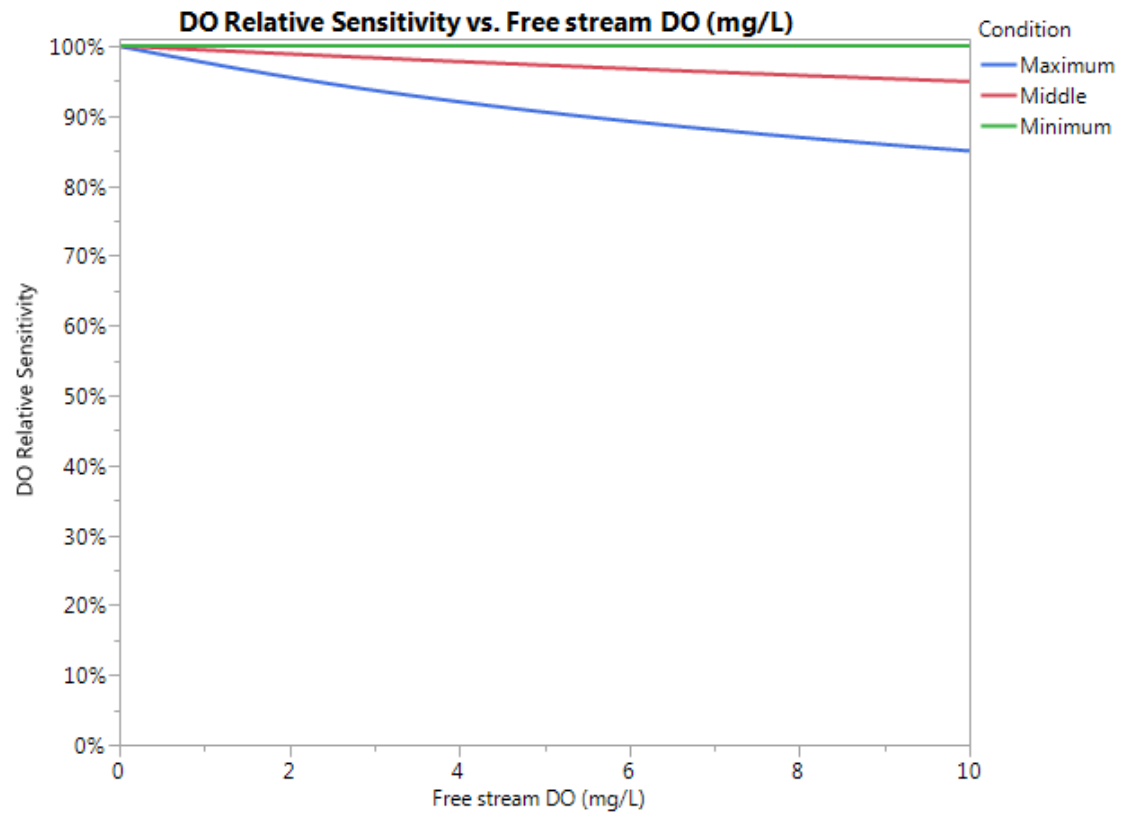
Figure 30: Graph of the M-C method's relative sensitivity to free stream DO under simulated minimum (green), median (red), and maximum (blue) mass transfer conditions.
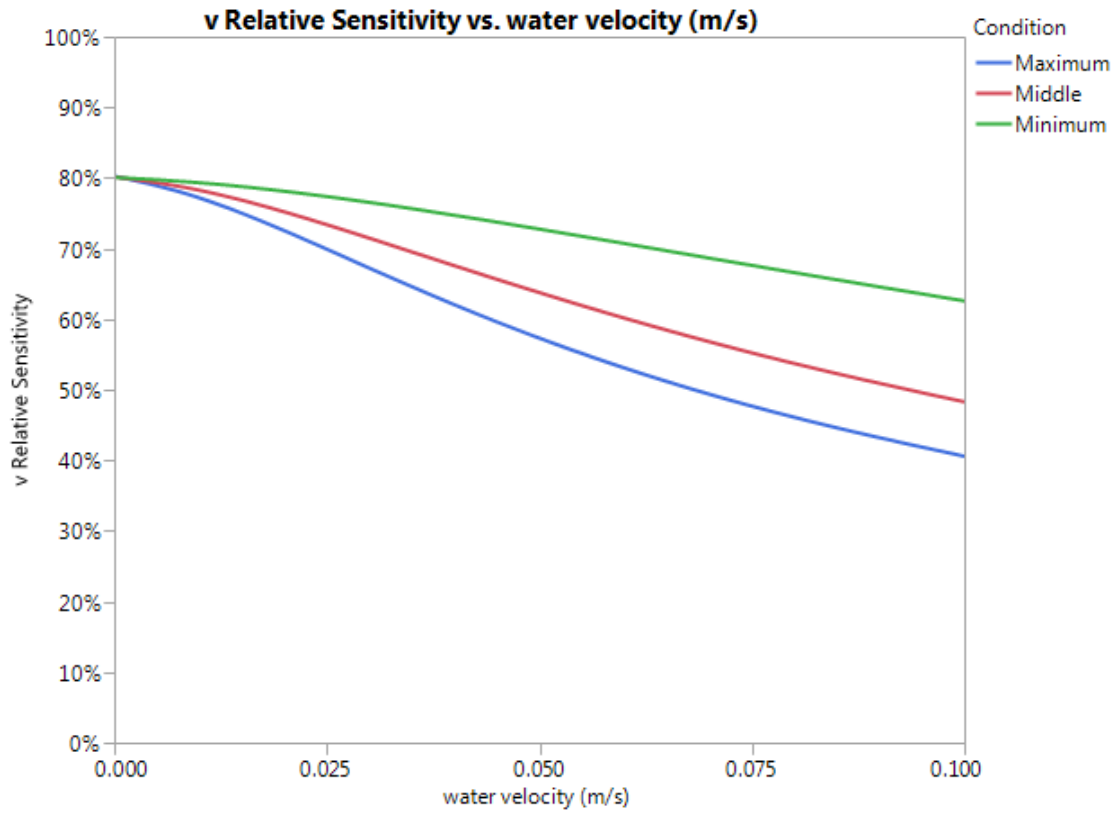
Figure 31: Graph of the M-C method's relative sensitivity to water velocity under simulated minimum (green), median (red), and maximum (blue) mass transfer conditions.

4.3 Applying The M-C Method To Core Inputs - Mass Transfer Dynamics

This study focuses on comparing the ICI method as commonly used with the M-C method applying a realistic range of simulated lake inputs for water velocity and free stream DO. It was shown that SOD obtained using the M-C method bracketed ICI SOD data. However, the ICI method does not measure SOD under *in-situ* conditions for water velocity and free stream DO. The SOD results from the M-C method can range from less than to greater than ICI SOD results depending upon the values of water velocity and free stream DO input to the model. This indicates that the value for water velocity and free stream DO that would cause the model to predict SOD values obtained using ICI are between the minimum and maximum model input values. If the M-C model can predict ICI SOD using equivalent input values occurring inside the incubated core for water velocity and DO, confidence in the model's accuracy would increase and "equivalent" water velocity and free stream DO values relating core conditions to *in-situ* conditions could be estimated.

Because the oxygen profile in the water above the sediment and the water velocity profile inside the incubated core are not well understood for this specific set of circumstances, it presents a number of complications in attempting to adapt the M-C method mass diffusion model for in-situ conditions to modeling a core. In a lake environment, the free stream DO concentration and water velocity above the sediment can be and have been measured directly. Because of the size of the lake systems, changes in water velocity and DO occur over a larger scale that is more easily measured or generalized (meters to hundreds of meters) than the conditions inside cores that describe the ICI environment (millimeters). Sediment typically has several meters of water overlying it in lakes. However, in the intact core tubes used in this study,

sediment only has on average 30cm of water overlying it, with a very low water inflow and outflow rate following an entirely different flow regime. The M-C model assumes a large, unbounded flow pattern of water flowing over sediment to estimate h_m , but core flows are bounded in the cylinder leading to a potentially more complex flow regime and the potential for the entire column to be a boundary layer, meaning there may not be a distinct free stream DO concentration.

The model requires two numerical inputs that could not be directly measured in the core: the DO concentration overlying the sediment and mass transfer coefficient, h_m. In order to obtain an estimate of either, several assumptions were made. Calculations show that the highest velocity in the incubated core, inside the inflow tube, follows laminar flow (average $Re \approx 740$), meaning that the entire column must be laminar. Because cores are incubated at constant temperature, it is assumed that there are no temperature gradients to drive convection currents. This was confirmed anecdotally by observing the horizontal delineation between the slightly cloudy lake water and the clear inflow water. Using a flashlight shone through the side of the core during incubation, it was observed that the inflow water slowly displaced the lake water without mixing (plug flow) from the sediment-water interface upward to the top of the core.

Following the assumption that plug flow is dominant, the oxygen profile in the tube can be deduced. Because the inflow tube is placed approximately 1 cm above the sediment, it is assumed that the inflow water spreads out in a very thin layer above the sediment, mixes with existing water, and reaches a steady state DO concentration as oxygen is added to the layer from the inflow and diffused down into the sediment. As the layer is constantly replenished with oxygenated inflow water, older water must move up (as seen by the turbidity delineation), where it is finally measured after exiting the outflow at the top. Oxygen removed from the water

column is from SOD that occurs in the thin convective layer just above the sediment and from consumption by the water occurring between the equilibrium concentration in the thin, mixed convective layer and the outflow. The rate of water oxygen uptake is determined from the control core (Eq. 21). Total oxygen removal from the water column is calculated from the hydraulic retention time given by the height of the water column above the sediment and the difference between inflow and outflow oxygen mass flow rates. This leaves a concentration slightly higher than outflow, referred to as DO1, which is assumed to be the free stream DO concentration above the sediment that drives the gradient between the free stream and the sediment (Eq. 22).

$$OUR = \frac{(DO_{in,ctrl} - DO_{out,ctrl})Q_{ctrl}}{Vol_{ctrl}} \tag{21}$$

$$DO1_{core} = DO_{out,core} - \frac{OUR*Vol_{Core}}{Q_{core}} \tag{22}$$

where:

$DO1$ = DO overlying the boundary layer (mg-L^{-1})

DO_{out} = DO of outflow, as measured for ICI (mg-L^{-1})

OUR = Volumetric oxygen uptake rate of control water measured from the same sample batch (mg-L^{-1}-min^{-1})

Vol = Volume of water in core (L)

Q = Flow rate (mL-min^{-1})

The next assumption to be made in order to model the intact core directly is the value of the mass transfer convection coefficient between the sediment and DO1. The SOD from the M-C model was calculated assuming no boundary layer ($h_m \approx \infty$), which thereby assumes equilibrium between the sediment surface to the free stream DO1. Using this assumption, the M-C method over-predicted SODs (up to 4.4 g/m2-d, see fig. 31), indicating a finite boundary layer exists.

68

The mass transfer convection coefficient was estimated using Equations 23-27 for laminar flow over a flat plate and the known exit velocity out of the inflow tube. This approach resulted in an h_m value within an order of magnitude of the h_m calculated by Charbonnet (for conditions occurring inside closed-system benthic chambers) (also see Fig. 32). Using this estimated h_m, the range of M-C core adapted SOD predictions within the range of measured core SOD. Results of M-C core SOD predictions and ICI SOD values, along with associated DO1, velocity, and h_m are shown in Appendix A, Tables 9-14.

For representing ICI conditions, the following equations were used (Datta, 2002):

$$h_m = \frac{h D_{O2,w}}{k} \tag{23}$$

$$h = \frac{Nu\,k}{L_c} \tag{24}$$

$$Nu = 0.664 Re^{1/2} Pr^{1/3} \tag{25}$$

$$Re = \frac{\rho_w v L_c}{\mu} \tag{26}$$

$$Pr = \frac{\mu * C_p}{k} \qquad *(27)$$

(*This input may also be found using a

water property table)

where:

v = flow velocity (m-s^{-1}), in ICI assumed to remain at the inflow velocity as it spreads out across the core surface before slowing to vertical plug flow.

L_c = characteristic length, in this case calculated as the average length of travel from the edge of a circle (where the inflow tube was always located) to every other point on the circle's perimeter, which converged to 0.6366*diameter as the number of points around the perimeter increased.

69

α = thermal diffusivity of water (m^2-s^{-1})

k = thermal conductivity of water (W-m^{-1}-K^{-1})

μ = dynamic viscosity of water (Pa-s)
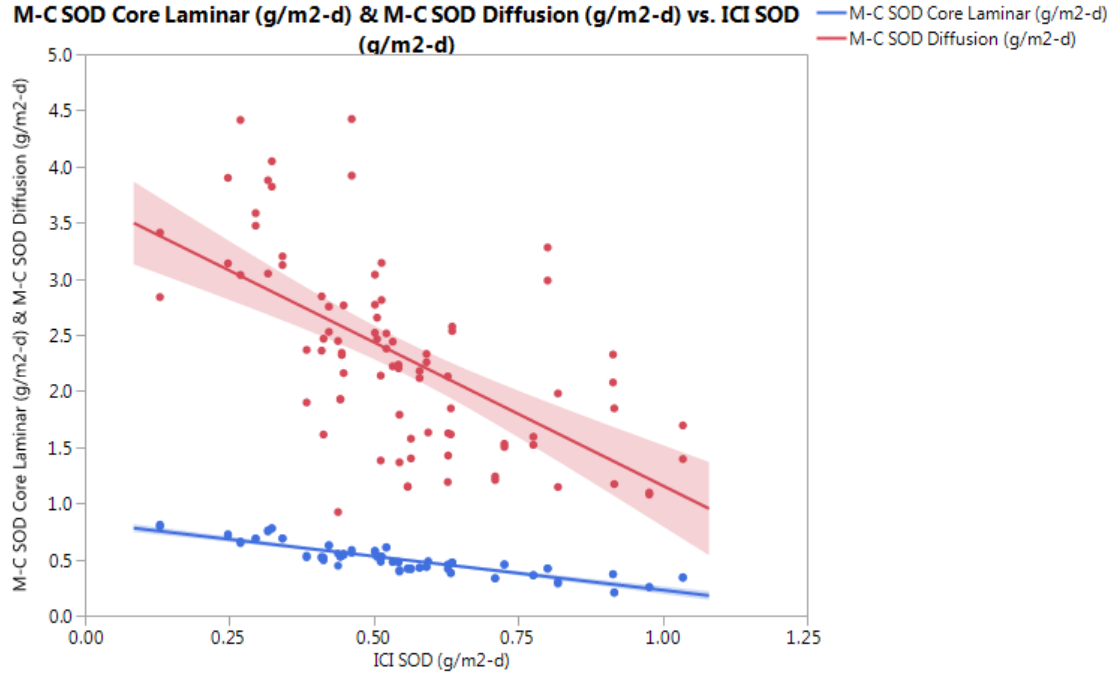
Figure 32: Graph of ICI SOD vs. M-C Core SOD (g/m^2-d) using both the assumption of diffusion only (no boundary layer, red), and the assumption of a laminar boundary layer (blue), with linear regressions and CIs of means.

If there is a finite mass transfer convection boundary layer as the results indicate, then any changes in water flow rate into the cores should affect measured SOD. The effect of h_m on SOD is controlled in the ICI method by conducting all tests using similar temperatures and water flow rates. However, measured flow through each core did vary slightly. Figure 33 shows the variation in flow rate plotted against ICI SOD. Linear regression analysis indicated a significant positive correlation (α=0.05; p=0.0028), however this could be fully or partially an artifact of flow rate being used in the SOD calculation.
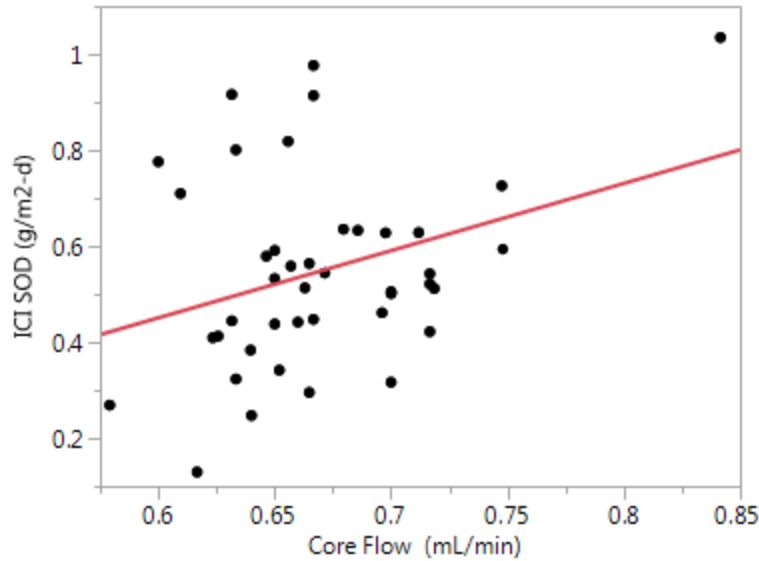
Figure 33: Graph of bivariate fit of ICI SOD by Core Flow, with linear regression in red. ANOVA p=0.0028.

4.4 Measure-Calculate Prediction Of ICI Core SOD

A paired t-test using data from all cores combined showed that M-C Core SOD was not significantly different from observed SOD (α=0.05; p=0.19). Paired t-tests using data subcategorized by lake showed that M-C data was significantly different than ICI SOD in each case (p=0.0002 for Fayetteville, p=0.0008 for Wedington, p=0.0002 for Wister). This result was explained in part by plotting observed ICI SOD versus M-C SOD (Table 9). Rather than the usual positive correlation expected between observed and predicted outcomes, the graph reveals an unexpected and strong negative correlation (p<0.0001; R^2 = 0.79), with data from all 3 lakes contributing. Mean M-C predicted core SOD was lower than ICI SOD for lakes Fayetteville and Wedington, and higher for Wister (see Table 9, Fig. 34).

Table 9: M-C SOD results using core inputs, with ICI SOD results for comparison.

Lake	M-C SOD Core (g-m^{-2}-d^{-1})				ICI SOD (g-m^{-2}-d^{-1})			
	Min	Mean	Max	CV	Min	Mean	Max	CV
Fayetteville	0.291	0.42	0.526	17.96	0.442	0.669	1.035	25.19
Wedington	0.205	0.394	0.533	26.49	0.384	0.677	0.977	33.05
Wister	0.414	0.583	0.81	19.77	0.13	0.439	0.636	29.14
All	0.205	0.501	0.81	27.23	0.13	0.548	1.035	36.56
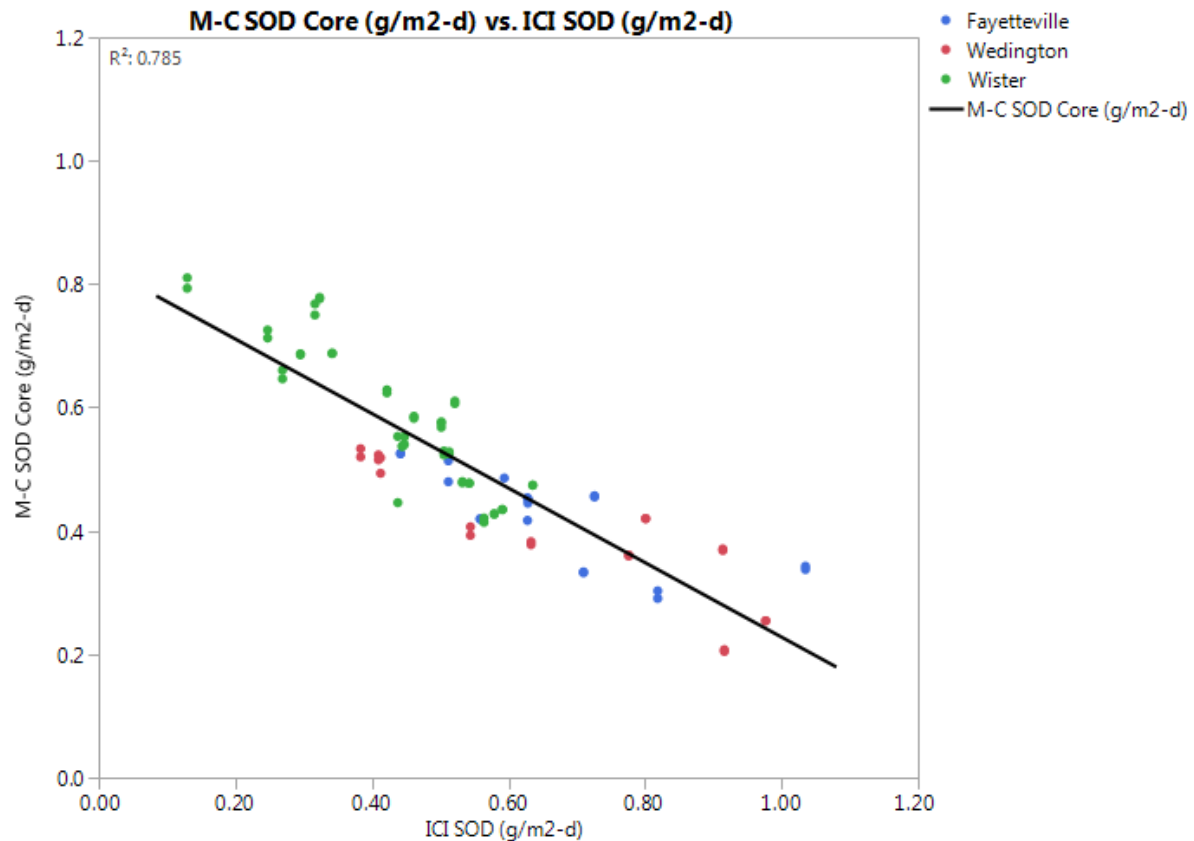
Figure 34: Graph of predicted vs. observed SOD (g/m^2-d) (M-C Core vs. ICI SOD), with linear regression. ANOVA p<0.0001

4.5 Other Correlations

The effect various inputs have on SOD outputs was next evaluated, in hopes of illuminating insightful relationships.

Plotting ICI SOD versus $\dot{N}_{sed}$ reveals a counterintuitive relationship. When data from all lakes are evaluated together, they show a visually unconvincing but statistically significant negative correlation ($\alpha=0.05$; $p=0.008$), where high $\dot{N}_{sed}$ correlates with low SOD (Fig. 35). However, when evaluated on a lake-by-lake basis, the correlation is revealed to be the product of several insignificant and disagreeing lake datasets (Fig. 36). No significant correlation could be found in any single lake dataset ($p=0.26$, 0.44, 0.18 respectively in Fayetteville, Wedington, and Wister). 2 of 3 lakes (Fayetteville and Wedington) showed insignificant positive correlations.
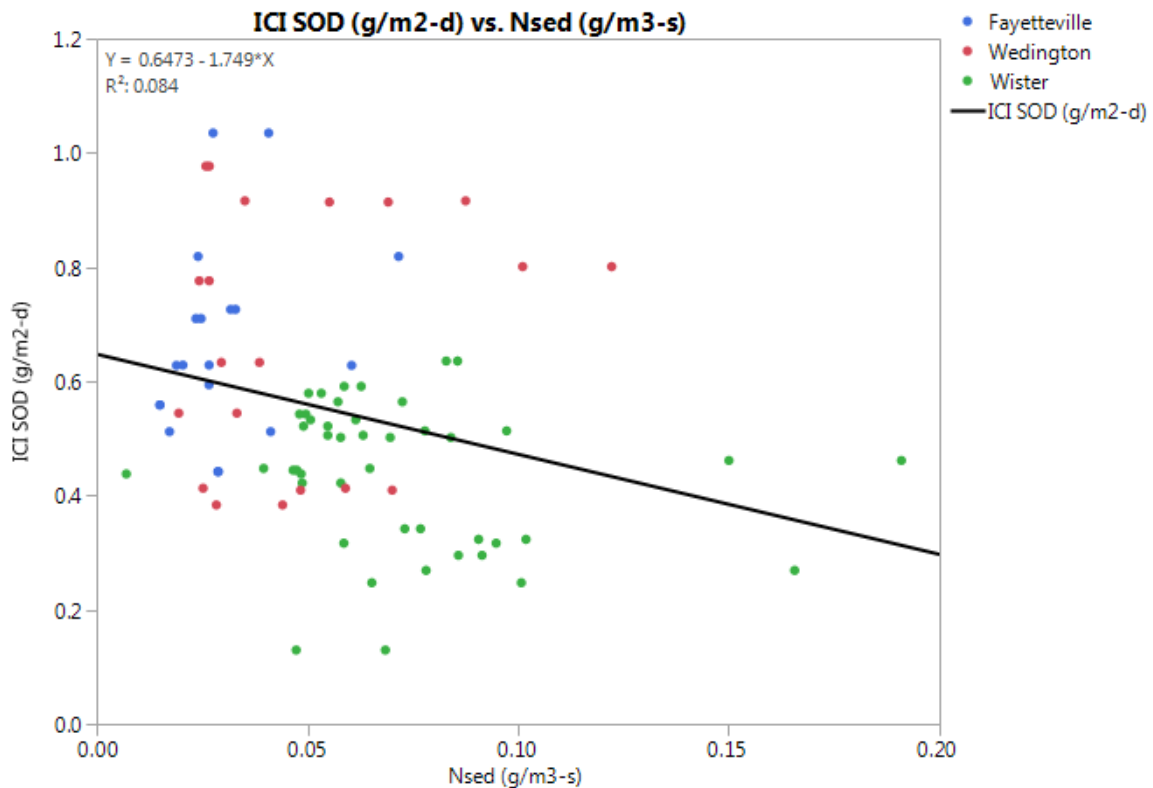
Figure 35: Graph of ICI SOD (g-m-^{2}-d^{-1}) vs. $\dot{N}_{sed}$ (g/m^3-s) with linear regression. ANOVA p=0.008.
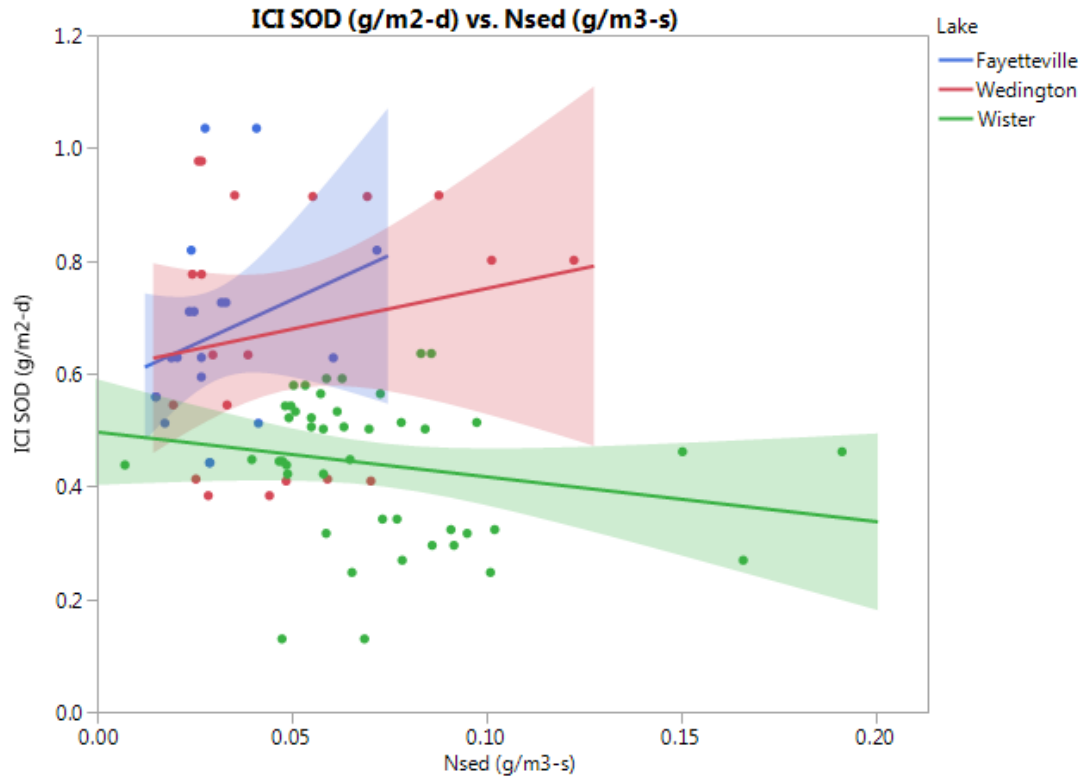
Figure 36: Graph of ICI SOD (g/m^2-d) vs. $\dot{N}_{sed}$ (g/m^3-s), with linear regressions by lake and CIs of means. ANOVA p = 0.26, 0.44, 0.18 respectively for Fayetteville, Wedington, and Wister

Using selected inputs, including additional data not used by the M-C model, several multiple linear regression (MLR) models were created (outputs available in Appendix B). These inputs included Lake Depth, Water Core Height, Core Flow, Inflow DO, Density, MC, P_{sed}, and $\dot{N}_{sed}$. Because DO1 (the oxygen driver for M-C predicted core SOD) is dependent on outflow DO data that also determines ICI SOD, DO1 is not a useful input (because it is really an output) for model comparisons.

The MLR model was capable of an R^2 of 0.44. The most significant parameter estimate was Core Flow, with a positive contribution (α=0.05; p<0.0001). Other significant parameters were Inflow DO (+, p=0.0002), Lake Depth (-, p=0.0021), P_{sed} (-, p=0.0032), and MC (+, p=0.0060).

While it can be seen from the calculation methods that ICI SOD is driven by $\Delta DO_{(in\text{-}out)}$ and M-C SOD is driven by the DO above the sediment (DO1 in the case of cores), it was not immediately obvious that these drivers directly contradicted each other, as shown in Fig. 37. This is further discussed in the following section.
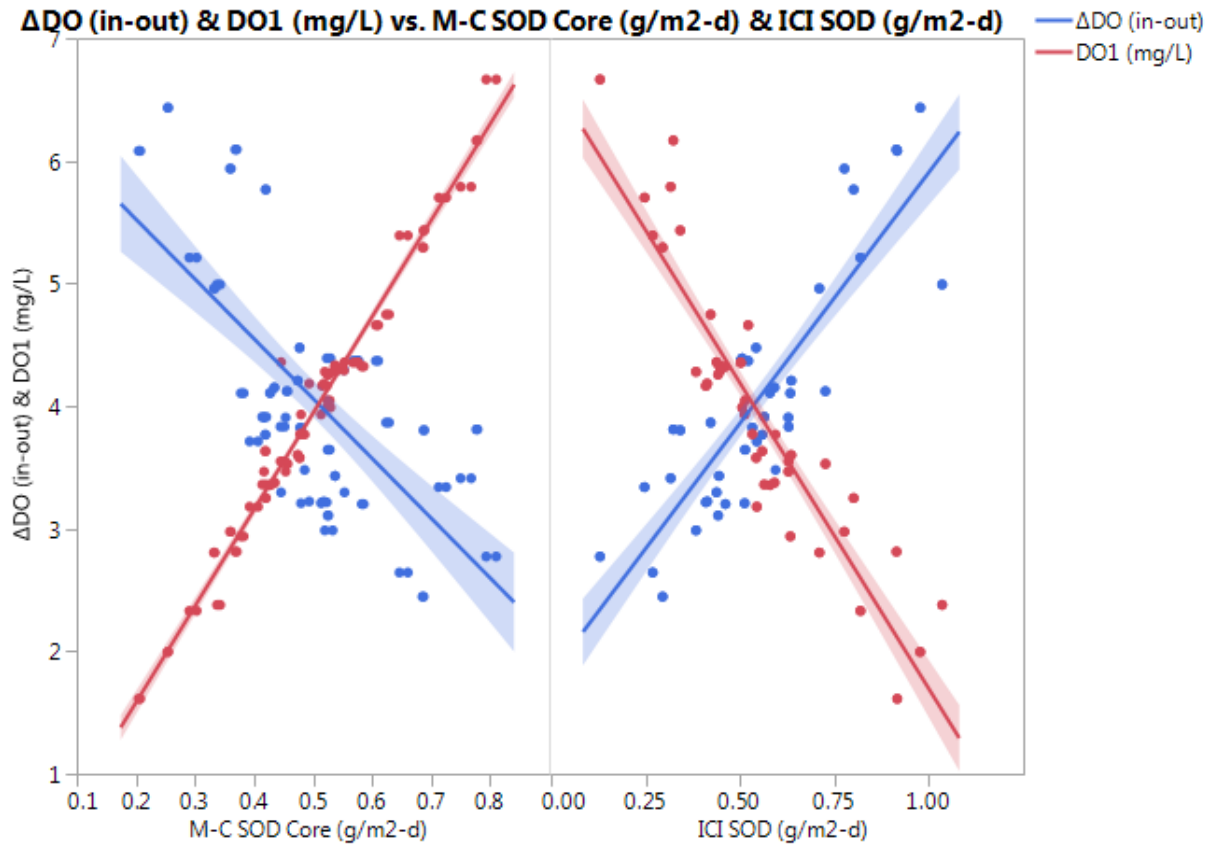
Figure 37: DO1 and ΔDO(in-out) (mg/L) vs. M-C and ICI SODs (g/m²-d) with linear regressions and CIs of means.

5. DISCUSSION

5.1 Sediment Extraction

The method used to extract intact sediment cores in this study failed to collect sediment at multiple locations. Originally, sediments were planned to be collected from Lake Brittany in Bella Vista, AR rather than from Lake Wister. However, the bottom of Lake Brittany proved to be so rocky that no intact cores were extracted in over two hours of attempts. Impenetrable sediment was also found in parts of Lake Wedington, however other parts of that lake contained very soft and non-cohesive sediment that would not remain in the corer during retrieval to the surface. Both of these issues limit the ability of the ICI method to comprehensively sample lakes for SOD. It was not able to evaluate SOD in Lake Brittany. For the same reasons, the deployment of benthic chambers would likely have been problematic due to leakage around the bottom of the chamber. The M-C method may be able to use smaller amounts of sediment scooped from the lake bottom using a sampler such as the Wildco Ekman Sampler used by Richardson (2014), and thus may be able to determine SOD in Lake Brittany and others where ICI or benthic chamber use is excluded. Care should likely be taken to disturb collected sediments as little as possible.

5.2 Observations On $\dot{N}_{sed}$ Methods

While the model used for the M-C method remained the same between this and previous studies, a departure from previous methods was the calculation of $\dot{N}_{sed}$. When planning and developing this experiment, emphasis was placed on obtaining as accurate readings as possible. Equipment was set up for electronic data collection every 15 seconds rather than manual recordings. While the model used only the later steady state portion of the data, much care was

taken to precisely measure early oxygen consumption (t = 0 - 30 s). Great care was taken in correctly timing the recording and stirring of the BOD bottle tests and it appears that this increased quantity of data has allowed for developing a model (Eq. 8) that precisely describes sediment oxygen uptake throughout the recorded DO versus time curve for this study. It is speculated that accuracy in the earlier portion of the uptake test contributes to the regression's ability to accurately predict steady state consumption, especially when the test ends before steady state consumption is observed. Because previous studies had fewer data points and used linear regressions on nonlinear data with decreasing first derivatives, their methods over-predict the steady state consumption rate compared to the methods used here.

In analysis of initial consumption rates, it was shown that they were much more variable than steady state consumption rates, even between duplicates of the same sediment samples. This was due in part to the extreme influence of the timing of the start of the recording relative to when the sediment was actually added and suspended in the BOD bottle. This should be taken into consideration if the earlier portions of the DO versus time regression (i.e. non-steady-state) are used in any future studies (e.g. modeling a sediment resuspension event).

Early testing of $\dot{N}_{sed}$ methods using refrigerated, previously collected sediment revealed the importance of using ambient temperature, freshly collected sediment in these studies. Refrigerated sediments, though they had been stored in glass beakers covered with cellophane film, contained sufficiently high DO that they contributed DO to the test water rather than consumed it.

5.3 Validity of Comparing ICI and M-C SOD Results

Miller-Way and Twilley (1996) conducted an SOD study using ICI and found that dilution rate (inflow rate) can affect values determined for ICI SOD. The study provided stirring likely producing a large h_m value (thin boundary layer), so the effect of flow rate over the sediment surface would have been primarily from a change in oxygen mass flow rate into the system and resulting water DO and not via a boundary layer. The study found that there is a range of inflow rates that are optimal. For inflow rates below this range, feedback occurs. For inflow rates above this range, washout occurs. Feedback is defined as the process whereby SOD drives a significant decrease in overlying DO, which in turn limits the oxygen availability to the sediment and reduces SOD. Washout occurs when the differences between inflow and outflow DO are smaller than the error associated with the measurements, so no significant results can be obtained. Because the optimum ranges will vary according to the core dimensions and SOD, a direct relationship between inflow rates and SOD may vary between tests and optimal, feedback, and washout inflow rates may not be compared directly between studies. Because of different sized cores and potentially different SOD values between this study and that of Miller-Way and Twilley, it may be that the target inflow rate used in this research was below the optimal range and contributed to feedback. However, data confirms that the ICI SOD results obtained were statistically similar to literature values although the variability of SOD values measured was large both for this study and those in the literature. If the data was compromised because of non-optimal flow rates, it does not appear compromised significantly more than these other studies. One problem this raises is that SOD comparisons using these methods may be relative to each study, not absolute. A method to determine the real, true value of SOD *in-situ* was not available. Thus, the comparisons made were between methods that either change conditions (water DO and

convection coefficient) under which SOD is measured (ICI) or assume these conditions in the model and therefore hold them constant (M-C). In this case, consensus is the only guide. That two independent methods for calculating SOD both found similar results increases confidence in the validity of both.

5.4 Limiting Factors For SOD In This Study And Their Implications

By analyzing differences in predicted SOD relative sensitivity based on the M-C model (at all three conditions), it can be shown that M-C SOD was limited most by free stream DO, then water velocity, P_{sed}, and $\dot{N}_{sed}$ in descending order. Coefficient of variation (CV) data supports the conclusion that $\dot{N}_{sed}$ is not the most limiting factor in that $\dot{N}_{sed}$ had the highest CV (~50), with ICI SOD next (~30) and M-C lake SOD having the smallest CV (~7 for median conditions). These differences in variations indicate the closeness of relationship between each data set and directly measured values from the environment. $\dot{N}_{sed}$ and ICI SOD were determined from direct measurement of sediment, while M-C SOD was the result of model calculations where the variability of $\dot{N}_{sed}$ did not translate to SOD because of the insensitivity of the model to $\dot{N}_{sed}$ at those conditions. Since the M-C model is most sensitive to inputs that are held constant during simulations, it is not surprising the CV for M-C SOD is relatively low. According to the mechanisms of mass transfer used by the model, using ICI conditions for DO and water velocity that do not mimic lake conditions is likely to influence ICI SOD away from its true *in-situ* value. Experimental methods outlined in previous studies appear to address these sensitive inputs, such as constant impeller stirring, and a DO mass flow rate that is selected to maintain a constant free stream DO across different cores (Miller-Way and Twilley, 1996). However, constant impeller stirring is unlikely to replicate in-situ flow patterns or boundary layer thickness as represented by h_m, and finding the optimal DO mass flow rate for each core would add equipment expense (one

variable-speed pump per core rather than per batch), complication, and labor to an already

intensive process. If these inputs are not controlled adequately, they may introduce SOD

variability that overshadows differences in sediment P_{sed} and $\dot{N}_{sed}$.

Given these complications, the M-C Method has the advantage in accounting for these

limiting inputs and either standardizing or replicating *in-situ* conditions mathematically at

reduced error, labor, and cost.

5.5 Efficacy Of The M-C Method

The study has shown that the ICI method was able to measure SOD in each of the study

lakes with reasonable results compared to the literature, and that the M-C Method was able,

using reasonable flow and DO conditions, to bracket all measured ICI values, between

approximately 0 and 1.2 $g\text{-}m^{-2}\text{-}d^{-1}$ and provide statistically similar values (p=0.77) for median

conditions. Furthermore, when the M-C model was adapted to predict core conditions, it was

able to return a mean SOD value that was not significantly different than the ICI method

(p=0.19). However, the indirect relationship between SOD results obtained using each method

indicates the M-C model is likely not appropriate for describing the SOD mechanisms occurring

inside the core during ICI testing. Considering that the M-C method was able to produce

reasonable SOD values compared to the ICI method using physics equations and only measured

or calculated inputs without optimized empirical constants, improves confidence in the M-C

method's validity.

5.6 Explaining The Inverse Relation Between ICI SOD And M-C Core SOD

One of the most interesting relationships that the data revealed when comparing M-C

method results modeling SOD inside the core was a negative relationship between ICI SOD and

M-C predicted core SOD. This relationship may reveal an inherent flaw with using the M-C model to predict ICI SOD.

The M-C model assumes that in a lake, convection boundary conditions control SOD. However, in the intact core incubation method, SOD may control the boundary conditions by controlling the oxygen gradient (creating a self-limiting condition). For both lake and core SOD, the rate of transfer of DO to the sediment is the result of DO demand ($\dot{N}_{sed}$), DO supply (free stream DO), DO demand access (P_{sed} and $D_{O2\text{-}sed}$), and DO supply access (water velocity). In the core there is a finite supply rate of DO, which over time becomes depleted by SOD and it is the rate of this depletion that is measured to determine SOD. The M-C model assumes that in the short time required to reach steady state, SOD does not affect the DO of overlying water. In the longer term, both the ability of SOD to control boundary conditions (ICI's working assumption) and the ability of boundary conditions to control SOD (M-C method's working assumption) hold true, and create a feedback loop that may or may not lead to the problem of water body oxygen depletion. However, when compounded and confined over the duration of the core incubation, neither working assumption fully describes what takes place, and so they show a trend discrepancy.

While both the M-C and ICI methods correlate an increasing DO differential with increasing SOD, they are opposite in how they measure this differential. Whereas the M-C method calculates this differential as the difference between the sediment and the overlying DO concentration (DO1), the core incubation calculates it as the difference between the inflow and the outflow. These calculations contradict one another when directly compared (shown previously in Fig. 34 and 37). A hypothetical example may clarify this point. Suppose two cores have no water OUR and identical inflow DOs of 7 mg/L. Core A has an outflow DO of 0 mg/L,

and core B has an outflow DO of 7 mg/L. In this scenario, the core incubation calculation would show that core A has the larger SOD, as all of the oxygen must have been consumed by the sediment. In contrast, the M-C calculation would calculate that core B has the larger SOD, because of the higher free stream water DO and thus higher gradient into the sediment. The M-C model would calculate an SOD of 0 for Core A because sediment cannot consume oxygen that does not exist.

Another potential explanation is that a consumptive boundary layer may be creating feedback. The water flow rate may not be sufficient in relation to the SOD to control the thickness of the boundary layer resulting in a diffusion limited condition in the water, thus the boundary layer may be driven by SOD, ergo SOD may be limiting itself. Put in economic terms, the import of a commodity (oxygen) is limited by a number of factors: demand ($\dot{N}_{sed}$), market access (P_{sed} and $D_{O2,sed}$), world supply (DO), and transportation availability (water flow velocity). If the delivery is insufficient, the demand will outstrip the supply to an extent that the boundary layer is controlled no longer by supply but by demand, and the gradient created becomes an impediment to oxygen transfer. The M-C model assumes an infinite supply of oxygen (at the given concentration) in the lake over the time period required to reach steady state, whereas the core method relies on the consumption of this supply in order to calculate SOD- a more complex scenario.

6. CONCLUSIONS

6.1 Summary Of Conclusions

6.1.1 Data Supports Further Exploration Of M-C Method

While possibly coincidental, the fact that ICI SOD, M-C Core SOD, and M-C Lake SOD converged to similar SOD values that fall well within literature ranges likely attests that both methods generally agree despite being entirely different in approach. This is especially impressive considering that the M-C model contains no fitted parameters. Using only measured and calculated inputs, it reproduced mean SOD results that were not significantly different from the independent ICI method, with considerably lower variability.

6.1.2 Data Shows That M-C Model As Applied To Core Conditions Was Not Appropriate

While the mean values were not significantly different, trends between M-C Core SOD and ICI SOD showed clear disagreement, likely indicating that the core incubation system was not described well by the model, which is meant to represent lake dynamics.

6.2 Potential Impact

This study should encourage further investigation and validation studies of the M-C Method, towards the eventual goal that it be a fully defensible field method. If successful, the method will grant a much wider array of environmental workers access to SOD data through decreased cost and decreased testing time, and may improve the accuracy and precision of SOD data- both in direct, individual sampling and potentially on the scale of environmental modeling.

6.3 Future Work

6.3.1 Sediment Collection

An advantage the MC method offers over the intact core method is the ability to collect sediment from a broader range of environments. Because it only requires a small sample of sediment, creative methods could collect sediment from rocky or non-cohesive sediments with much simpler equipment. Additional experiments could determine the sensitivity of sediment properties to depth below the sediment surface, the degree to which the sediment is disturbed before testing, and the time elapsed between collection and testing under various circumstances and using various methods.

6.3.2 $\dot{N}_{sed}$ Procedure for Future Use

Because the study showed that $\dot{N}_{sed}$Lin (the longest-term, linear slope of the curve) was the best performing and most logical $\dot{N}_{sed}$ input to the model, a simplified method may also perform well. Sediment in the BOD bottle could be aerated for a predetermined length of time before taking the initial $\dot{N}_{sed}$ measurement. This should quench any immediate chemical demand and encourage the more stable (linear) consumption presumably driven by bacterial consumption. A regression of this slope should yield $\dot{N}_{sed}$ without the need for a complicated 6-parameter regression and without the precision required to correctly time the $\dot{N}_{sed}$ procedure used in this study.

6.3.3 Temperature and Seasonality

Future studies should investigate and improve the M-C Method's ability to correctly account for the various effects temperature has on SOD. They should also investigate the

seasonal behavior of $\dot{N}_{sed}$, to determine the number of tests necessary to accurately model SOD throughout the year, in order to give the model the ability to accurately model SOD both historically and predictively.

REFERENCES

Avnimelech, Y., Ritvo, G., Meijer, L. E., & Kochba, M. (2001). Water content, organic carbon and dry bulk density in flooded sediments. *Aquacultural engineering, 25*(1), 25-33.

Berg, P. (n.d.). *Eddy Research Correlation Lab at University of Virginia.* Retrieved from http://faculty.virginia.edu/berg/

Berg, P., Røy, H., Janssen, F., Meyer, V., Jørgensen, B. B., Huettel, M., et al. (2003). Oxygen uptake by aquatic sediments measured with a novel non-invasive eddy-correlation technique. *Marine Ecology Progress Series, 261*, 75-83.

Bowman, G. T., & Delfino, J. J. (1980). Sediment oxygen demand techniques: A review and comparison of laboratory and in situ systems. *Water Research, 14*(5), 491-499.

Brand, A., McGinnis, D. F., Wehrli, B., & Wüest, A. (2008). Intermittent oxygen flux from the interior into the bottom boundary of lakes as observed by eddy correlation. *Limnology and Oceanography, 53*(5), 1997-2006.

Buck, S. D. (2014). *Concentrations, Loads, and Yields of Total Phosphorus, Total Nitrogen, and Suspended Sediment and Bacteria Concentrationsin the Wister Lake Basin, Oklahoma and Arkansas, 2011-13.* Poteau Valley Improvement Authority. USGS.

Chapra, S. C. (2008). *Surface water-quality modeling.* Long Grove, Illinois: Waveland Press, Inc.

Charbonnet, D. A. (2003). A finite difference model for predicting sediment oxygen demand in streams. *MS Thesis.* Fayetteville, AR: University of Arkansas, Dept. of Biological and Agricultural Engineering.

Charbonnet, D. A., Osborn, G. S., Haan, P. K., & Matlock, M. D. (2006). Application and validation of the spreadsheet method for determining SOD. *Transactions of the ASABE, 49*(6), 2039-2050.

Committee on Environment and Natural Resources. (2010). *Scientific assesment of hypoxia in U.S. coastal waters.* Washington, D.C.: Interagency Working Group on Harmful Algal Blooms, Hypoxia, and Human Health of the Joint Subcommittee.

Cornett, R. J., & Rigler, F. H. (1987). Decomposition of seston in the hypolimnion. *Canadian Journal of Fisheries and Aquatic Sciences, 44*(1), 146-51.

Datta, A. K. (2002). *Biological and bioenvironmental heat and mass transfer.* New York: CRC Press.

Del Giorgio, P. A., & Williams, P. J. (Eds.). (2005). *Respiration in aquatic ecosystems.* New York: Oxford University Press.

Duchscherer. (2010). *Dissolved Oxygen TMDL for the Souris River in Renville and Burke Counties, North Dakota.* North Dakota Department of Public Heath, Division of Water Quality.

Edberg, N., & Hofsten, B. V. (1973). Oxygen uptake of bottom sediments studied in situ and in the laboratory. *Water Research, 7*(9), 1285-1294.

Fennel, K., Jiatang, H., Arnaud, L., Marta-Almeida, M., & Hetland, R. (2013). Sensitivity of hypoxia predictions for the northern Gulf of Mexico to sediment oxygen consumption and model nesting. *Journal of Geophysical Research: Oceans, 118*(2), 990-1002.

Fillos, J., & Molof, A. H. (1972). Effect of benthal deposits on oxygen and nutrient economy of flowing waters. *Journal of the Water Pollution Control Federation, 44*(4), 644-662.

Gardner, W. S., McCarthy, M. J., An, S., Sobolev, D., Sell, K. S., & Brock, D. (2006). Nitrogen fixation and dissimilatory nitrate reduction to ammonium (DNRA) support nitrogen dynamics in Texas estuaries. *Limnology and Oceanography, 51*(1 part 2), 558-568.

Gloor, M., Wuest, A., & Munnich, M. (1994). Benthic boundary mixing and resuspension induced by internal seiches. *Hydrobiologia, 284*, 59-68.

Glud, R. N., Gundersen, J. K., & Holby, O. (1999). Benthic in situ respiration in the upwelling area off central Chile. *Marine Ecology Progress Series, 186*(September), 9-18.

Glud, R. N., Gundersen, J. K., Røy, H., & Jørgensen, B. B. (2003). Seasonal dynamics of benthic O2 uptake in a semienclosed bay: Importance of diffusion and faunal activity. *Limnology and Oceanography, 48*(3), 1265-76.

Glud, R. N., Holby, O., Hoffman, F., & Canfield, D. E. (1998). Benthic mineralization and exchange in Arctic sediments (Svalbard, Norway). *Marine Ecology Progress Series, 173*(November), 237-51.

Grantz, E. M., Kogo, A., & Scott, J. T. (2012). Partitioning whole-lake denitrification using in situ dinitrogen gas accumulation and intact sediment core experiments. *Limnology and Oceanography, 57*(4), 925-35.

Haan, C. T. (2002). *Statistical methods in hydrology* (2nd ed.). Ames, IA: Iowa State University Press.

Haggard, B. E., Scott, J. T., & Patterson, S. (2012). Sediment phosphorous flux in an Oklahoma reservoir suggest reconsideration of watershed management planning. *Lake and Reservoir Management, 28*, 59-69.

Hall, D. C., & Berkas, W. R. (1988). Comparison of instream and laboratory methods of measuring sediment oxygen demand. *Water Resources, 24*(3), 571-575.

Hall, P. O., Anderson, L. G., van der Loeff, M. M., Sundby, B., & Westerlund, S. F. (1989). Oxygen uptake kinetics in the benthic boundary layer. *Limnology and Oceanography, 34*(4), 734-746.

Hatcher, K. J. (1986). Sediment oxygen demand: processes, modeling, and measurement. *In 56th WPCF Conference, Atlanta, Ga. (USA), 1983.* Institute of Natural Resources, University of Georgia.

He, Y., & Liu, C. (2011). Optimizing the design of in situ sediment oxygen demand measurement chambers. *International Journal of Sediment Research, 26*(2), 222-229.

Higashino, M., & Gantzer, C. J. (2004). Unsteady diffusional mass transfer at the sediment/water interface: Theory and significance for SOD measurement. *Water Research, 38*(1), 1-12.

Horn, W., Mortimer, C. H., & Schwab, D. J. (1986). Wind-induced internal seiches in Lake Zurich observed and modeled. *Limnology and Oceanography, 31*(6), 1232-1254.

Huettel, M., Ziebis, W., Forster, S., & Luther, G. W. (1998). Advective transport affecting metal and nutrient distributions and interfacial fluxes in permeable sediments. *Geochimica et Cosmochimica Acta, 62*(4), 613-631.

James, A. (1974). The measurement of benthal respiration. *Water Resources, 8*(11), 955-959.

Jorgensen, B. B., & Revsbech, N. P. (1985). Diffusive boundary layers and the oxygen uptake of sediments and detritus. *Limnology and Oceanography, 30*(1), 111-122.

Kalff, J. (2002). *Limnology: Inland water ecosystems.* Upper Saddle River, N.J.: Prentice Hall.

Kasprzak, K. R. (2001). Modeling in situ sediment oxygen demand in the Arroyo Colorado. *MS Thesis*. College Station, TX: Texas A&M University, Department of Agricultural Engineering.

Kemp, M. H., & Sampou, P. A. (1992). Seasonal depletion of oxygen from bottom waters of Chesapeake bay- Roles of benthic and planktonic respiration and physical exchange processes. *Marine Ecology Progress Series, 85*(1-2), 137-52.

Lavery, P. S., Oldham, C. E., & Ghisalberti, M. (2001). The use of Fick's First Law for predicting porewater nutrient fluxes under diffusive conditions. *Hydrobiological Processes, 15*, 2435-2451.

Lee, J. H., Kuang, C. P., & Yung, K. S. (2000). Fluid mechanics of triangular sediment oxygen demand chamber. *Journal of Environmental Engineering, 126*(3), 208-216.

Lorrai, C., McGinnis, D. F., Berg, P., Brand, A., & Wüest, A. (2010). Application of oxygen eddy correlation in aquatic systems. *Journal of Atmospheric and Oceanic Technology, 27*(9), 1533-1546.

Mackenthun, A. A., & Stefan, H. G. (1998). Effect of flow velocity on sediment oxygen demand: Experiments. *Journal of Environmental Engineering, 124*(3), 222-230.

Matlock, M. D., Kasprzak, K. R., & Osborn, G. S. (2003). Sediment oxygen demand in the Arroyo Colorado River. *Journal of American Water Research, 39*(2), 267-275.

Matthews, D. A., & Effler, S. W. (2006). Long-term changes in the areal hypolimnetic oxygen deficit (AHOD) of Onondaga Lake: Evidence of sediment feedback. *Limnology and Oceanography, 51*(1 part 2), 702-714.

McCarthy, M. J., Gardner, W. S., Lavrentyev, P. J., Moats, K. M., Jochem, F. J., & Klarer, D. M. (2007). Effects of hydrological flow regime on sediment-water interface and water column nitrogen dynamics in a Great Lakes coastal wetland (Old Woman Creek, Lake Erie). *Journal of Great Lakes Research, 33*(1), 219-231.

Miller-Way, T., & Twilley, R. R. (1996). A comparison of batch and continuous flow methodologies for determining benthic fluxes. *Marine Ecology Progress Series, 140*, 257-269.

Miller-Way, T., Boland, G. S., Rowe, G. T., & Twilley, R. R. (1994). Sediment oxygen consumption and benthic nutrient fluxes on the Louisiana continental shelf: a methodological comparison. *Estuaries, 17*(4), 809-815.

Murphy, P. J., & Hicks, D. B. (1986). In-situ method for measuring sediment oxygen demand: Theory. In K. J. Hatcher (Ed.), *Sediment oxygen demand: Processes, modeling, and measurement* (pp. 307-322). Athens, GA: University of Georgia, Institute of Natural Resources.

Nakamura, Y., & Stefan, H. G. (1994). Effect of flow velocity on sediment oxygen demand: Theory. *Journal of Environmental Engineering, 120*(5), 996-1016.

Osborn, G. S., Charbonnet, D. A., Smith, P. K., & Matlock, M. D. (2008). A chamberless method for determining SOD. *Transactions of the ASABE, 51*(3), 1123-1131.

Pamatmat, M. M., & Banse, K. (1969). Oxygen consumption by the sea bed: II. In situ measurements to depth of 180m. *Limnology and Oceanography, 14*(2), 250-259.

Rabouille, C., Denis, L., Dedieu, K., Stora, G., Lansard, B., & Grenz, C. (2003). Oxygen demand in coastal marine sediments: Comparing in situ microelectrodes and laboratory core incubations. *Journal of Experimental Marine Biology and Ecology, 285*, 49-69.

Rasmussen, H., & Jorgensen, B. B. (1992). Microelectrode studies of seasonal oxygen uptake in a coastal sediment: Role of molecular diffusion. *Marine Ecology Progress Series, 81*, 289-303.

Richardson, G. (2014). Lab-scale experiment for assessing the effect of resuspension and oxygenation on sediment oxygen demand. *MS Thesis*. Fayetteville, AR: University of Arkansas, Dept. of Biological and Agricultural Engineering.

Rounds, S., & Doyle, M. C. (1997). *Sediment oxygen demand in the Tualatin River Basin, Oregon, 1992-1996.* US Geological Survey; Branch of Information Services.

Rutherford, J. C., Wilcock, R. J., & Hickey, C. W. (1991). Deoxygenation in a mobile-bed river: I. Field studies. *Water Research, 25*(12), 1487-1497.

Scott, J. T., & Grantz, E. M. (2013). N2 fixation exceeds internal nitrogen loading as a phytoplankton nutrient source in perpetually Nitrogen-limited reservoirs. *Freshwater Science, 32*(3), 849-61.

Scott, J. T., McCarthy, M. J., Gardner, W. S., & Doyle, R. D. (2008). Denitrification, dissimilatory nitrate reduction to ammonium, and nitrogen fixation along a nitrate concentration gradient in a created freshwater wetland. *Biogeochemistry, 87*, 99-111.

Seiki, T., Izawa, H., & Date, E. (1989). Benthic nutrient remineralization and oxygen consumption in the coastal area of Hiroshima Bay. *Water Research, 23*(2), 219-228.

Seiki, T., Izawa, H., Date, E., & Sunahara, H. (1994). Sediment oxygen demand in Hiroshima Bay. *Water Research, 28*(2), 385-393.

Sweerts, J. P., Bär-Gilissen, M. J., Cornelese, A. A., & Cappenberg, T. E. (1991). Oxygen-consuming processes at the profundal and littoral sediment-water interface of a small meso-eutrophic lake (Lake Vechten, the Netherlands). *Limnology and Oceanography, 36*(6), 1124-33.

Sweerts, J. P., Louis, V. S., & Cappenberg, T. E. (1989). Oxygen concentration profiles and exchange in sediment cores with circulated overlying water. *Freshwater Biology, 21*(3), 401-409.

Thomann, R. V., & Mueller, J. A. (1987). *Principles of surface water quality modeling and control.* Harper & Row, Pubishers.

Truax, R. V., Shindala, A., & Sartain, H. (1995). Comparison of two sediment oxygen demand measurement techniques. *Journal of Environmental Engineering, 121*(9), 619-624.

US EPA. (2015). *National Summary of Impaired Waters and TMDL Information.* US EPA.

Walker, R., & Snodgrass, W. (1986). Model for sediment oxygen demand in lakes. *Journal of Environmental Engineering, 112*(1), 25-43.

Waterman, D. M., Waratuke, A. R., Motta, D., Cataño-Lopera, Y. A., Zhang, H., & García, M. H. (2011). In situ characterization of resuspended-sediment oxygen demand in Bubbly Creek, Chicago, Illinois. *Journal of Environmental Engineering, 137*(8), 717-730.

Whittemore, R. C. (1986). The significance of interfacial water velocity on the measurement of sediment oxygen demand. In K. J. Hatcher (Ed.), *Sediment oxygen demand: Processes, modeling, and measurement* (pp. 63-74). Athens, GA: University of Georgia, Institute of Natural Resources.

APPENDIX A. STUDY DATA

Table 10: Selected study data– collection and ICI SOD, Lakes Fayetteville and Wedington

Lake	ID	Run ID	Site	Lat	Long	Sample Date	Depth (m)	Core Height (m)	Core Flow (mL/min)	Core Flushes	DO Inflow (mg/L)	DO Out (mg/L)	Control (mg/L-min) Flow* ΔDO(in-out)	ICI SOD (g/m2-d)	DO1 (mg/L)
Fayetteville	F02	F02AA	F02	36.14098	-94.12199	6/29/2015	0.9	0.275	0.657	1.37	6.75	2.99	-0.000295	0.56	3.63
Fayetteville	F02	F02AB	F02	36.14098	-94.12199	6/29/2015	0.9	0.275	0.657	1.37	6.75	2.99	-0.000295	0.56	3.63
Fayetteville	F04	F04AA	F04	36.13922	-94.12575	6/29/2015	1.0	0.400	0.610	0.88	6.75	1.79	-0.000295	0.71	2.81
Fayetteville	F04	F04AB	F04	36.13922	-94.12575	6/29/2015	1.0	0.400	0.610	0.88	6.75	1.79	-0.000295	0.71	2.81
Fayetteville	F08	F08AA	F08	36.13572	-94.13328	6/29/2015	4.6	0.180	0.719	2.29	6.75	3.55	-0.000295	0.51	3.93
Fayetteville	F08	F08AB	F08	36.13572	-94.13328	6/29/2015	4.6	0.180	0.719	2.29	6.75	3.55	-0.000295	0.51	3.93
Fayetteville	F10	F10AA	F10	36.13397	-94.13705	6/29/2015	7.5	0.337	0.842	1.43	6.75	1.76	-0.000295	1.03	2.38
Fayetteville	F10	F10AB	F10	36.13397	-94.13705	6/29/2015	7.5	0.337	0.842	1.43	6.75	1.76	-0.000295	1.03	2.38
Fayetteville	F12	F12AA2	F12	36.13799	-94.12698	6/29/2015	2.7	0.280	0.698	1.43	6.75	2.85	-0.000295	0.63	3.47
Fayetteville	F12	F12AB	F12	36.13799	-94.12698	6/29/2015	2.7	0.280	0.698	1.43	6.75	2.85	-0.000295	0.63	3.47
Fayetteville	F14	F14AA	F14	36.13659	-94.12591	6/29/2015	3.0	0.335	0.656	1.12	6.75	1.54	-0.000295	0.82	2.33
Fayetteville	F14	F14AB	F14	36.13659	-94.12591	6/29/2015	3.0	0.335	0.656	1.12	6.75	1.54	-0.000295	0.82	2.33
Fayetteville	F16	F16AA	F16	36.13750	-94.13378	6/29/2015	0.8	0.435	0.748	0.99	6.75	2.63	-0.000295	0.73	3.53
Fayetteville	F16	F16AB	F16	36.13750	-94.13378	6/29/2015	0.8	0.435	0.748	0.99	6.75	2.63	-0.000295	0.73	3.53
Fayetteville	F18	F18AA	F18	36.13591	-94.13281	6/29/2015	5.5	0.262	0.660	1.45	6.75	3.65	-0.000295	0.44	4.26
Fayetteville	F18	F18AB	F18	36.13591	-94.13281	6/29/2015	5.5	0.262	0.660	1.45	6.75	3.65	-0.000295	0.44	4.26
Fayetteville	F20	F20AA	F20	36.13433	-94.13185	6/29/2015	3.7	0.240	0.748	1.79	6.75	3.27	-0.000295	0.59	3.77
Fayetteville	FDup	FDupAA	F18	36.13591	-94.13281	6/29/2015	5.5	0.290	0.712	1.41	6.75	2.92	-0.000295	0.63	3.55
Fayetteville	FDup	FDupAB	F18	36.13591	-94.13281	6/29/2015	5.5	0.290	0.712	1.41	6.75	2.92	-0.000295	0.63	3.55
Wedington	W03	W03BA	W03	36.09493	-94.37055	7/13/2015	3.7	0.263	0.640	1.43	6.53	3.55	-0.000342	0.38	4.28
Wedington	W03	W03BB	W03	36.09493	-94.37055	7/13/2015	3.7	0.263	0.640	1.43	6.53	3.55	-0.000342	0.38	4.28
Wedington	W05	W05BA	W05	36.09339	-94.36923	7/13/2015	7.7	0.135	0.672	2.92	6.53	2.82	-0.000342	0.54	3.18
Wedington	W05	W05BB	W05	36.09339	-94.36923	7/13/2015	7.7	0.135	0.672	2.92	6.53	2.82	-0.000342	0.54	3.18
Wedington	W11	W11BA	W11	36.08967	-94.37027	7/13/2015	5.9	0.196	0.686	2.05	6.53	2.43	-0.000342	0.63	2.94
Wedington	W11	W11BB	W11	36.08967	-94.37027	7/13/2015	5.9	0.196	0.686	2.05	6.53	2.43	-0.000342	0.63	2.94
Wedington	W13	W13BA	W13	36.08873	-94.37228	7/13/2015	3.7	0.411	0.632	0.90	6.53	0.45	-0.000342	0.92	1.61
Wedington	W13	W13BB	W13	36.08873	-94.37228	7/13/2015	3.7	0.411	0.632	0.90	6.53	0.45	-0.000342	0.92	1.61
Wedington	W14	W14BA	W14	36.08826	-94.37328	8/3/2015	3.4	0.383	0.633	0.99	7.44	1.68	-0.000499	0.80	3.25
Wedington	W14	W14BB	W14	36.08826	-94.37328	8/3/2015	3.4	0.383	0.633	0.99	7.44	1.68	-0.000499	0.80	3.25
Wedington	W15	W15BA	W15	36.08779	-94.37429	7/13/2015	2.6	0.306	0.626	1.20	6.53	3.31	-0.000342	0.41	4.18
Wedington	W15	W15BB	W15	36.08779	-94.37429	7/13/2015	2.6	0.306	0.626	1.20	6.53	3.31	-0.000342	0.41	4.18
Wedington	W16	W16BA	W16	36.08732	-94.37529	8/3/2015	1.5	0.253	0.667	1.45	7.44	1.01	-0.000499	0.98	2.00
Wedington	W16	W16BB	W16	36.08732	-94.37529	8/3/2015	1.5	0.253	0.667	1.45	7.44	1.01	-0.000499	0.98	2.00
Wedington	W18	W18BA	W18	36.09159	-94.36727	8/3/2015	9.8	0.339	0.600	0.98	7.44	1.50	-0.000499	0.78	2.98
Wedington	W18	W18BB	W18	36.09159	-94.36727	8/3/2015	9.8	0.339	0.600	0.98	7.44	1.50	-0.000499	0.78	2.98
Wedington	W2Dup	W2DupBA	W14	36.08826	-94.37328	8/3/2015	3.4	0.375	0.667	0.98	7.44	1.35	-0.000499	0.91	2.81
Wedington	W2Dup	W2DupBB	W14	36.08826	-94.37328	8/3/2015	3.4	0.375	0.667	0.98	7.44	1.35	-0.000499	0.91	2.81
Wedington	WDup	WDupBA	W15	36.08779	-94.37429	7/13/2015	2.6	0.296	0.623	1.23	6.53	3.32	-0.000342	0.41	4.17
Wedington	WDup	WDupBB	W15	36.08779	-94.37429	7/13/2015	2.6	0.296	0.623	1.23	6.53	3.32	-0.000342	0.41	4.17

Table 11: Selected study data– collection and ICI SOD, Lake Wister

Lake	ID	Run ID	Site	Lat	Long	Sample Date	Depth (m)	Core Height (m)	Core Flow (mL/min)	Core Flushes	DO Inflow (mg/L)	DO Out (mg/L)	Control (mg/L-min)	ICI SOD (g/m2-d)	DO1 (mg/L)
													Flow* ΔDO(in-out)		
Wister	R01	R01BA	R01	34.92699	-94.78947	7/20/2015	4.0	0.316	0.640	1.44	6.94	3.60	-0.000816	0.25	5.70
Wister	R01	R01BB	R01	34.92699	-94.78947	7/20/2015	4.0	0.316	0.640	1.44	6.94	3.60	-0.000816	0.25	5.70
Wister	R02	R02AA	R02	34.92839	-94.78164	7/27/2015	3.1	0.376	0.579	1.00	6.80	4.15	-0.000365	0.27	5.39
Wister	R02	R02AB	R02	34.92839	-94.78164	7/27/2015	3.1	0.376	0.579	1.00	6.80	4.15	-0.000365	0.27	5.39
Wister	R03	R03BA	R03	34.92979	-94.77380	7/20/2015	4.8	0.352	0.652	1.32	6.94	3.13	-0.000816	0.34	5.43
Wister	R03	R03BB	R03	34.92979	-94.77380	7/20/2015	4.8	0.352	0.652	1.32	6.94	3.13	-0.000816	0.34	5.43
Wister	R04	R04AA	R04	34.93119	-94.76596	7/27/2015	3.0	0.311	0.663	1.18	6.80	3.15	-0.000365	0.51	4.05
Wister	R04	R04AB	R04	34.93119	-94.76596	7/27/2015	3.0	0.311	0.663	1.18	6.80	3.15	-0.000365	0.51	4.05
Wister	R05	R05BA	R05	34.93259	-94.75812	7/20/2015	10.1	0.237	0.700	2.10	6.94	2.55	-0.000816	0.51	3.99
Wister	R05	R05BB	R05	34.93259	-94.75812	7/20/2015	10.1	0.237	0.700	2.10	6.94	2.55	-0.000816	0.51	3.99
Wister	R06	R06AA	R06	34.93399	-94.75028	7/27/2015	5.1	0.266	0.696	1.44	6.80	3.60	-0.000365	0.46	4.32
Wister	R06	R06AB	R06	34.93399	-94.75028	7/27/2015	5.1	0.266	0.696	1.44	6.80	3.60	-0.000365	0.46	4.32
Wister	R07	R07BA	R07	34.93539	-94.74245	7/20/2015	7.2	0.188	0.717	2.72	6.94	2.46	-0.000816	0.54	3.58
Wister	R07	R07BB	R07	34.93539	-94.74245	7/20/2015	7.2	0.188	0.717	2.72	6.94	2.46	-0.000816	0.54	3.58
Wister	R08	R08AA	R08	34.93679	-94.73461	7/27/2015	4.0	0.293	0.650	1.22	6.80	3.50	-0.000365	0.44	4.36
Wister	R08	R08AB	R08	34.93679	-94.73461	7/27/2015	4.0	0.293	0.650	1.22	6.80	3.50	-0.000365	0.44	4.36
Wister	R09	R09BA	R09	34.93819	-94.72677	7/20/2015	8.0	0.258	0.667	1.84	6.94	2.64	-0.000816	0.45	4.29
Wister	R09	R09BB	R09	34.93819	-94.72677	7/20/2015	8.0	0.258	0.667	1.84	6.94	2.64	-0.000816	0.45	4.29
Wister	R10	R10AA	R10	34.93960	-94.71893	7/27/2015	6.7	0.166	0.665	2.21	6.80	2.88	-0.000365	0.56	3.36
Wister	R10	R10AB	R10	34.93960	-94.71893	7/27/2015	6.7	0.166	0.665	2.21	6.80	2.88	-0.000365	0.56	3.36
Wister	R11	R11BA	R11	34.92990	-94.73072	7/20/2015	6.0	0.294	0.700	1.70	6.94	2.57	-0.000816	0.50	4.36
Wister	R11	R11BA2	R11	34.92990	-94.73072	7/20/2015	6.0	0.294	0.700	1.70	6.94	2.57	-0.000816	0.50	4.36
Wister	R11	R11BB	R11	34.92990	-94.73072	7/20/2015	6.0	0.294	0.700	1.70	6.94	2.57	-0.000816	0.50	4.36
Wister	R12	R12AA	R12	34.93196	-94.73069	7/27/2015	3.7	0.361	0.680	1.04	6.80	2.59	-0.000365	0.64	3.60
Wister	R12	R12AB	R12	34.93196	-94.73069	7/27/2015	3.7	0.361	0.680	1.04	6.80	2.59	-0.000365	0.64	3.60
Wister	R13	R13BA	R13	34.93401	-94.73067	7/20/2015	5.1	0.352	0.717	1.45	6.94	2.57	-0.000816	0.52	4.66
Wister	R13	R13BB	R13	34.93401	-94.73067	7/20/2015	5.1	0.352	0.717	1.45	6.94	2.57	-0.000816	0.52	4.66
Wister	R14	R14AA	R14	34.93607	-94.73064	7/27/2015	6.7	0.249	0.650	1.44	6.80	2.65	-0.000365	0.59	3.38
Wister	R14	R14AB	R14	34.93607	-94.73064	7/27/2015	6.7	0.249	0.650	1.44	6.80	2.65	-0.000365	0.59	3.38
Wister	R15	R15BA	R15	34.93813	-94.73061	7/20/2015	8.8	0.452	0.633	1.00	6.94	3.13	-0.000816	0.32	6.17
Wister	R15	R15BB	R15	34.93813	-94.73061	7/20/2015	8.8	0.452	0.633	1.00	6.94	3.13	-0.000816	0.32	6.17
Wister	R16	R16AA	R16	34.94018	-94.73058	7/27/2015	5.0	0.226	0.646	1.58	6.80	2.69	-0.000365	0.58	3.36
Wister	R16	R16AB	R16	34.94018	-94.73058	7/27/2015	5.0	0.226	0.646	1.58	6.80	2.69	-0.000365	0.58	3.36
Wister	R17	R17BA	R17	34.94224	-94.73056	7/20/2015	5.5	0.362	0.617	1.21	6.94	4.16	-0.000816	0.13	6.66
Wister	R17	R17BB	R17	34.94224	-94.73056	7/20/2015	5.5	0.362	0.617	1.21	6.94	4.16	-0.000816	0.13	6.66
Wister	R18	R18AA	R18	34.94430	-94.73053	7/27/2015	4.1	0.320	0.632	1.09	6.80	3.37	-0.000365	0.44	4.33
Wister	R18	R18AB	R18	34.94430	-94.73053	7/27/2015	4.1	0.320	0.632	1.09	6.80	3.37	-0.000365	0.44	4.33
Wister	R19	R19BA	R19	34.94635	-94.73050	7/20/2015	5.4	0.372	0.700	1.34	6.94	3.53	-0.000816	0.32	5.79
Wister	R19	R19BB	R19	34.94635	-94.73050	7/20/2015	5.4	0.372	0.700	1.34	6.94	3.53	-0.000816	0.32	5.79
Wister	R20	R20AA	R20	34.94841	-94.73048	7/27/2015	3.8	0.329	0.665	1.11	6.80	4.35	-0.000365	0.30	5.29
Wister	R20	R20AB	R20	34.94841	-94.73048	7/27/2015	3.8	0.329	0.665	1.11	6.80	4.35	-0.000365	0.30	5.29
Wister	R2Dup	R2DupAA	R08	34.93679	-94.73461	7/27/2015	4.0	0.273	0.650	1.31	6.80	2.97	-0.000365	0.53	3.77
Wister	R2Dup	R2DupAB	R08	34.93679	-94.73461	7/27/2015	4.0	0.273	0.650	1.31	6.80	2.97	-0.000365	0.53	3.77
Wister	RDup	RDupBA	R05	34.93259	-94.75812	7/20/2015	10.1	0.282	0.717	1.81	6.94	3.07	-0.000816	0.42	4.75
Wister	RDup	RDupBB	R05	34.93259	-94.75812	7/20/2015	10.1	0.282	0.717	1.81	6.94	3.07	-0.000816	0.42	4.75

Table 12: Selected study data – M-C SOD and inputs, Lakes Fayetteville and Wedington

Lake	Run ID	Density (g/cm3)	MC %	Psed,w	Nsed (g/m3-s)	hm ICI (m/s)	M-C SOD Core (g/m2-d)	hm Lake MIN (m/s)	hm Lake MAX (m/s)	hm Lake MID (m/s)	M-C SOD Lake MIN (g/m2d)	M-C SOD Lake MAX (g/m2d)	M-C SOD Lake MID (g/m2d)
						(temp corrected)	(@ DO1, core flow)				(2 mg/L, 0.01 m/s)	(9.09 mg/L, 0.05 m/s)	(5.5 mg/L, 0.02 m/s)
Fayetteville	F02AA	1.3152	63.48%	0.834	0.0149	1.542E-06	0.419	2.682E-08	1.896E-06	1.199E-06	0.005	1.019	0.499
Fayetteville	F02AB	1.3152	63.48%	0.834	0.0149	1.542E-06	0.419	2.682E-08	1.896E-06	1.199E-06	0.005	1.019	0.499
Fayetteville	F04AA	1.3152	60.58%	0.795	0.0235	1.482E-06	0.332	2.682E-08	1.896E-06	1.199E-06	0.005	1.104	0.517
Fayetteville	F04AB	1.3152	60.58%	0.795	0.0247	1.483E-06	0.334	2.682E-08	1.896E-06	1.199E-06	0.005	1.116	0.519
Fayetteville	F08AA	1.1348	79.28%	0.898	0.0412	1.605E-06	0.514	2.682E-08	1.896E-06	1.199E-06	0.005	1.264	0.544
Fayetteville	F08AB	1.1348	79.28%	0.898	0.0172	1.606E-06	0.480	2.682E-08	1.896E-06	1.199E-06	0.005	1.089	0.514
Fayetteville	F10AA	1.11	83.01%	0.920	0.0275	1.744E-06	0.337	2.682E-08	1.896E-06	1.199E-06	0.005	1.200	0.534
Fayetteville	F10AB	1.11	83.01%	0.920	0.0407	1.738E-06	0.343	2.682E-08	1.896E-06	1.199E-06	0.005	1.270	0.544
Fayetteville	F12AA2	1.2124	64.91%	0.786	0.0188	1.588E-06	0.417	2.682E-08	1.896E-06	1.199E-06	0.005	1.047	0.505
Fayetteville	F12AB	1.2124	64.91%	0.786	0.0605	1.587E-06	0.454	2.682E-08	1.896E-06	1.199E-06	0.005	1.283	0.546
Fayetteville	F14AA	1.254	65.28%	0.817	0.0716	1.540E-06	0.303	2.682E-08	1.896E-06	1.199E-06	0.005	1.319	0.551
Fayetteville	F14AB	1.254	65.28%	0.817	0.0240	1.543E-06	0.286	2.682E-08	1.896E-06	1.199E-06	0.005	1.069	0.510
Fayetteville	F16AA	1.3228	57.41%	0.758	0.0317	1.643E-06	0.455	2.682E-08	1.896E-06	1.199E-06	0.005	1.150	0.525
Fayetteville	F16AB	1.3228	57.41%	0.758	0.0329	1.645E-06	0.457	2.682E-08	1.896E-06	1.199E-06	0.005	1.157	0.526
Fayetteville	F18AA	1.1164	83.49%	0.931	0.0288	1.541E-06	0.525	2.682E-08	1.896E-06	1.199E-06	0.005	1.213	0.536
Fayetteville	F18AB	1.1164	83.49%	0.931	0.0287	1.545E-06	0.526	2.682E-08	1.896E-06	1.199E-06	0.005	1.212	0.536
Fayetteville	F20AA	1.218	71.72%	0.872	0.0266	1.637E-06	0.486	2.682E-08	1.896E-06	1.199E-06	0.005	1.171	0.529
Fayetteville	FDupAA	1.0948	81.82%	0.894	0.0204	1.607E-06	0.445	2.682E-08	1.896E-06	1.199E-06	0.005	1.125	0.521
Fayetteville	FDupAB	1.0948	81.82%	0.894	0.0266	1.597E-06	0.452	2.682E-08	1.896E-06	1.199E-06	0.005	1.182	0.531
Wedington	W03BA	1.0504	87.75%	0.920	0.0441	1.519E-06	0.533	2.682E-08	1.896E-06	1.199E-06	0.005	1.283	0.546
Wedington	W03BB	1.0504	87.75%	0.920	0.0283	1.520E-06	0.520	2.682E-08	1.896E-06	1.199E-06	0.005	1.205	0.535
Wedington	W05BA	1.0196	91.26%	0.929	0.0332	1.561E-06	0.407	2.682E-08	1.896E-06	1.199E-06	0.005	1.238	0.540
Wedington	W05BB	1.0196	91.26%	0.929	0.0194	1.558E-06	0.393	2.682E-08	1.896E-06	1.199E-06	0.005	1.131	0.522
Wedington	W11BA	1.0492	88.35%	0.925	0.0295	1.574E-06	0.378	2.682E-08	1.896E-06	1.199E-06	0.005	1.215	0.536
Wedington	W11BB	1.0492	88.35%	0.925	0.0386	1.575E-06	0.383	2.682E-08	1.896E-06	1.199E-06	0.005	1.263	0.543
Wedington	W13BA	1.2092	68.75%	0.830	0.0351	1.514E-06	0.205	2.682E-08	1.896E-06	1.199E-06	0.005	1.207	0.535
Wedington	W13BB	1.2092	68.75%	0.830	0.0876	1.507E-06	0.207	2.682E-08	1.896E-06	1.199E-06	0.005	1.348	0.555
Wedington	W14BA	1.1544	75.94%	0.875	0.1223	1.522E-06	0.420	2.682E-08	1.896E-06	1.199E-06	0.005	1.392	0.560
Wedington	W14BB	1.1544	75.94%	0.875	0.1011	1.524E-06	0.420	2.682E-08	1.896E-06	1.199E-06	0.005	1.375	0.558
Wedington	W15BA	1.2104	69.38%	0.838	0.0590	1.501E-06	0.519	2.682E-08	1.896E-06	1.199E-06	0.005	1.299	0.548
Wedington	W15BB	1.2104	69.38%	0.838	0.0252	1.506E-06	0.493	2.682E-08	1.896E-06	1.199E-06	0.005	1.143	0.524
Wedington	W16BA	1.2056	66.51%	0.801	0.0266	1.560E-06	0.254	2.682E-08	1.896E-06	1.199E-06	0.005	1.135	0.523
Wedington	W16BB	1.2056	66.51%	0.801	0.0258	1.561E-06	0.254	2.682E-08	1.896E-06	1.199E-06	0.005	1.128	0.521
Wedington	W18BA	1.0236	93.24%	0.953	0.0266	1.480E-06	0.361	2.682E-08	1.896E-06	1.199E-06	0.005	1.207	0.535
Wedington	W18BB	1.0236	93.24%	0.953	0.0242	1.481E-06	0.359	2.682E-08	1.896E-06	1.199E-06	0.005	1.188	0.532
Wedington	W2DupBA	1.1112	79.85%	0.886	0.0552	1.564E-06	0.368	2.682E-08	1.896E-06	1.199E-06	0.005	1.305	0.549
Wedington	W2DupBB	1.1112	79.85%	0.886	0.0692	1.565E-06	0.371	2.682E-08	1.896E-06	1.199E-06	0.005	1.335	0.553
Wedington	WDupBA	1.1936	74.44%	0.887	0.0483	1.503E-06	0.515	2.682E-08	1.896E-06	1.199E-06	0.005	1.286	0.547
Wedington	WDupBB	1.1936	74.44%	0.887	0.0701	1.505E-06	0.523	2.682E-08	1.896E-06	1.199E-06	0.005	1.337	0.553

Table 13: Selected study data – M-C SOD and inputs, Lake Wister

Lake	Run ID	Density (g/cm3)	MC %	Psed,w	Nsed (g/m3-s)	hm ICI (m/s)	M-C SOD Core (g/m2-d)	hm Lake MIN (m/s)	hm Lake MAX (m/s)	hm Lake MID (m/s)	M-C SOD Lake MIN (g/m2d)	M-C SOD Lake MAX (g/m2d)	M-C SOD Lake MID (g/m2d)
						(temp corrected)	(@ DO1, core flow)				(2 mg/L, 0.01 m/s)	(9.09 mg/L, 0.05 m/s)	(5.5 mg/L, 0.02 m/s)
Wister	R01BA	1.20	72.47%	0.866	0.0653	1.526E-06	0.713	2.682E-08	1.896E-06	1.199E-06	0.005	1.322	0.552
Wister	R01BB	1.20	72.47%	0.866	0.1008	1.526E-06	0.725	2.682E-08	1.896E-06	1.199E-06	0.005	1.373	0.558
Wister	R02AA	1.25	63.00%	0.787	0.1658	1.450E-06	0.661	2.682E-08	1.896E-06	1.199E-06	0.005	1.400	0.561
Wister	R02AB	1.25	63.00%	0.787	0.0781	1.454E-06	0.646	2.682E-08	1.896E-06	1.199E-06	0.005	1.320	0.551
Wister	R03BA	1.22	68.48%	0.835	0.0768	1.537E-06	0.688	2.682E-08	1.896E-06	1.199E-06	0.005	1.334	0.553
Wister	R03BB	1.22	68.48%	0.835	0.0731	1.539E-06	0.687	2.682E-08	1.896E-06	1.199E-06	0.005	1.327	0.552
Wister	R04AA	1.19	70.74%	0.843	0.0779	1.555E-06	0.525	2.682E-08	1.896E-06	1.199E-06	0.005	1.338	0.554
Wister	R04AB	1.19	70.74%	0.843	0.0973	1.555E-06	0.528	2.682E-08	1.896E-06	1.199E-06	0.005	1.363	0.557
Wister	R05BA	1.09	81.84%	0.889	0.0548	1.590E-06	0.523	2.682E-08	1.896E-06	1.199E-06	0.005	1.305	0.549
Wister	R05BB	1.09	81.84%	0.889	0.0632	1.600E-06	0.529	2.682E-08	1.896E-06	1.199E-06	0.005	1.325	0.552
Wister	R06AA	1.27	64.35%	0.818	0.1502	1.595E-06	0.559	2.682E-08	1.896E-06	1.199E-06	0.005	1.264	0.544
Wister	R06AB	1.27	64.35%	0.818	0.1911	1.596E-06	0.586	2.682E-08	1.896E-06	1.199E-06	0.005	1.416	0.563
Wister	R07BA	1.17	76.41%	0.893	0.0496	1.618E-06	0.477	2.682E-08	1.896E-06	1.199E-06	0.005	1.292	0.547
Wister	R07BB	1.17	76.41%	0.893	0.0481	1.620E-06	0.477	2.682E-08	1.896E-06	1.199E-06	0.005	1.287	0.547
Wister	R08AA	1.12	79.84%	0.894	0.0069	1.544E-06	0.445	2.682E-08	1.896E-06	1.199E-06	0.005	0.861	0.458
Wister	R08AB	1.12	79.84%	0.894	0.0484	1.548E-06	0.553	2.682E-08	1.896E-06	1.199E-06	0.005	1.288	0.547
Wister	R09BA	1.17	75.95%	0.884	0.0648	1.552E-06	0.552	2.682E-08	1.896E-06	1.199E-06	0.005	1.327	0.552
Wister	R09BB	1.17	75.95%	0.884	0.0395	1.554E-06	0.540	2.682E-08	1.896E-06	1.199E-06	0.005	1.252	0.542
Wister	R10AA	1.12	47.98%	0.537	0.0725	1.561E-06	0.421	2.682E-08	1.896E-06	1.199E-06	0.005	1.178	0.530
Wister	R10AB	1.12	47.98%	0.537	0.0572	1.562E-06	0.414	2.682E-08	1.896E-06	1.199E-06	0.005	1.128	0.521
Wister	R11BA	1.21	70.28%	0.847	0.0841	1.590E-06	0.577	2.682E-08	1.896E-06	1.199E-06	0.005	1.348	0.555
Wister	R11BA2	1.21	70.28%	0.847	0.0579	1.590E-06	0.568	2.682E-08	1.896E-06	1.199E-06	0.005	1.299	0.548
Wister	R11BB	1.21	70.28%	0.847	0.0696	1.596E-06	0.575	2.682E-08	1.896E-06	1.199E-06	0.005	1.325	0.552
Wister	R12AA	1.37	56.98%	0.780	0.0830	1.578E-06	0.474	2.682E-08	1.896E-06	1.199E-06	0.005	1.326	0.552
Wister	R12AB	1.37	56.98%	0.780	0.0856	1.578E-06	0.474	2.682E-08	1.896E-06	1.199E-06	0.005	1.330	0.553
Wister	R13BA	1.23	68.53%	0.839	0.0548	1.611E-06	0.610	2.682E-08	1.896E-06	1.199E-06	0.005	1.288	0.547
Wister	R13BB	1.23	68.53%	0.839	0.0490	1.611E-06	0.606	2.682E-08	1.896E-06	1.199E-06	0.005	1.270	0.544
Wister	R14AA	1.20	71.22%	0.852	0.0587	1.547E-06	0.434	2.682E-08	1.896E-06	1.199E-06	0.005	1.303	0.549
Wister	R14AB	1.20	71.22%	0.852	0.0627	1.545E-06	0.435	2.682E-08	1.896E-06	1.199E-06	0.005	1.312	0.550
Wister	R15BA	1.21	71.50%	0.860	0.1019	1.517E-06	0.778	2.682E-08	1.896E-06	1.199E-06	0.005	1.372	0.558
Wister	R15BB	1.21	71.50%	0.860	0.0907	1.520E-06	0.776	2.682E-08	1.896E-06	1.199E-06	0.005	1.360	0.556
Wister	R16AA	1.15	75.60%	0.868	0.0502	1.535E-06	0.427	2.682E-08	1.896E-06	1.199E-06	0.005	1.285	0.547
Wister	R16AB	1.15	75.60%	0.868	0.0533	1.535E-06	0.428	2.682E-08	1.896E-06	1.199E-06	0.005	1.294	0.548
Wister	R17BA	1.25	68.56%	0.852	0.0685	1.492E-06	0.810	2.682E-08	1.896E-06	1.199E-06	0.005	1.324	0.552
Wister	R17BB	1.25	68.56%	0.852	0.0473	1.495E-06	0.793	2.682E-08	1.896E-06	1.199E-06	0.005	1.269	0.544
Wister	R18AA	1.13	77.36%	0.870	0.0474	1.515E-06	0.537	2.682E-08	1.896E-06	1.199E-06	0.005	1.277	0.545
Wister	R18AB	1.13	77.36%	0.870	0.0466	1.517E-06	0.537	2.682E-08	1.896E-06	1.199E-06	0.005	1.274	0.545
Wister	R19BA	1.17	75.22%	0.881	0.0586	1.596E-06	0.750	2.682E-08	1.896E-06	1.199E-06	0.005	1.312	0.550
Wister	R19BB	1.17	75.22%	0.881	0.0948	1.598E-06	0.760	2.682E-08	1.896E-06	1.199E-06	0.005	1.342	0.554
Wister	R20AA	1.17	74.17%	0.867	0.0859	1.559E-06	0.685	2.682E-08	1.896E-06	1.199E-06	0.005	1.356	0.556
Wister	R20AB	1.17	74.17%	0.867	0.0915	1.560E-06	0.687	2.682E-08	1.896E-06	1.199E-06	0.005	1.363	0.557
Wister	R2DupAA	1.13	75.89%	0.855	0.0507	1.538E-06	0.478	2.682E-08	1.896E-06	1.199E-06	0.005	1.282	0.546
Wister	R2DupAB	1.13	75.89%	0.855	0.0615	1.532E-06	0.480	2.682E-08	1.896E-06	1.199E-06	0.005	1.310	0.550
Wister	RDupBA	1.10	80.65%	0.884	0.0579	1.617E-06	0.629	2.682E-08	1.896E-06	1.199E-06	0.005	1.311	0.550
Wister	RDupBB	1.10	80.65%	0.884	0.0487	1.619E-06	0.624	2.682E-08	1.896E-06	1.199E-06	0.005	1.286	0.547

Table 14: Selected study data – $\dot{N}_{sed}$ calculation inputs, Lakes Fayetteville and Wedington

Run	N (datapoints)	Duration (sec)	Duration (min)	a	b	c	d	e	f	Wed Sed (g)	T AVG (°C)	Density (g/cm^3)	Nsed uncorr. (g/m3-s)	Nsed (g/m3-s)
F01AA	181	2700	45.0	3.92673	-0.00086	1.712427	-0.00193	2.007177	-0.02656	11.81	19.83	1.329	0.02902	0.02865
F01AB	57	840	14.0	2.942151	-0.00293	2.717144	-0.00791	2.516524	-0.05877	13.02	19.96	1.329	0.08984	0.08960
F02AA	181	2700	45.0	2.364187	-0.00044	2.580646	-0.00187	2.521235	-0.03857	12.04	20.34	1.315	0.01449	0.01487
F02AB	181	2700	45.0	2.51863	-0.00047	2.684411	-0.00189	2.763351	-0.03876	12.71	20.37	1.315	0.01449	0.01491
F03AA	74	1095	18.3	2.897627	-0.00221	2.048419	-0.00629	3.167965	-0.05559	11.94	20.02	1.264	0.07033	0.07045
F03AB	57	840	14.0	2.854016	-0.00283	2.183997	-0.00731	3.279536	-0.05241	13.64	20.08	1.264	0.07870	0.07917
F04AA	181	2700	45.0	3.083606	-0.00066	2.647409	-0.0022	2.260541	-0.03986	11.06	19.93	1.315	0.02359	0.02346
F04AB	181	2700	45.0	3.68768	-0.00063	2.396013	-0.00223	2.000262	-0.03613	10.16	20.12	1.315	0.02446	0.02469
F05AA	181	2700	45.0	3.681263	-0.00037	2.550094	-0.00143	1.439733	-0.04735	10.08	19.59	1.541	0.01681	0.01628
F05AB	181	2700	45.0	4.242859	-0.00068	2.533019	-0.00174	1.568767	-0.03843	9.94	19.85	1.541	0.03175	0.03140
F06AA	43	630	10.5	1.566449	-0.00174	3.181944	-0.0069	3.209387	-0.03387	12.53	19.76	1.226	0.05103	0.05009
F06AB	181	2700	45.0	2.026382	-0.00052	2.570427	-0.00152	3.325358	-0.01874	8.59	19.94	1.226	0.02227	0.02216
F07AA	78	1155	19.3	2.190625	-0.00147	3.066086	-0.00706	2.617751	-0.09613	11.46	19.70	1.155	0.04456	0.04353
F07AB	153	2280	38.0	2.8703	-0.00108	2.293658	-0.00363	2.97206	-0.03333	9.77	20.35	1.155	0.03813	0.03918
F08AA	53	780	13.0	1.628975	-0.00147	3.181623	-0.00639	2.661866	-0.05311	11.58	19.40	1.135	0.04316	0.04121
F08AB	181	2700	45.0	4.446665	-0.0003	1.787234	-0.00322	1.554951	-0.05385	5.68	19.53	1.135	0.01782	0.01719
F09AA	46	675	11.3	2.06713	-0.00239	3.178965	-0.00741	2.923622	-0.08765	12.95	20.61	1.098	0.06073	0.06366
F09AB	181	2700	45.0	3.488148	-0.00069	2.477036	-0.00374	1.729442	-0.046	7.49	20.80	1.098	0.03055	0.03248
F10AA	181	2700	45.0	3.263328	-0.00065	2.256228	-0.00256	2.309985	-0.02852	8.02	20.24	1.110	0.02702	0.02751
F10AB	121	1789	29.8	2.831745	-0.00134	2.805281	-0.00426	2.376435	-0.03941	10.62	19.60	1.110	0.04201	0.04074
F11AA	168	2505	41.8	2.906216	-0.00099	3.915689	-0.002	1.140121	-0.04697	16	19.88	1.679	0.03121	0.03092
F11AB	181	2700	45.0	2.908022	-0.00092	3.832583	-0.00181	1.383616	-0.03241	15.39	20.60	1.679	0.03010	0.03153
F12AA2	181	2700	45.0	1.797882	-0.0004	2.857643	-0.00142	3.209435	-0.02508	7.95	20.24	1.212	0.01851	0.01885
F12AB	88	1305	21.8	2.653634	-0.00169	2.099571	-0.00481	3.386123	-0.03338	10.24	20.12	1.212	0.05988	0.06045
F13AA2	136	2025	33.8	2.671494	-0.00111	2.018757	-0.00299	3.042115	-0.02982	10.11	19.84	1.170	0.03839	0.03792
F13AB2	124	1860	31.0	2.843327	-0.0013	2.032818	-0.00436	2.816239	-0.04358	10.04	19.92	1.170	0.04548	0.04521
F14AA	57	840	14.0	2.119298	-0.00195	2.695801	-0.00805	3.147922	-0.0443	10.49	20.29	1.254	0.07006	0.07165
F14AB	180	2700	45.0	2.253116	-0.00036	2.466026	-0.00137	2.540373	-0.01921	7.48	20.67	1.254	0.01812	0.01907
F15AA	180	2700	45.0	5.211116	-0.00069	1.69843	-0.00146	0.489448	-0.00751	15.24	20.01	1.896	0.02575	0.02577
F15AB	100	1500	25.0	2.464169	-0.00147	4.634614	-0.00201	0.40695	-0.02559	30.08	20.77	1.896	0.02770	0.02940
F16AA	181	2700	45.0	3.690154	-0.00108	2.705527	-0.00213	1.519561	-0.04646	13.68	20.12	1.323	0.03140	0.03170
F16AB	181	2700	45.0	4.994267	-0.00076	1.967296	-0.00209	1.073372	-0.0393	9.51	20.42	1.323	0.03183	0.03287
F17AA	92	1365	22.8	2.728318	-0.00168	2.965964	-0.00653	2.845433	-0.04534	10.51	19.84	1.254	0.05998	0.05924
F17AB	181	2700	45.0	2.323847	-0.00059	2.641034	-0.00154	3.54884	-0.0248	8.41	20.22	1.254	0.02619	0.02663
F18AA	181	2700	45.0	3.224509	-0.00074	2.051129	-0.00289	2.13018	-0.03108	8.46	19.78	1.116	0.02927	0.02878
F18AB	180	2685	44.8	2.725355	-0.00085	2.548844	-0.00322	2.400447	-0.05126	10.19	20.27	1.116	0.02809	0.02867
F19AA	181	2700	45.0	4.081851	-0.00069	2.100663	-0.00326	2.10954	-0.06602	7.61	20.09	1.124	0.03064	0.03086
F19AB	181	2700	45.0	3.856336	-0.00078	2.402939	-0.00303	1.846412	-0.04006	8.65	20.91	1.124	0.03042	0.03263
F20AA	142	2115	35.3	2.08118	-0.00081	2.823002	-0.00164	2.884347	-0.02791	10.6	19.33	1.218	0.02797	0.02657
F20AB	96	1425	23.8	3.215905	-0.00196	2.330801	-0.00494	2.402771	-0.05354			1.218		
FDupAA	181	2700	45.0	3.233307	-0.00049	2.450231	-0.00381	2.378122	-0.04239	8.27	20.65	1.095	0.01935	0.02035
FDupAB	171	2544	42.4	2.599872	-0.00085	2.564522	-0.00332	2.918929	-0.03069	10.03	19.40	1.095	0.02785	0.02659
W02BA	181	2700	45.0	3.973117	-0.0005	2.184289	-0.00215	1.620243	-0.02228	8.85	21.49	1.389	0.02359	0.02644
W02BB	181	2700	45.0	2.58848	-0.00071	3.306862	-0.00234	2.278686	-0.02676	12.67	22.01	1.389	0.02333	0.02723
W03BA	99	1470	24.5	2.27922	-0.00125	3.675171	-0.00385	2.419116	-0.04327	8.97	20.07	1.050	0.04381	0.04405
W03BB	171	2550	42.5	2.139068	-0.00066	3.628897	-0.00234	2.541138	-0.02282	7.48	20.16	1.050	0.02800	0.02833
W05BA	131	1950	32.5	2.509465	-0.00106	3.434412	-0.00276	1.9289	-0.04953	10.25	20.65	1.020	0.03155	0.03317
W05BB	181	2700	45.0	3.121726	-0.00075	3.183836	-0.00195	1.747666	-0.02214	12.16	20.30	1.020	0.01891	0.01935
W11BA	181	2700	45.0	3.098999	-0.00077	3.189566	-0.00239	1.895218	-0.0519	8.33	20.24	1.049	0.02896	0.02949
W11BB	104	1545	25.8	2.488965	-0.00132	3.674242	-0.00327	2.139835	-0.0456	11	20.29	1.049	0.03770	0.03855
W13BA	167	2490	41.5	2.187338	-0.00145	3.660304	-0.00241	2.322676	-0.03441	7.63	20.24	1.209	0.03338	0.03511
W13BB	42	611	10.2	2.184503	-0.00291	4.496352	-0.0068	1.898135	-0.06893	11.86	19.80	1.209	0.08891	0.08755
W14BA	44	645	10.8	2.061939	-0.00258	4.038641	-0.00587	1.938837	-0.04842	8.12	21.37	1.154	0.11002	0.12227
W14BB	69	1020	17.0	2.280133	-0.0018	4.007516	-0.00438	1.997676	-0.03903	7.04	21.72	1.154	0.08859	0.10112
W15BA	65	960	16.0	2.227376	-0.00187	3.648667	-0.0047	2.610314	-0.04468	11.38	19.83	1.210	0.05977	0.05899
W15BB	177	2640	44.0	2.067175	-0.00061	3.765568	-0.00246	2.654187	-0.02925	9.26	20.55	1.210	0.02411	0.02515
W16BA	181	2700	45.0	2.464451	-0.00053	3.061749	-0.00225	2.346119	-0.02302	7.93	21.20	1.206	0.02428	0.02663
W16BB	181	2700	45.0	3.347056	-0.00044	2.758433	-0.00214	1.943738	-0.02414	6.88	21.30	1.206	0.02335	0.02580
W18BA	181	2700	45.0	4.811376	-0.00049	2.163651	-0.00175	0.871586	-0.031	6.17	21.21	1.024	0.02426	0.02661
W18BB	181	2700	45.0	3.74909	-0.00067	3.155376	-0.00177	1.259018	-0.03219	9.42	21.31	1.024	0.02190	0.02423
W2DupBA	128	1905	31.8	2.269018	-0.00095	3.638785	-0.00261	2.344588	-0.02607	6.57	21.70	1.111	0.04842	0.05520
W2DupBB	90	1335	22.3	2.376606	-0.00145	3.927553	-0.00358	2.04135	-0.03828	8.08	21.85	1.111	0.06001	0.06918
WDupBA	95	1410	23.5	2.388138	-0.00138	3.439336	-0.0041	2.425954	-0.05781	10.65	20.49	1.194	0.04656	0.04834
WDupBB	64	945	15.8	2.519411	-0.00219	3.441891	-0.00547	2.394949	-0.0577	11.83	20.72	1.194	0.06632	0.07009

Table 15: Selected study data – $\dot{N}_{sed}$ calculation inputs, Lake Wister

Run	N (datapoints)	Duration (sec)	Duration (min)	a	b	c	d	e	f	Wed Sed (g)	T AVG (°C)	Density (g/cm^3)	Nsed uncorr. (g/m3-s)	Nsed (g/m3-s)
R01BA	157	2340	39.0	2.469803	-0.00086	3.3033	-0.00226	2.223518	-0.08204	5.07	20.89	1.198	0.06094	0.06526
R01BB	66	975	16.3	2.089573	-0.00174	3.439752	-0.00367	2.731641	-0.03382	6.65	20.87	1.198	0.09427	0.10082
R02AA	34	510	8.5	2.003714	-0.00321	3.777459	-0.00674	3.531582	-0.06273	7.69	20.74	1.251	0.15653	0.16576
R02AB	144	2160	36.0	2.445521	-0.00093	3.594237	-0.00225	2.178195	-0.02337	4.88	21.22	1.251	0.07115	0.07815
R03BA	74	1095	18.3	2.028136	-0.00146	3.18873	-0.00375	2.330689	-0.03497	7.25	20.50	1.221	0.07392	0.07684
R03BB	66	975	16.3	1.779814	-0.00144	3.366536	-0.00335	2.712059	-0.02742	7.61	20.72	1.221	0.06915	0.07309
R04AA	115	1710	28.5	2.44132	-0.00117	3.523698	-0.00289	2.647613	-0.03168	5.86	21.17	1.194	0.07119	0.07790
R04AB	84	1245	20.8	2.468269	-0.00163	3.521612	-0.0036	2.586107	-0.03844	6.56	21.14	1.194	0.08909	0.09729
R05BA	30	435	7.3	1.098314	-0.00182	3.566993	-0.00644	3.108485	-0.05077	11	20.20	1.088	0.05397	0.05480
R05BB	86	1275	21.3	2.335084	-0.00127	3.11224	-0.00354	2.891856	-0.03633	7.28	21.39	1.088	0.05677	0.06318
R06AA	78	1155	19.3	0.790049	-0.0006	4.126016	-0.00202	3.628479	-0.01527	5.08	21.26	1.274	0.04511	0.04972
R06AB	36	525	8.8	1.934948	-0.00298	4.036708	-0.00659	3.954723	-0.04165	6.66	21.45	1.274	0.17090	0.19114
R07BA	120	1785	29.8	1.935472	-0.00083	3.079209	-0.00248	3.228145	-0.05164	6.51	21.28	1.171	0.04493	0.04957
R07BB	155	2310	38.5	2.593215	-0.0008	2.999061	-0.00245	2.730173	-0.03048	6.50	21.47	1.171	0.04297	0.04810
R08AA	181	2700	45.0	3.363799	-7.3E-05	3.176439	-0.00166	1.826191	-0.03137	4.06	21.72	1.121	0.00605	0.00691
R08AB	181	2700	45.0	2.313181	-0.00069	3.531568	-0.00222	2.58328	-0.03226	5.68	22.18	1.121	0.04098	0.04845
R09BA	86	1275	21.3	1.949984	-0.00118	2.997373	-0.00325	2.611373	-0.03253	6.51	20.23	1.166	0.06364	0.06477
R09BB	181	2700	45.0	2.179815	-0.00059	3.026485	-0.00198	2.467096	-0.02573	5.41	20.50	1.166	0.03805	0.03954
R10AA	71	1050	17.5	1.910502	-0.00142	3.316783	-0.00361	2.744071	-0.03326	7.42	21.56	1.121	0.06434	0.07253
R10AB	181	2700	45.0	3.383153	-0.00067	2.636049	-0.00207	2.143413	-0.02588	4.54	21.76	1.121	0.04995	0.05720
R11BA	71	1050	17.5	2.22124	-0.00169	3.1642	-0.00467	2.206236	-0.05459	7.4	20.22	1.207	0.08264	0.08405
R11BA2	111	1650	27.5	2.265071	-0.0011	3.129735	-0.00336	2.094055	-0.04453	6.95	20.17	1.207	0.05710	0.05787
R11BB	97	1440	24.0	2.192297	-0.0012	3.130969	-0.00334	2.39757	-0.0327	6.71	20.91	1.207	0.06495	0.06964
R12AA	134	1995	33.3	2.44571	-0.001	3.585843	-0.00244	2.520152	-0.02453	5.64	21.64	1.370	0.07312	0.08297
R12AB	107	1590	26.5	2.268945	-0.00116	3.802158	-0.0027	2.61327	-0.02882	6.31	21.58	1.370	0.07584	0.08564
R13BA	144	2145	35.8	2.344771	-0.00088	3.147701	-0.00265	2.171105	-0.0406	6.08	20.43	1.226	0.05302	0.05479
R13BB	173	2580	43.0	2.47739	-0.00078	3.115215	-0.00223	2.151059	-0.02599	6.04	20.39	1.226	0.04757	0.04904
R14AA	181	2700	45.0	2.547135	-0.00077	3.565445	-0.00212	2.393702	-0.03072	5.53	22.09	1.198	0.04998	0.05871
R14AB	181	2700	45.0	2.947972	-0.00078	3.422417	-0.00221	2.138645	-0.0306	5.14	21.75	1.198	0.05483	0.06272
R15BA	60	885	14.8	2.046058	-0.00184	3.406781	-0.00422	2.655224	-0.03887	6.91	20.75	1.205	0.09618	0.10191
R15BB	88	1305	21.8	2.300182	-0.00142	3.407625	-0.00349	2.507377	-0.03754	6.16	21.13	1.205	0.08310	0.09066
R16AA	145	2160	36.0	2.20811	-0.00082	3.560342	-0.00253	2.602919	-0.02977	6.1	21.10	1.150	0.04616	0.05023
R16AB	181	2700	45.0	2.63569	-0.00073	3.361933	-0.00225	2.449331	-0.02909	5.16	21.11	1.150	0.04890	0.05326
R17BA	103	1530	25.5	2.197444	-0.00114	3.151947	-0.0032	2.171086	-0.03625	6.25	20.05	1.245	0.06821	0.06848
R17BB	175	2610	43.5	2.427414	-0.00075	3.187291	-0.00223	2.230909	-0.02934	6.18	20.47	1.245	0.04563	0.04729
R18AA	118	1755	29.3	2.085307	-0.00093	3.578161	-0.00273	2.641494	-0.02729	7.07	20.80	1.127	0.04457	0.04742
R18AB	181	2700	45.0	2.824171	-0.00073	3.478779	-0.00217	2.322549	-0.03337	5.78	21.08	1.127	0.04285	0.04657
R19BA	160	2385	39.8	2.511613	-0.00086	3.132257	-0.00238	2.137648	-0.03458	5.55	20.92	1.173	0.05462	0.05862
R19BB	80	1185	19.8	1.945735	-0.0013	3.294695	-0.00295	2.900027	-0.02805	6.79	21.14	1.173	0.06762	0.07381
R20AA	116	1725	28.8	2.544484	-0.00122	3.483812	-0.00297	2.368926	-0.03106	5.53	21.39	1.170	0.07715	0.08585
R20AB	96	1425	23.8	2.514043	-0.00145	3.612345	-0.00331	2.449357	-0.03191	6.23	21.44	1.170	0.08185	0.09146
R2DupAA	161	2400	40.0	2.354933	-0.00079	3.383248	-0.00226	2.442984	-0.02481	5.66	20.90	1.129	0.04730	0.05070
R2DupAB	116	1708	28.5	2.415026	-0.00116	3.495414	-0.00285	2.33443	-0.03284	6.43	20.10	1.129	0.06099	0.06146
RDupBA	109	1620	27.0	2.234972	-0.0011	3.15694	-0.00374	2.266787	-0.05275	6.87	21.18	1.098	0.05285	0.05789
RDupBB	181	2700	45.0	2.642249	-0.00073	2.954102	-0.00243	2.039814	-0.03858	5.5	21.46	1.098	0.04356	0.04873

APPENDIX B. ICI METHOD MLR REGRESSION

Table 16: MLR results for predicting ICI SOD using various inputs, with highly significant contributions in orange and significant contributions in red.

Summary of Fit

RSquare	0.440535
RSquare Adj	0.380859
Root Mean Square Error	0.157538
Mean of Response	0.547658
Observations	84

Analysis of Variance

Source	DF	Sum of Squares	Mean Square	F Ratio
Model	8	1.4656828	0.18321	7.3821
Error	75	1.8613701	0.024818	**Prob > F**
C. Total	83	3.3270528		<.0001

Parameter Estimates

Term		Estimate	Std Error	t Ratio	Prob>|t|
Intercept		-6.108067	1.888088	-3.24	0.0018
Depth (m)		-0.030995	0.009714	-3.19	0.0021
Core Height (m)		0.3504833	0.307832	1.14	0.2585
Core Flow (mL/min)		1.8279788	0.402678	4.54	<.0001
DO Inflow (mg/L)		0.3233524	0.081063	3.99	0.0002
Density (g/cm3)		3.3758528	1.482522	2.28	0.0256
MC %		6.8068801	2.405454	2.83	0.0060
Psed		-6.579104	2.159262	-3.05	0.0032
Nsed (g/m3-s)		-1.151611	0.603247	-1.91	0.0601

APPENDIX C. LITERATURE DATA

Table 17: Literature data for SOD, density, MC, P$_{sed}$, and $\dot{N}_{sed}$

Author	Waterbody	Description	SOD (g/m2-d)	Density (g/cm3)	MC %	Psed	Nsed (g/m3-s)
Charbonnet et al. (2008)	Arroyo Colorado	1015 Bridge Aug01R1	2.03	1.64	0.3811	0.625	0.1500
Charbonnet et al. (2008)	Arroyo Colorado	1015 Bridge Aug01R2	2.43	1.64	0.3811	0.625	0.1490
Charbonnet et al. (2008)	Arroyo Colorado	106 Bridge Aug01R1	0.553	1.31	0.6198	0.812	0.2370
Charbonnet et al. (2008)	Arroyo Colorado	106 Bridge Aug01R2	0.589	1.31	0.6198	0.812	0.2400
Charbonnet et al. (2008)	Arroyo Colorado	493 Bridge Aug01R1	0.984	1.5	0.3200	0.48	0.0550
Charbonnet et al. (2008)	Arroyo Colorado	1015 Bridge Apr02R1	1.65	1.64	0.3787	0.621	0.1640
Haggard et al. (2010)	Lake Wister	1 min	0.43				
Haggard et al. (2010)	Lake Wister	2 min	0.39				
Haggard et al. (2010)	Lake Wister	3 min	0.23				
Haggard et al. (2010)	Lake Wister	1 max	0.66				
Haggard et al. (2010)	Lake Wister	2 max	0.64				
Haggard et al. (2010)	Lake Wister	3 max	0.27				
Higashino et al. (2004)		(range of theoretical values for μ (Nsed)					0.0006
Higashino et al. (2004)		(range of theoretical values for μ (Nsed)					0.0012
Higashino et al. (2004)		(range of theoretical values for μ (Nsed)					0.0023
Higashino et al. (2004)		(range of theoretical values for μ (Nsed)					0.0116
Higashino et al. (2004)		(range of theoretical values for μ (Nsed)					0.0231
Matlock et al. (2003)	Arroyo Colorado	281 Bridge			0.2600		0.0064
Matlock et al. (2003)	Arroyo Colorado	907 Bridge			0.4710		0.0107
Matlock et al. (2003)	Arroyo Colorado	493 Bridge			0.2620		0.0026
Matlock et al. (2003)	Arroyo Colorado	1015 Bridge			0.5540		0.0135
Matlock et al. (2003)	Arroyo Colorado	2556 Bridge			0.2100		0.0004
Matlock et al. (2003)	Arroyo Colorado	800 Bridge			0.2100		0.0011
Matlock et al. (2003)	Arroyo Colorado	499 Bridge			0.1570		0.0002
Matlock et al. (2003)	Arroyo Colorado	Port of Harlingen			0.5590		0.0322
Matlock et al. (2003)	Arroyo Colorado	493 Bridge July 99	1.36				
Matlock et al. (2003)	Arroyo Colorado	2556 Bridge July 99	0.13				
Matlock et al. (2003)	Arroyo Colorado	800 Bridge July 99	0.15				
Matlock et al. (2003)	Arroyo Colorado	499 Bridge July 99	0.14				
Matlock et al. (2003)	Arroyo Colorado	Port of Harlingen July 99	0.66				
Matlock et al. (2003)	Arroyo Colorado	281 Bridge Sept 99	0.44				
Matlock et al. (2003)	Arroyo Colorado	907 Bridge Sept 99	0.79				
Matlock et al. (2003)	Arroyo Colorado	1015 Bridge Sept 99	0.88				
Matlock et al. (2003)	Arroyo Colorado	2556 Bridge Sept 99	1.2				
Matlock et al. (2003)	Arroyo Colorado	800 Bridge Sept 99	0.99				
Matlock et al. (2003)	Arroyo Colorado	499 Bridge Sept 99	0.44				
Matlock et al. (2003)	Arroyo Colorado	Port of Harlingen Sept 99	0.87				
Matlock et al. (2003)	Arroyo Colorado	907 Bridge Nov 99	0.42				
Matlock et al. (2003)	Arroyo Colorado	493 Bridge Nov 99	0.36				
Matlock et al. (2003)	Arroyo Colorado	Port of Harlingen Nov 99	0.53				
Richardson (2014)	Lake Wister	1	0.661				
Richardson (2014)	Lake Wister	2	0.456				
Richardson (2014)	Lake Wister	9/1/2013					0.1306
Richardson (2014)	Lake Wister	9/5/2013					0.1389
Richardson (2014)	Lake Wister	9/9/2013					0.1771
Richardson (2014)	Lake Wister	9/17/2013					0.1033
Richardson (2014)	Lake Wister	9/23/2013					0.1741
Richardson (2014)	Lake Wister	9/26/2013					0.2197
Richardson (2014)	Lake Wister	10/1/2013					0.2178
Richardson (2014)	Lake Wister	10/8/2013					0.2309
Thomann & Mueller (1987)		Estuarine mud minimum	1				
Thomann & Mueller (1987)		Sandy bottom minimum	0.2				
Thomann & Mueller (1987)		Mineral soils minimum	0.05				
Thomann & Mueller (1987)		Estuarine mud maximum	2				
Thomann & Mueller (1987)		Sandy bottom maximum	1				
Thomann & Mueller (1987)		Mineral soils maximum	0.1				
Truax et al. (1995)		Upper WI River min	0.022				
Truax et al. (1995)		Upper WI River max	0.92				
Truax et al. (1995)		Eastern US rivers min	0.11				
Truax et al. (1995)		Eastern US rivers max	0.19				
Truax et al. (1995)		SE US rivers min	0.33				
Truax et al. (1995)		SE US rivers max	0.77				
Truax et al. (1995)		E MI rivers min	0.1				
Truax et al. (1995)		E MI rivers max	5.3				
Truax et al. (1995)		N IL rivers min	0.27				
Truax et al. (1995)		N IL rivers max	9.8				
Truax et al. (1995)		NJ rivers min	1.1				
Truax et al. (1995)		NJ rivers max	12.8				
Truax et al. (1995)		E US rivers down from papermills min	0.1				
Truax et al. (1995)		E US rivers down from papermills max	33				